From the Department of Medicine, Solna
Karolinska Institutet, Stockholm, Sweden

THE EFFECT OF *PLASMODIUM* INFECTION ON CELLULAR AGING IN HUMANS

Aurelie Miglar

Karolinska Institutet

Stockholm 2023

Published by Karolinska Institutet.

Printed by Universitetsservice US-AB, 2023

ISBN 978-91-8016-931-8

Cover illustration: Aurelie Miglar

THE EFFECT OF *PLASMODIUM* INFECTION ON CELLULAR AGING IN HUMANS

THESIS FOR DOCTORAL DEGREE (Ph.D.)

By

Aurelie Miglar

The thesis will be defended in public at Rolf Luft Auditorium, L1:00, Karolinska University Hospital, Solna, 2023-03-10, 9:00

Principal Supervisor:
Professor Anna Färnert
Karolinska Institutet
Department of Medicine, Solna
Division of Infectious Diseases

Co-supervisor:
Associate Professor Eduardo Villablanca
Karolinska Institutet
Department of Medicine, Solna
Division of Immunology and Allergy

Opponent:
Professor Paul Shiels
University of Glasgow
Department of Cancer Science

Examination Board:
Associate Professor Linda Lindström
Karolinska Institutet
Department of Oncology-Pathology

Professor Marita Troye Blomberg
Stockholm University
Department of Molecular Bioscience

Associate Professor Karolina Kauppi
Umeå University
Department of Integrative Medical Biology

Internal Thesis Reviewer:
Professor Akira Kaneko
Karolinska Institutet
Department of Microbiology, Tumor and Cell Biology

External Thesis Reviewer:
Professor Karl-Heinz Wagner
University of Vienna
Department of Nutritional Sciences

Aging is a process of mind over matter – if you don't mind, it does not matter.

-Samuel Langhorne Clemens (Mark Twain)

POPULAR SCIENCE SUMMARY OF THE THESIS

The relationship of malaria and cellular aging – friends or enemies?

Life expectancy in populations living in Sub-Saharan Africa is constantly increasing and the WHO has reported an increase by 10 years per person between 2000 and 2019. Nevertheless, evidence suggests that the proportion of life in good health has remained constant. The region faces a persistent burden of infectious diseases and an increase in non-communicable diseases. Malaria, an infectious disease caused by the protozoan parasite of the genus *Plasmodium* leads to millions of cases and thousands of deaths every year, predominately in children under the age of five. Little is known about the link between biological aging and the impact of infections, such as malaria, in humans. It is hypothesized that increased age further increases the susceptibility to infection; yet, the relationship might be mutual, implying that the exposure to infectious diseases might accelerate biological aging – which resembles our age based on body functionality rather than chronological age.

By unravelling the principles of aging on a cellular and molecular level, we can identify pharmaceutical targets and understand the impact of environmental factors, such as infections, to facilitate healthy aging and a healthier life. So far, scientific advances have identified tentative cellular and molecular hallmarks that represent common denominators of aging in most species, including humans. One such hallmark is telomere shortening. Telomeres cap and protect the ends of our chromosomes, similar to a helmet, protecting our head when bicycling. Their main function is to avoid DNA loss and damage during cell division. Recently, animal studies introduced malaria as a potential driver of aging by accelerating telomere shortening.

This thesis explores the causal link between malaria infection and cellular aging in humans. In the first study chapter, we look into the length of telomeres and markers of aging together with inflammation before, during and after malaria infection in humans. In the second study, we take a closer look at telomeres in different white blood cells during and after a malaria infection.

The last two study chapters consider the consequences of repeated febrile malaria episodes as well as 'non-symptomatic' carriage of malaria parasites on telomeres in people residing in Sub-Saharan Africa.

In **Study I**, we found that a mild acute malaria infection shortens telomere length in blood, which restored within the host after successful treatment. We further found that inflammation and accumulated oxidative stress were tightly associated with the telomere shortening effect.

As a follow-up in **Study II**, we show that telomere shortening due to malaria infection is not only occurring in one specific white blood cell type, but in a majority of cell types that are part of the human immune system.

Study III revealed that the number of malaria infections experienced by children living in endemic areas does not seem to affect their telomere length. **Study IV** assessed children and adults followed over several decades in a malaria endemic area. It provides insights into telomere dynamics at different ages and shows that telomeres shorten over time within individuals and on a population level. Interestingly, we found that males and females start off with similar telomere length in infancy, but once reaching adolescence, females have longer telomeres throughout life.

This thesis exhibits telomere dynamics across life, including age and sex-specific differences, and further reveals that an acute malaria infection triggers telomere shortening that is restored once the infection is cleared. Moreover, repeated malaria infections did not seem to cause lasting consequences on telomere length in children, which suggests the presence of resistance mechanisms that might protect people living in malaria endemic areas. Despite still being far from understanding the mutual relationship between aging and infections, the findings in this thesis might lead the way to further comprehend how infections affect aging biology, and raise awareness of the importance of battling infectious diseases in the context of living healthier lives.

ABSTRACT

Telomeres play an essential role in maintaining chromosomal integrity and stability. Telomere shortening is part of the natural aging process, nevertheless, accelerated telomere shortening has been linked to chronic diseases and premature aging. Recently, malaria infections have been found to affect cellular aging and lifespan in birds, and telomere shortening was detected in travellers treated for malaria. The aim of this thesis was to study the effect of single and repeated malaria infections on cellular aging in humans, and to explore potential mechanisms underlying telomere attrition during infection.

Within a closely monitored controlled human malaria infection (CHMI) study, we detected that *Plasmodium falciparum* parasiteamia resulted in accelerated TL in peripheral blood, which was fully reversed after treatment and parasite clearance. Moreover, we found a correlation between TL and CDKN2A, a marker of cellular senescence, and identified increased cytokine production and low expression levels of antioxidant enzymes as potential drivers of accelerated telomere shortening during infection.

We further evaluated whether infection driven telomere attrition is synchronized across immune cell-subtypes, or if it is rather cell-type specific. By assessing TL dynamics in peripheral blood mononuclear cells (PBMC) of travellers with acute malaria, we found that TL is largely synchronized across cell types, nevertheless, we identified cell-type specific differences during the course of malaria infection that are likely to reflect the host immune reaction.

Next, we investigated the impact of repeated clinical episodes of malaria and asymptomatic carriage of parasites on telomere dynamics in naturally exposed individuals, living in malaria endemic areas. Studying children with different malaria exposure in Kenya, we did not find evidence of that repeated *Plasmodium* infections in children impact cellar aging by accelerating telomere shortening, however, asymptomatic *Plasmodium* infection seem to have a slightly

positive effect on TL, which requires further studies to provide a comprehensive explanation, in particular the study of TL during immune reactions.

Finally, we explored telomere dynamics in all aged individuals in a longitudinal followed population cohort in Tanzania over a period of three decades. The study provides detailed information on age and sex specific changes in telomere length, revealing that the sex-difference with females having longer TL than males emerges during adolescence and remains throughout life.

Together, this thesis adds fundamental knowledge to the relationship of malaria infection and cellular aging in humans. The work contributes to the expanding field of aging biology by showing a transient effect of acute infection on TL, while identifying inflammation and oxidative stress as contributing mechanisms, and further provides age and sex-specific characteristics of telomere dynamics during different life stages. Future studies are needed in endemic areas to further investigate potential long-term consequences of infectious diseases on aging.

CONTENTS

LIST OF ABBREVIATIONS

ACT	Artemisinin-based combination therapy
AIDS	Acquired immunodeficiency syndrome
DNA	Deoxyribonucleic acid
CAT	Catalase
CDKN	Cyclin dependent kinase
CDKN2a	Cyclin dependent kinase inhibitor 2a
cDNA	Complementary DNA
CHMI	Controlled human malaria infection
CMV	Cytomegalovirus
DDR	DNA damage repair
DNase	Deoxyribonuclease
EBV	Epstein Barr virus
GSTK1	Glutathione S-transferase kappa 1
Hb	Hemoglobin
HCV	Hepatitis C virus
HIV	Human immunodeficiency virus
HRP-2	Histidine-rich protein 2
ICC	Intraclass correlation coefficient
IL-1β	Interleukin 1beta
IL-6	Interleukin 6

IL-8	Interleukin 8
IL-10	Interleukin 10
IL12p70	Interleukin 12p70
IL-17A	Interleukin 17A
IL-18	Interleukin 18
IL-33	Interleukin 33
INF-α	Interferon alpha
INF-γ	Interferon gamma
kb	Kilobase
KEMRI	Kenya Medical Research Institute
LTL	Leukocyte telomere length
MCP-1	Monocyte chemoattractant protein 1
NOS3	Nitric oxide synthase 3
PBMC	Peripheral blood mononuclear cells
PCA	Principal component analysis
PCR	Polymerase chain reaction
pfHRP2	*Plasmodium falciparum* Histidine Rich Protein 2
pLDH	*Plasmodium* Lactate Dehydrogenase
POT1	Protection of telomere 1
PRC	Polycomb repressive complex
qPCR	Quantitative polymerase chain reaction
RAP1	Repressor/Activator protein 1

RDT	Rapid diagnostic test
rRNA	ribosomal RNA
RNA	Ribonucleic acid
ROS	Reactive oxygen species
SASP	Senescence associated secretory phenotype
SOD 1	Superoxide dismutase 1
SOD2	Superoxide dismutase 2
TERC	Telomerase RNA component
TERT	Telomerase reverse transcriptase
TIN2	TRF1-and TRF2-interacting nuclear protein 2
TL	Telomere length
TNF-α	Tumor necrosis factor - alpha
TPP1	Adrenocortical dysplasia protein homolog gene
TRF1	Telomere repeat binding factor 1
TRF2	Telomere repeat binding factor 2
mL	Milliliter
pg	Picogram
µg	Microgram
µL	Microliter

1 INTRODUCTION

Aging is a process that encompasses measurable modifications by both, genetic and environmental factors. As a consequence, understanding factors that accelerate aging is important to improve population health. It is therefore imperative to study and unravel the fundamental aging processes and to gain a more comprehensive picture of aging-related mechanisms, as well as the impact of environmental factors. Advanced biological aging is accompanied by the accumulation of a variety of molecular and cellular deterioration and a gradual decline in immune function, which results in increased susceptibility to age-related pathologies, but also infectious diseases[1]. Moreover, the impact of infectious diseases on aging and long-term consequences on the host need further understanding.

1.1 AGING AND INFECTIOUS DISEASES

Despite medical advances, public health measures, effective vaccines and the availability of antibiotics, infectious diseases remain responsible for a large burden of deaths and morbidity, particularly in Africa. Recent advances in the field of aging have revealed that the relationship of biological age and disease susceptibility is mutual, and suggests that exposure to infectious diseases can accelerate cellular aging[2,3]. Malaria, a vector-borne infectious disease has been investigated in this context and recent studies in animal models have revealed that both, its acute and chronic form affect cellular aging by driving telomere attrition. Nevertheless, a study in travellers suggests accelerated cellular aging after a single acute malaria infection[4]. Yet, not much is known about the effect of acute, multiple or chronic infections on cellular aging in humans, and the underlying cellular and molecular mechanisms are yet to be understood.

In this thesis, we study the effect of single acute malaria infection on telomere length (TL) in a controlled human infection model and in a prospective immunological study in travellers treated for malaria in Sweden, as well as the effect of repeated malaria infection on TL in epidemiological longitudinal study cohorts including children and adults in Kenya and

Tanzania. This thesis provides updated evidence of aging dynamics across life and provides insight into molecular and cellular mechanisms underlying infectious diseases driving cellular aging in humans.

1.2 BIOLOGICAL AGING

Aging is characterized as age-progressive loss of intrinsic physiological integrity, leading to deteriorated physical function, while accelerated aging leads to increased age-specific mortality and decreased lifespan[5]. Age and lifespan characteristics are highly species-specific, despite also showing intra-species variability[6]. While chronological age is defined as years of life since birth, biological age represents the cellular and molecular functionality of the body, including physical and mental capacity. In 2013, Lopez-Odin et al. defined nine tentative hallmarks that represent common denominators of biological aging in mammalian organisms (**Figure 1**).

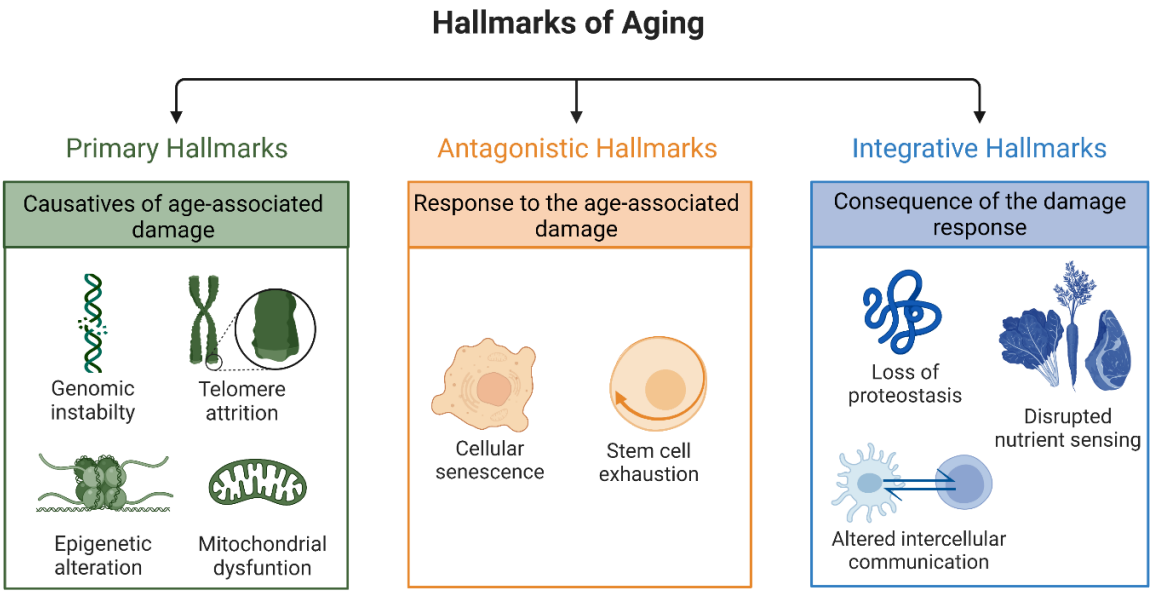

Figure 1. Fundamental hallmarks of aging*. Figure by A. Miglar, designed in BioRender.com, adopted from Lopez-Odin et al., Cell. 2013.*

These nine mechanistic hallmarks can be divided into three categories: 1) Primary hallmarks or causatives of age-associated damage, including genomic instability, telomere attrition,

epigenetic alterations and mitochondrial dysfunction, 2) Antagonistic hallmarks or response to the age-associated damage, including cellular senescence, stem cell exhaustion and in most cases chronic inflammation, and 3) Integrative hallmarks or the consequence of the damage response leading to loss of proteostasis, disrupted nutrient sensing, and altered intercellular communication. The nine hallmark candidates are fundamental pathways expressed during the normal aging process, while alteration and imbalance in their expression provoke accelerated and pathological aging. All hallmarks of aging have been associated with human pathologies, including cardiovascular diseases, cognitive impairments, metabolic dysfunction and cancer[5]. To improve healthy aging in humans, and to target novel pharmaceutic interventions implementing a long healthy life expectancy, the challenge is to dissect the interconnectivity between these hallmarks, including telomere attrition and cellular senescence, and to determine the underlying molecular mechanisms contributing to accelerated aging during disease.

1.2.1 Telomeres

One of the primary hallmarks of aging is accelerated telomere attrition. Telomeres are non-coding tandem repeats of (TTAGGG)n sequences, capping the ends of eukaryotic linear chromosomes[7]. The nucleoprotein-DNA structures play an important role in genome stability and integrity and are well-described biomarkers of biological aging[8]. The end structure of telomeric sequence is characterized by a single stranded G-rich 3´ overhang, which varies in length and exact sequence between organisms[7]. To avoid activation of the DNA damage response (DDR), telomeres protect their single stranded overhang by the formation of a telomere-loop (T-loop), formed by the strand invasion of the 3´-end into the duplex part of the telomeric sequence, further creating a displacement-loop (D-loop) in which the terminal overhang sequence displaces the G-rich strand of the double stranded telomeric sequence (**Figure 2**)[9,10]. The maintenance and protection of this complex structure is provided by the

shelterin complex, a multi-protein complex that consists of six major components (TRF1, TRF2, TIN2, TPP1, POT1 and RAP1)[11].

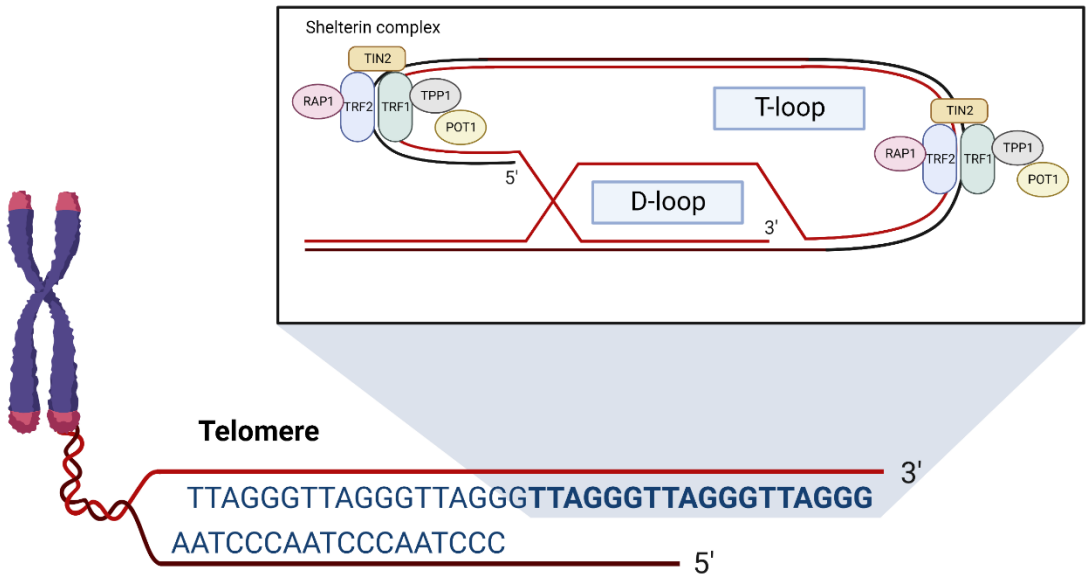

Figure 2. The structure of telomeric sequence and schematic overview of the shelterin complex*. To avoid recognition of the single stranded 3' overhang by the DDR, telomeres form a complex structure, including the incorporation of the single stranded 3' end back into the duplex telomere sequence, forming a T-loop and D-loop. The structure is stabilized by the shelterin complex, which consists of six major proteins. TRF1 and TRF2 bind with high specificity to the telomeric sequence and are bridged by TIN2. TIN2 recruits the molecule TPP1, which recruits POT1. POT1 binds the telomeric overhang and RAP1 presents in a 1:1 complex with TRF2. (Figure by A. Miglar, designed in BioRender.com).*

Telomeres undergo age-dependent incremental attrition, due to the so called end-replication problem, leading to the incomplete synthesis of the lagging strand during DNA replication and thus, to progressive shortening of telomeric DNA[12]. Telomere length and the rate of telomere-loss are substantially inter- and intra-species variable, and are influenced by genetic and environmental factors [13,14]. Telomere length in peripheral blood is at its maximum at birth and decreases progressively with advanced age, therefore being considered as a biomarker of biological age. In humans, the average TL at birth is 11- 15kb (rodents 10 -72 kb; ungulates 7-23 kb; lagomorphs 2-50 kb), including a 3´ overhang of approximately 50-300 nucleotides [14,15].

The average loss of telomeric sequence during the replication process varies between 50-100bp per cell division, however, the rate of telomere loss shows substantial intra-species variation[16] and further depends on the individual's life-stage [14].

Once reaching a critical length, telomeres are associated with cell-deterioration and cell-senescence, a state in which the cell exits the cell cycle and enters irreversible cell arrest or apoptosis[17]. To counteract progressive telomere shortening, germlines and stem cells express telomerase, a holoenzyme composed of two catalytic units, TERT and TERC. TERT is a reverse transcriptase, capable of adding telomeric sequence to the ends of chromosomes, which together with TERC, an RNA molecule carrying an RNA template, promotes restoration and maintenance of telomeric sequence. Despite its variable expression in cells of the immune system[18], telomerase expression is downregulated in most somatic cells, as its overexpression causes uncontrolled cell-proliferation and tumor formation in the majority of cancer types[19].

1.2.2 Telomeres and cellular senescence

The accumulation of short telomeres promotes aging-processes, in particular cellular senescence, which is associated with multiple changes on cellular and molecular levels[20]. By reaching a critical length, telomeres are unable to form the protective T-loop structure and are recognized as double strand breaks by the DDRs, which leads to the cell entering a state of replicative senescence. Cellular senescence was first described by the American anatomists Leonard Hayflick and Paul Moorhead in 1961 and describes the remission of cell proliferation (to a maximum 50 divisions/cell) and induction of stable cell arrest to damaged or aged cells [21]. Senescence plays an important role in embryogenic morphology, while in adults it is mainly a response to cellular damage and dysfunction. With increasing age, senescent cells accumulate in the body and are characterized by distinct phenotypic alterations, including the remodelling of chromatin-structure, metabolic reprogramming, elevated autophagy, and a pro-inflammatory secretome, known as SASP, secreting IL-6 and IL-8 [22,23]. A recent study in mice

revealed that accumulation of senescent cells leads to physical impairment and shortened lifespan[24]. Senescent mediated cell arrest is driven by two major pathways: p16INK4a/Rb and p53/p21CIP1, both leading to repression of CDK 4/6, proteins involved in G1 phase progression of the cell cycle[22]. The protein p16 is encoded by CDKN2A, a gene located on the INK4/ARF locus. In general, cyclin dependent kinases regulate cell-proliferation by driving cell cycle progression, and regulating transcription[25]. In young cells, the gene locus INK4/ARF is epigenetically silenced and controlled by PRC proteins, however, it gets activated by senescence induced inflammation and ROS-mediated DNA damage[22]. The p53/p21CIP1 pathway is activated by DNA segments with chromatin alterations reinforced senescence (DNA-SCARS), leading to p53 activation, which induces transcription of the cyclin-dependent kinase inhibitor p21[22]. Activated p21 levels repress CDK 4/6, leading to hypo-methylation of the tumor suppressor protein Rb and the terminal exit of the cell cycle[22].

1.2.3 Telomeres and the immune system

Vellejo et al. found that during infection, it is in particular immune cells that are susceptible to accelerated telomere shortening and consequently to senescence, due to their high proliferation rate and large production of ROS and inflammation as part of the immune response[26]. Increased age has been shown to have a profound effect on the phenotype, number and functionality of cells triggering the innate and adaptive immune response that include neutrophils, macrophages, natural killer cells, and dendritic cells[27]. The effects of innate immune-senescence are characterized by impaired neutrophil function, such as reduced phagocytic capacity, impaired production of reactive oxygen intermediates, and reduced capacity of intercellular-killing of pathogens[28]. Age-related changes in the abundance of macrophages and dendritic cell-subsets lead to alteration in phagocytic activity, defective activation and decreased chemotaxis and cytokine production, impaired signal transduction and antigen presentation[27,29].

The decrease in functionality in the adaptive immune system has been shown to be impaired with physiological changes in primary lymphoid tissues, including thymic involution and decrease in haematopoietic bone marrow, leading to a decline in T-cell and B-cell generation[30]. Respectively, fewer naïve T-cells ($CD8^+$ and $CD4^+$ T-cells) and B-cells are exported to the periphery of the secondary lymphoid tissue. Changes in the T-cell repertoire of $CD8^+$ cells represent most age-related changes of the adaptive immune system[30]. Increased age leads to a major proliferation-limit of $CD8^+$ T-cells, which was further linked to progressive telomere loss[31]. Furthermore, increased age leads to an oligo-clonal expansion of $CD8^+$ T-cells, which results in an increased accumulation of terminally differentiated, exhausted cells in the peripheral tissue (spleen, lymph nodes, and mucosa-associated lymphoid tissues), reducing space for the few newly generated naïve T-cells[30]. Another consequence of the oligo-clonal T-cell expansion is decreased T-cell memory, a population-shift towards previous encountered antigens, limiting the ability of the $CD8^+$ T cells respond to yet unexposed pathogens[32,33]. The impaired capacity of the T cell repertoire during aging and aging itself leads to a decline in the quantity of serum antibodies, decreased diversity of antibody responses and low affinity antibodies for foreign antibodies, despite no detectable changes in the number of B-cells[34].

1.2.4 Telomeres in human pathologies

After the discovery of the direct relation between TL and chronical aging in 1990 by Harley et al.[35], increasing evidence suggested that telomeres are key-regulators in variable human pathologies, including metabolic, inflammatory and vascular diseases, as well as cancer [36]. Consecutively, TL has been linked to higher mortality in cardiovascular diseases, as shown in a comparative human telomere length study by Cawthon et al. [37]. Besides aging-associated pathologies, shorter telomeres were further linked to infectious diseases, including acute human immunodeficiency virus (HIV) infection[38], Epstein-Barr virus (EBV) infection[39], Hepatitis C virus (HCV) infection[40] and chronic Cytomegalo virus (CMV) infection[41], with HCV and

CMV infection also being significantly correlated to changes in the cellular senescent marker p16INK4a, and in levels of CDKN-inhibitors[42,43]. An experimental bacterial mouse study by Ilmonen et al. revealed that mice with *Salmonella* infection that have longer telomeres in a subset of leukocytes were able to clear infection quicker than infected mice having shorter leukocyte telomere length (LTL)[44]. Similarly, in an experimental human infection study, Choen et al. revealed that TL in overall PBMCs and T cell subsets were associated with an increased risk of acquiring experimental upper respiratory infection. In their study, participants with shorter TL had greater odds of infection, while longer TL in infected volunteers contributed to a decreased risk of developing clinical illness[45].

Studies in animals have further revealed an effect of malaria on biological aging [46,47]. Asghar et al. have shown that chronic asymptomatic malaria infection in birds results in accelerated biological aging, mediated by telomere shortening in whole blood [46]. The observed effect was directly correlated to individual lifespan and fitness, with chronically malaria infected birds living 45% shorter and producing less lifetime offspring than uninfected birds. To elaborate whether the telomere shortening effect is confined to whole blood or rather appears to be synchronized in other body tissues and organs, Asghar et al. performed an experimental bird study, revealing that a single acute malaria infection results in telomere shortening in whole blood and six major organs (liver, lungs, spleen, heart, kidney, and brain) [47]. To translate the results to humans, aging markers were assessed within a one-year longitudinal study of individuals diagnosed and treated for imported malaria, revealing that a single acute malaria infection in humans affects cellular aging dynamics (TL, CDKN2A) in whole blood with apparent recovery upon successful treatment[4]. However, it remains unknown whether TL in these individuals were completely restored and whether it is a specific cell sub-type that is most susceptible to infection driven telomere shortening. To confirm that TL is fully restored after the infection is cleared would require a controlled infection setting with a sample prior to infection. Moreover, as TL is measured in whole blood further studies are needed to reveal if

changes in TL are cell-subtype specific. Importantly, results from the traveller study urge the need to investigate the effect of repeated malaria episodes and persistent asymptomatic infection on cellular aging (similarly to the observation in birds) in populations living in malaria endemic areas, and to investigate whether there are hidden long-term costs from malaria through life.

1.3 MALARIA

Malaria is a vector-borne infectious disease caused by the protozoan parasite of the *Plasmodium* genus. Despite sustained malaria elimination efforts globally, infection by the parasite *Plasmodium* still caused more than 247 million malaria cases worldwide and accounted for 619.000 deaths in 2021[48]. Out of the 84 malaria endemic countries to date, infants and children under five years, pregnant women, patients with HIV/AIDS and non-immune migrants are at considerably higher risk of contracting malaria[48] and of developing severe pathology[4]. In humans, malaria is caused by five *Plasmodium* species (*P. falciparum, P. vivax, P.ovale*, *P. malariae* and *P. knowlesi*). Out of the five species, *P. falciparum* is the most prevalent malaria parasite in the African Region, and also responsible for most morbidity and mortality globally (99.7% of all cases in Sub-Saharan Africa in 2018)[49]. Outside of Sub-Saharan Africa, the most dominating malaria parasite is *P. vivax*. There are 30 anopheline vector species, which can transmit the malaria parasite to humans, with the female Anopheles mosquito being the "carrier of malaria". Transmission of the malaria parasite profoundly depends on the long lifespan of the mosquito species, in addition to climatic conditions, which affect the number of surviving mosquitos and the rate of *Plasmodium* parasites surviving within the mosquito. Transmission is often seasonal and peaks during and after the raining season. In many parts of sub-Saharan Africa, two main malaria transmission seasons occur, following two rain seasons, May-July and September-December[50].

1.3.1 Life cycle of *Plasmodium*

The life cycle of *Plasmodium* starts with an infected female Anopheles mosquito taking a blood meal, inoculating sporozoites into the human host (**Figure 3**). The sporozoites invade the liver, infect hepatocytes, followed by asexually multiplication of the parasite for 7-10 days. *P. vivax* and *P. ovale* have dormant liver stages (hypnozoites) that can be re-activated after weeks, months or years after initial infection [51]. After multiplication, schizonts burst and release multiple merozoites into the blood stream, initiating the asexual erythrocytic stage of the parasite. Within erythrocytes, the parasite undergoes morphological changes, including ring stage trophozoites, schizonts and merozoites. The asexual erythrocytic stage is repeated after approximately 48 hours for *P. falciparum*, *P. vivax* and *P. ovale*, 72 hours for *P. malariae* and 24 hours for *P. knowlesi* hours, and is responsible for the clinical outcome and manifestations of the disease. Some of the immature ring stage parasites leave the cycle of asexual multiplication and differentiate into the sexual stage of the parasite (gametocytes), which circulate in the blood and are crucial for the transmission between human and mosquito. With a female Anopheles taking a blood meal, male and female gametocytes mature into gametes in the mosquito's mid-gut lumen. Fertilized female gametes further develop into ookinetes that break through the mid-gut wall and form oocysts on the exterior surface. When bursting, oocysts release thousands of sporozoites that migrate to the mosquito's salivary glands. The inoculation of sporozoites into a new human host maintains the malaria life cycle and ensures transmission.

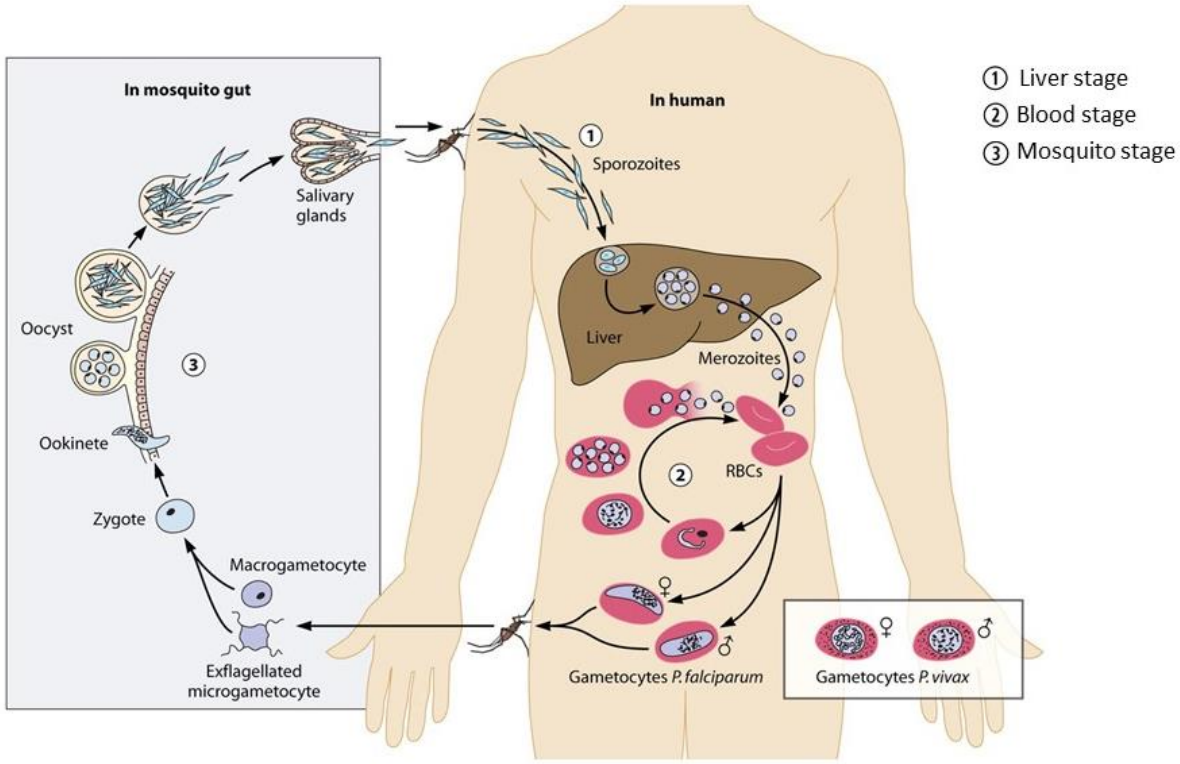

Figure 3. Life cycle of the Plasmodium parasite*. The parasite is released in the form of sporozoites into the human bloodstream when an infected female Anopheles mosquito takes a blood meal. The majority of sporozoites then migrate to the liver, where they invade hepatocytes and multiply. Merozoites are formed and released into the bloodstream, where they invade erythrocytes, initiating the asexual multiplication cycle of the parasite. Some of the merozoites are released from infected erythrocytes form gametocytes, the transmissible parasite form. (Figure adapted from Bousema et al., 2011 with permission of the American Society for Microbiology publishing group).*

1.3.2 Disease pathogenesis and long-term impairments

Plasmodium falciparum infections can be classified as asymptomatic, uncomplicated or severe, with the later form of infection manifesting itself with life-threatening symptoms. Uncomplicated malaria usually manifests itself with unspecific first symptoms, such as fever, nausea, headache, chills and vomiting, 7-14 days after infection. If not treated within 24 hours, uncomplicated *P. falciparum* infection can lead to severe illness, in particular in young children. Complications of severe malaria can include severe anemia, organ failure, pulmonary complications, acidosis, hypoglycaemia, cerebral malaria and death, respectively. Furthermore, the sequestration of infected erythrocytes with later stage- *P. falciparum* parasites into the deep

vasculature can lead to acute organ dysfunction in severe malaria. Currently, efficacious treatment for severe *P. falciparum* infection leads to an apparent complete recovery, however, survivors might suffer long-term impairments, including epilepsy, deficiency in motor function and cognitive impairments in children, and persistent neurocognitive sequel in adults [52-54]. Repeated malaria exposure in endemic areas have further been linked to the development of lymphomas, including Burkitt lymphoma[55]. Asymptomatic infection refers to circulating malarial parasites in the absence of fever or other clinical symptoms and is usually an infection state acquired after having experience multiple episodes that have led to the acquisition of partial immunity. However, asymptomatic infection have been associated with recurrent episodes of symptomatic parasitaemia, chronic anemia, cognitive impairment and co-infection with bacteria and helminths[56]. Furthermore, asymptomatic infection can lead to severe complications during pregnancy, including maternal anemia, accumulation of parasites in the placenta, as well as low birth weight and infant mortality[57].

1.3.3 Diagnostics and treatment

The gold standard for laboratory-based diagnosis of malaria remains microscopy. The method allows for the identification of the parasite species, the stage of the parasite and the quantification of parasite density. The technique requires a few drops of blood, typically obtained from a finger-prick test, to prepare a "thick" (three blood drops) and a "thin" (one blood drop) blood smear. The thick blood smear is used to detect the presence or absence of the parasite, while the thin blood smear usually determines the species of malaria parasite causing infection. The slides are stained with Giemsa or Field and for thin films, cells are chemically fixed with methanol to facilitating parasite detection. The microscopic detection of the parasite is relatively cheap and accessible in rural settings. However, it is very labour intensive and requires a high level of technical skills for preparation and interpretation of the

slides, which might vary between individuals and laboratories [58,59]. Microscopy is thus, a rather insensitive detection method, with the lowest detection sensitivity of ~50 parasites /µL blood.

Within the clinical setting, another developed detection method of malaria has been rapid diagnostic tests (RDTs). RDTs are immunochromatography-based tools that rely on the principle of detecting species-specific antigens (HRP-2, pLDH, and *Plasmodium* aldolase) from the malaria parasite that circulate in the blood of infected individuals. The application requires blood from a finger-prick that will be applied to the assay. If *Plasmodium* antigens are present in the blood, these stick to the band on the assay and form a coloured line in the test area of the assay within 15-30 minutes. RDTs provide rapid low-cost quantitative results on malaria positivity, nevertheless, it cannot differentiate between non -*P. falciparum* species.

Both, microscopy and RDTs are rather insensitive towards the detection of low parasite densities and primarily used for the diagnosis of clinical malaria. For the detection of low density e.g. asymptomatic infections, which account for 80% of all malaria infections in endemic areas, other, more sensitive diagnostic methods have been developed, which are based on nucleic acid amplification[60]. The most prominent is qPCR, which allows for qualitative and quantitative detection of the malaria parasite, as well as identification of the *Plasmodium* species. The qPCR approach is based on the detection of conserved regions of parasite DNA, most commonly encoding the 18S ribosomal RNA and using fluorescent probes that bind to the amplified DNA to facilitate quantification. Compared to RDTs and microscopy approaches, PCR is highly sensitive method, which can detect very low density malaria infections (< 1 parasite/µL) [59].

Once diagnosed with malaria, treatment has to be initiated immediately. The drug regimen used for treatment depends on the clinical status of the patient, the parasite species and the geographical area of acquired infection, as well as pregnancy status. Treatment guidelines are set by the WHO and include all risk groups[61]. The treatment for uncomplicated malaria caused

by *P. falciparum* is generally consists of an artemisinin-based combination therapy. The doses and treatment time are dependent on age and condition. Individuals with severe disease manifestations are commonly treated with intravenous artesunate, followed by artemisinin-based combination therapy[61]. Despite of immediate treatment leading to complete recovery, anti-malarial drug resistance has become a continuous challenge, in particular with resistance to artemisinin-based combination therapy (ACT). Genetic mutations in parasite proteins and particularly, mutations in the parasite genes coding for PfCRT (Chloroquine Resistance Transporter) are the reason why first-line treatments, such as chloroquine are no longer used in areas where *P. falciparum* is dominant[62]. Furthermore, artemisinin –resistant *P. falciparum* parasites have emerged in the Greater Mekong Subregion and in East Africa[49]

1.3.4 Malaria immunology

Partial immunity against malaria can be acquired, which controls disease symptoms and severity, however it is not believed to prevent infections completely[63]. The level of natural acquired immunity develops with age and is dependent on the degree of parasite exposure and the level of transmission[64]. The higher the transmission intensity, the earlier the age of infection, but also, acquired protection and maternal derived immunity[63,65]. Non-sterile immunity in repeatedly exposed children protects against high density parasitaemia and risk of severe disease, while in adults defines the asymptomatic carrier status[63,66]. In contrast, the majority of *P. falciparum* infections in malaria naïve individuals can manifest themselves in clinical symptoms already at low-density parasitaemia [63].

In areas of high and stable *Plasmodium* transmission, immunity to severe disease is acquired roughly within the first five years of life, after that the risk of severe malaria declines gradually with age and is limited to naïve individuals and pregnant women. Yet, complete disease protection is ever achieved, and asymptomatic *Plasmodium* infections remain common in individuals of all age [67]. In low- malaria transmission areas, the disease risk is highest,

particularly during childhood and adolescence[64,68]. Significant associations have been shown between malaria protection and genetic traits in the human host. The hemoglobin genotype AS (HbAS), causative of the sickle trait, is the main host genetic factor that confers resistance to severe and complicated malaria. The mutation causes sickle cell shaped erythrocytes that hinder the parasites invasion, growth and development [69].

1.3.5 Experimental malaria challenge model

Controlled human infection models haven been applied in medical research since the intentional exposure to yellow fever and dengue performed in the early 1900s[70]. Decades later, these infection models became highly regulated standard models in science and are exponentially increasing in implementation worldwide, with controlled human malaria infections (CHMI) being the most frequently practiced[71]. The first CHMI was performed in 1920, as effective treatment for neurosyphilis[72] and has been a standardized model to study malaria pathophysiology and immunology in the Netherlands, the United Kingdom, the USA and more recently also in endemic malaria countries such as Kenya and Gambia. CHMIs have received a central role in developing novel drugs and vaccines, with the bigger aim to prevent disease severity and disease transmission [71,73]. The basic principle of a CHMI is the intentional and closely controlled exposure of healthy individuals to the *Plasmodium* parasite, followed by strict monitoring and prompt treatment. In one of the studies in this thesis, aging markers were studied in volunteers infected by mosquito bites, which mimics the most mature and frequently used model, and resembles the natural life cycle of *Plasmodium* parasites in the human host. During the infections, qPCR was used as standard diagnosis of the malaria parasites, which is highly sensitive and can diagnose the malaria infection 2-4 days earlier than conventional microscopy[71]. Upon detected positive by qPCR, all study participants were treated promptly with a sub-curative treatment.

1.4 THESIS OBJECTIVES

1.4.1 Rationale

Animal models suggest that acute *Plasmodium* infection affects cellular aging by accelerating telomere shortening in multiple body tissues, and that chronic exposure leads to long-term impairments, such as reduced host fitness and lifespan[46,47]. In human, a study in travellers revealed a transient effect of a single acute malaria infection on cellular aging[4]. Nevertheless, the potential underlying molecular mechanisms remain largely unknown and whether TL is completely restored after treatment and recovery needs to be determined.

Furthermore, in addition to the findings in birds, results from the traveller study urge the need to evaluate the effect of repeated clinical malaria episodes and asymptomatic infections on TL in populations living in malaria endemic areas, as well as possible long-term consequences.

In this thesis, data is analyzed from a CHMI model to underpin infection driven changes in telomere dynamics, to explore potential underlying mechanisms involved and to evaluate cell-specific responses to acute malaria infection. Secondly, we take advantage of large cohort studies of all aged individuals living in malaria endemic areas to investigate the impact of malaria infection on cellular dynamics and to explore telomere dynamics across life.

1.4.2 Aims

I. To evaluate the relationship of TL and other hallmarks of aging, including pro-inflammatory cytokines and antioxidant defence enzymes during an induced *P. falciparum* infection (**Chapter 3**).

II. To explore whether infection driven telomere attrition is a synchronized process across immune cell types or if it is rather cell-type specific in travellers treated for malaria (**Chapter 4**).

III. To determine whether TL dynamics are affected by the level of malaria exposure in children living in a malaria endemic area (**Chapter 5**).

IV. To study TL dynamics across all aged individuals and to assess whether repeated malaria exposure and asymptomatic infections cause long-term consequences on cellular aging in individuals living in a high malaria transmission area (**Chapter 6**).

1.4.3 Study outline

Chapter 3: Analyses of cellular and molecular responses to a CHMI in previously malaria naïve individuals

Chapter 4: Cell-specific telomere dynamics in adults with naturally acquired acute malaria infection

Chapter 5: The effect of repeated symptomatic and asymptomatic malaria infections on telomere length in longitudinally followed children in Kenya

Chapter 6: Long-term consequences of symptomatic and asymptomatic malaria on cellular aging in a three-decade longitudinal cohort study in Tanzania

2 MATERIALS AND METHODS

2.1 STUDY DESIGN

This thesis includes four chapters based on four studies of prospectively, closely monitored and longitudinally followed cohorts of individuals exposed to different degrees of malaria infection.

2.2 STUDY POPULATIONS

The study populations consist of: **Chapter 3)** a CHMI cohort of adult volunteers, recruited at the Radboud University Medical Center, Nijmegen, the Netherlands, **Chapter 4)** a prospective immunological cohort of travellers treated for malaria at the Karolinska University Hospital in Stockholm, Sweden, **Chapter 5)** a longitudinal cohort of children in Junju and Ngerenya, Kilifi District, Kenya and **Chapter 6)** a longitudinal cohort of all-aged individuals in Nyamisati, the Rufiji River Delta region in Tanzania. A detailed description of each study cohort including ethical considerations is outlined in the respective study chapters.

2.3 LABORATORY METHODS

2.3.1 Malaria diagnostics

Methods for diagnosing malaria varied between chapters and brief descriptions of the procedures are outlined in each study chapter individually. Some work was performed as part of collaborative study procedures from which data is incorporated in this thesis. An overview of study-specific diagnostics of the *Plasmodium* parasite is provided in **Table 1**.

Table 1. Overview of malaria diagnostic methods used in individual studies.

Diagnostic tool	Thesis chapter	Cohort	Short description of the method
Light microscopy	Chapter 4 Chapter 5 Chapter 6	Traveller Junju and Ngerenya Nyamisati	Light microscopy of Field or Giemsa stained thick and thin blood films
qPCR	Chapter 3 Chapter 5 Chapter 6	CHMI Junju and Ngerenya Nyamisati	qPCR targeting the ribosomal subunit of the 18S gene, which is conserved across all *Plasmodium* species
RDT	Chapter 5 Chapter 6	Junju and Ngerenya Nyamisati	Chromatographic methods to detect pfHRP2 and pLDH in blood obtained from a finger-prick

2.3.2 Quantitative real time PCR (qPCR)

2.3.2.1 Plasmodium prevalence and species identification by qPCR

Parasite prevalence and species identification in **Chapter 6** was based on qPCR, referring to the protocol by Shokoples et al.[74]. The master mix for a single reaction included fluorophore-labelled probes and species-specific primers for four *Plasmodium* parasites (*P. falciparum*; *P. ovale*; *P. vivax* and *P. malariae*) used in combination with a conserved reverse *P. falciparum* primer (**Table 2**). A single reaction consisted of 25 µl, including 12.5 µl TagMan universal master mix, 0.5µl of each species-specific forward primer and the conserved reverse primer, 0.25µl of each probe and nuclease-free water. The thermal profile was the following: 20s at 95°C, followed by 45 cycles of 95°C for 1s and of 60°C for 20s. A serially diluted sample (10^{-1} to 10^{-5}) containing 0.01% *P. falciparum*-parasitaemia was used as standard and positive control for *P. falciparum*. All samples, standards, positive controls, and negative controls were placed on a 96-well-plate and ran in duplicates. Analyses were performed on the Thermo Fisher Scientific Cloud software. A cutoff of 40 cycles was used to define positive samples

Table 2. Primer sequences for species-specific qPCR and TL qPCR.

Species	Primer/Probe	Yield (nM)	Sequence (5'-3')	Supplier
Plasmodium spp.	reverse primer	200	AAC CCA AAG ACT TTG ATT TCT CAT AA	Biosearch Technologies
P. falciparum	forward primer	200	CCG ACT AGG TGT TGG ATG AAA GTG TTA A	Applied Biosystems
P. vivax	forward primer	50	CCG ACT AGG CTT TGG ATG AAA GAT TTT A	Applied Biosystems
P. ovale	forward primer	50	CCG ACT AGG TTT TGG ATG AAA GAT TTT T	Biosearch Technologies
P. malariae	forward primer	50	CCG ACT AGG TGT TGG ATG ATA GAG TAA A	Biosearch Technologies
P. falciparum	probe	80	Quasar 670-AGC AAT CTA AAA GTC ACC TCG AAA GAT GAC T-BHQ-2	Applied Biosystems
P. vivax	probe	80	TAMRA-AGC AAT CTA AGA ATA AAC TCC GAA GAG AAA ATT CT-BHQ-2	Applied Biosystems
P. ovale	probe	80	VIC-CGA AAG GAA TTT TCT TAT T-MGBNFQ	Biosearch Technologies
P. malariae	probe	80	FAM-CTA TCT AAA AGA AAC ACT CAT-MGBNFQ	Biosearch Technologies

2.3.2.2 Telomere length measurement

Telomere length was assessed in real-time by qPCR in all studies, following the principle described in Cawthon et al.[75] and Pfaffl et al.[76]. The high-throughput method estimates the amount of telomeric DNA sequence in a sample (T), relative to the amount of a single-copy gene sequence (S), which is equal to the relative change in telomere and single-copy gene sequences ($\Delta C_T = C_T$ (telomere) $/C_T$ (single-copy gene)). In this thesis, we use the single copy gene human β2-globulin (HBG). A telomere-specific amplicon set of primers (*T1, T2*) was used to quantify TL together with a single-copy gene amplicon set of primers (*S1, S2*), to control for total amount of DNA in each reaction[75]. Primer sequences are described in **Table**

3. Two master mixes of PCR reagents were prepared, one with the T primer pair, the other with the S primer pair. Each PCR reaction was prepared in a 25 µl final volume to the following concentrations: 1 × Platinum® Quantitative PCR SuperMix-UDG (Invitrogen, cat # 1730025), 0.1 pmol of each primer; 0.1x ROX reference dye (Invitrogen, cat # 12223012) and 5 µl of template DNA with a concentration of approximately 2 ng/µl. Primer sequences for *T1*, *T2* are presented in the table below. Extracted DNA was diluted to 2 ng/ul using dd water.

Telomere (T) PCRs and single copy gene (S) PCRs were performed in separate 96-well plates, with matching row and column coordinates to achieve the lowest variability in the T/S ratio. A standard curve was generated by performing serial dilutions (10^{-1} to 10^{-5}) of a randomly selected sample, and a human genomic DNA reference (2.5ng/ µl) was included on each plate to control for intra-plate variability. To avoid inter-plate variability, all samples from a single individual were placed on the same plate. All samples, standard dilution, reference sample and negative control (nuclease free water) were run in duplicates for each primer set, and each primer set was run on a separate plate. Quantity values were standardized across the plates by dividing them by the plate value of the reference sample to obtain plate adjusted amounts of telomere and single copy gene sequence. A cut-off for qPCR runs was set with a PCR efficiency of 100 ±15%. The mean C_T of duplicates was used as final data for analysis.

Thermal profile of the qPCR included a 2 min incubation period at 50 °C, and activation of the polymerase for 10 min at 95 °C, followed by 30 cycles of 95 °C for 15 s, 53 °C for 45 s and 72 °C for 45 s for the T primer set, and 40 cycles for the S primer set. To validate the specificity of the PCR product, we included a melt curve step at the end of each reaction following the thermal profile of 95 °C for 15 s, 62 °C for 1 min and 95 °C for 10s.

Relative TL were calculated using the $\Delta\Delta C_T$ method according to Cawthon et al.[75]. Some studies included in this thesis corrected for the PCR efficiency according to Pfaffl et al. [76] prior to calculating relative TL, which is mentioned in the respective study chapter. Telomere length

in kb was calculated using a human genomic DNA reference of known length that was included on each TL and single copy gene run and calculated as follows: relative ($2^{-\Delta\Delta C_T}$ value) × gDNA (kb) sample. The TL of a diploid cell was then divided by the number of chromosome ends (92) to receive the average TL at each chromosome end (($2^{-\Delta\Delta C_T}$ × gDNA(kb))/92). Analyses were performed in the Thermo Fisher Scientific Cloud software.

Table 3. Primers used for TL measurement by qPCR. *T for telomere and S for single-copy gene (HBG).*

Primer	Concentration (nM)	Sequence (5'-3')	Supplier
T forward	14.1	GGTTTTTGAGGGTGAGGGTGAGGGTGAGGGTGAGGGT	Eurofins genomics
T reverse	12.6	TCCCGACTATCCCTATCCCTATCCCTATCCCTATCCCTA	Eurofins genomics
S forward	27.7	GCTTCTGACACAACTGTGTTCACTAGC	Eurofins genomics
S reverse	28.5	CACCAACTTCATCCACGTTCACC	Eurofins genomics

2.3.3 Cytokine LEGENDplex™ assay

A LEGENDplex Multi-Analyte Flow Assay Kit was purchased from Biolegend to simultaneously analyze the levels of IL-1β, IFN-α2, IFN-γ, TNF-α, MCP-1 (CCL2), IL-6, IL-8 (CXCL8), IL-10, IL-12p70, IL-17A, IL-18, IL-23, and IL-33 in citrate-plasma. The principle of this method is based on a bead-based multiplex immunoassay, following the principle of sandwich immunoassays. The technology uses a customized human inflammation panel in combination with fluorescence-encoded beats for the use on flow cytometers. The assay was performed by our collaborators at the Radboud University Medical Center and details about the procedure are provided elsewhere[77].

2.3.4 PBMC isolation and preparation

2.3.4.1 PBMC isolation from human peripheral blood

Approximately 18 mL whole blood was diluted 1:1 with RPMI medium. A 50mL Leucosept tube was prepared with 15mL (0.5 x V) of Ficoll-Paque and centrifuged at 1000 G for one minute. The diluted blood was poured on top of a Leucosep filter and centrifuged at 800G for 15 minutes at room temperature without breaking at the end.

Next, the upper layer of plasma was removed using a Pasteur pipette, leaving the lymphocyte layer undisturbed at the interface. The mononuclear cell layer was removed and retained without disturbing erythrocyte/granulocyte pellet, followed by a resuspension in approximately three volumes of RPMI medium (2%FCS). After resuspension, the cell pellet was centrifuged at 300G for 10 min at room temperature, and the supernatant was discarded. The cell pellet was resuspended in 15 ml (0.5xV) of RPMI 2% FCS medium and centrifuged at 300G for 8 minutes at room temperature. The last two steps were repeated in 4mL of RPMI 2% FCS medium.

To determine the cell count of isolated PBMC, 10µl of the cell suspension were mixed 1:10 with Tryptan blue stain, and 10µl of this mixture were applied to a Burker chamber. The total number of cells in the sample was calculated by using the following formula : *Mean n cells in 4 squares x dilution (1 :10) x cell suspension volume in ml x* 10^4*).*

In the final step, the cell pellet was resuspended in an equal volume of RPMI 2% FCS and freezing medium (FCS + 20% DMSO) and stored in -80˚C overnight, before being transferred to liquid nitrogen (-155˚C). Each PBMC sample used in this study contained approximately five million cells/mL

2.3.4.2 PBMC preparation for cell sorting

Frozen PBMC vials were thawed by submersion in a 37°C water bath for approximately five minutes and the liquid transferred to a 5mL Falcon tube. 1 mL of PBS + 2% FBS + 2mM

EDTA was added, followed by a 30 min incubation at 4°C. Falcon tubes were centrifuged at 1500 rmp in 4°C for 5 min and supernatants were discarded. The cells were washed once more in 2 ml PBS. 300 µL of aqua fluorescent dilution (1µL of Aqua dead cell dye + 599µL of PBS) was added to each Falcon tube, followed by incubation of 20 min on ice and another washing step. Following another washing step in 1mL of PBS 2% FBS, the cells were stained with 70 µL of cell-specific fluorescent mix and incubated for 20 min on ice. The liquid was transferred to a Falcon tube with cell-strainer cap, centrifuged for 5 min in 4°C at 1500 rmp, and cells were suspended in 500 µL of PBS 2% FBS. Cells were sorted by flow cytometry on a BD Bioscience influx sorter (6-way sorter) and data were analyzed in FlowJo version 10.6.2 (TreeStar Inc). Cell-specific surface markers and gating strategies are found in **Chapter 4**, in section 4.3.3.

2.3.5 DNA extraction

DNA extraction procedures in this thesis varied between studies, as samples in **Chapter 3** and **Chapter 5** were processed at collaborative research facilities and samples in **Chapter 4** and **6** in our own laboratory. Nevertheless, all DNA samples for each individual study cohort were extracted using the same DNA extraction procedure, utilizing a single protocol, and thus, do not affect the individual study outcomes. Study specific DNA extraction methods are described in the respective study chapter.

2.3.6 RNA extraction and cDNA synthesis

RNA was isolated from total nucleic acid using the RNeasy Mini kit provided by Qiagen. To avoid DNA contamination, an additional DNase treatment-step was added, using the TURBO DNA-free Kit (Thermo Fisher Scientific). Quantification was carried out by fluorometric detection, using the Qubit RNA High Sensitivity (HS) assay (Invitrogen, Thermo Fisher Scientific). The cDNA synthesis was performed on approximately 100-150 ng RNA using the SuperScript VILO cDNA synthesis kit (Invitrogen, Thermo Fisher Scientific). For each reaction, 4 µl of SuperScript VILO reverse transcription master mix, 15 µl of extracted RNA

and 1 µl nuclease-free water were added per reaction in a 96-well PCR plate. Thermalcycling was performed on a QuantStudio 5 (Thermo Fisher Scientific) under the following conditions: 25°C for 10 min, 42°C for 60 min, 85°C for 5 min. cDNA was then stored at -20°C until further use.

2.3.7 Gene expression assays

Gene expression analysis was performed in real-time by multiplex qPCR on a QuantStudio 5 Real-Time PCR system (Applied Biosystems), using the cDNA processed in section 2.3.6. TagMan™ gene expression assays including pre-designed primers and pre-designed dye-labelled TaqMan™ probes for our genes of interest. Glyceraldehyde 3-phosphate dehydrogenase (GAPDH) was included in every assay as endogenous control. Reactions were set up with: 10 µl TagMan™ Universal Master mix (Thermo Fisher Scientific), 0.5µl TaqMan GAPDH expression assay, 0.5 µl TaqMan gene expression assay, 7 µl nuclease-free water and 2 µl cDNA. Thermocycling was performed under the following conditions: 20s at 95°C, followed by 45 cycles of 1s at 95°C and 20s at 60°C. The relative gene expression levels were calculated by applying a comparative calculation model $(\Delta C_T)^4$, in which the mean C_T value of the reference gene is subtracted from the mean C_T value of the genes of interest ($\Delta C_T = C_T$ Target-C_T GAPDH). The corresponding ratio refers to "expression of gene of interest".

2.4 STUDENT CONTRIBUTION TO THE INDIVIDUAL STUDIES

The research questions and design of the studies and experiments included in this work were defined jointly with the supervisors, the research group, and our collaborators. For all studies, the samples had already been collected within longitudinal studies. In the study on travellers in Stockholm (Study II, **Chapter 4**), I contributed to the processing of samples, including PBMC preparation. For all studies, I have contributed to the experimental set-up, and performed the laboratory analyses independently, including: 1) RNA and DNA extraction from total nucleic acid 2) RNA and DNA quantification 3) cDNA conversion 4) real-time PCR (qPCR) for

telomere measurement 5) data collection and documentation 6) relative gene expression assays 7) telomere length calculations upon supervision. For Study III (**Chapter 5**) the study design and all laboratory work with TL assays was performed by myself at the KEMRI, Kenya, where DNA was available. In Study IV (**Chapter 6**), I also performed species-specific multiplex PCR for parasite detection. In Study II (**Chapter 4**), FACS sorting of PBMCs into cell sub-populations, was performed jointly and under supervision. The measurement of cytokine levels and standard biochemical blood tests in Study I (**Chapter 3**) was performed by the study collaborators at the Radboud University Medical Center, Nijmengen, the Netherlands.

I have actively participated in the data analysis with supervisors and statisticians from the Biostatistics Core Facility at Karolinska Institutet, I have written all manuscript drafts upon supervision and generated all figures and graphs included. As the corresponding author of Study I (**Chapter 3**), I have contributed in selecting the journal for publication, in writing the cover letter and in writing the revised version and the rebuttal letter, to address the reviewer's response.

3 ANALYSES OF CELLULAR AND MOLECULAR RESPONSES TO A CONTROLLED HUMAN MALARIA INFECTION IN PREVIOUSLY NAÏVE INDIVIDUALS

3.1 AIM

The aim of this chapter was to investigate TL and other hallmarks of aging, including pro-inflammatory cytokines and antioxidant defence enzymes during an induced *P. falciparum* infection.

3.2 BACKROUND

With the given background and evidence of acute malaria infection affecting telomere dynamics in humans[4], it is important to acquire comprehensive understanding of the underlying cellular and molecular mechanisms involved in infection-driven telomere shortening, and to evaluate whether the effect is transient or remains after clearance of the infection.

Studying cellular aging dynamics in disease optimally requires a sample prior to disease and a well-controlled study setting. In natural infections, individuals are generally included at the time of ongoing infection and clinical presentation, while the duration of the infection can differ substantially between individuals, and for malaria, this is further dependent on the degree of parasite exposure and transmission[78]. In human malaria studies, another challenge to overcome is the high inter-species and spatio-temporal variation in telomere dynamics [79].

The focus of this chapter is on evaluating the significant interplay of telomere length, pro-inflammatory cytokine expression and antioxidant enzymes during an experimental malaria infection, and on investigating the relative relationship of telomere length and cellular senescence. This builds on results by Asghar and colleagues[4], who studied telomere length in travellers with naturally acquired acute malaria, prospectively followed over 12-month after successful treatment in Sweden. However, the study recruited patients with an ongoing acute clinical malaria infection and did not include a sample prior to infection. Here, data are

presented from a controlled human malaria infection study (CHMI) in healthy volunteers, providing insights into telomere dynamics and cellular senescence before, during and after a single malaria infection.

The chapter first describes the CHMI cohort and infection procedure, followed by study-specific methods. An analysis is then presented on the effect of *P. falciparum* on TL, followed by the inter-correlation of TL, cellular senescence and aging related mechanisms, and overall changes in study variable across the CHMI.

3.3 STUDY -SPECIFIC METHODS

3.3.1 Study population and controlled malaria infection

The CHMI was conducted between June and November 2015 at the Radboud University Medical Center. The samples were stored at -80˚C until shipped on dry ice to the Department of Medicine, Solna, Karolinska Institutet in 2017, where they were stored at -80˚C until analyses.

The CHMI study included 16 healthy malaria naïve Dutch volunteers, aged 18–35 years. Each of the study participants provided a complete medical history and a report including physical examination, blood hematological and biochemical parameters, serology for HIV, hepatitis B and C, and asexual *P. falciparum* levels [80]. Participants were infected with the *Plasmodium* strain NF54/3D7 by the one-time exposure to five infected *Anopheles stephensi* mosquitos[81,82], and followed over 64 days, respectively (**Figure 4**). Parasite levels were monitored by qPCR twice daily upon day six post infection. A sub-curative treatment (500 mg/25 mg sulfadoxine–pyrimethamine or 480 mg of piperaquine phosphate) was administered upon parasite density reaching ≥ 5000 Pf/mL (1E-04 % iRBC). With the administration of a second sub-curative treatment upon parasite density reaching ≥ 1500 Pf/mL (0.4E-04% iRBC), monitoring was pursued daily for three days, followed by three times a week until the final treatment with curative regiment of atovaquone/proguanil on day 42 post infection[83,84]. Participants continued

being monitored until 64 days post infection and blood samples were collected on every respective visit. The study reported no adverse events[77].

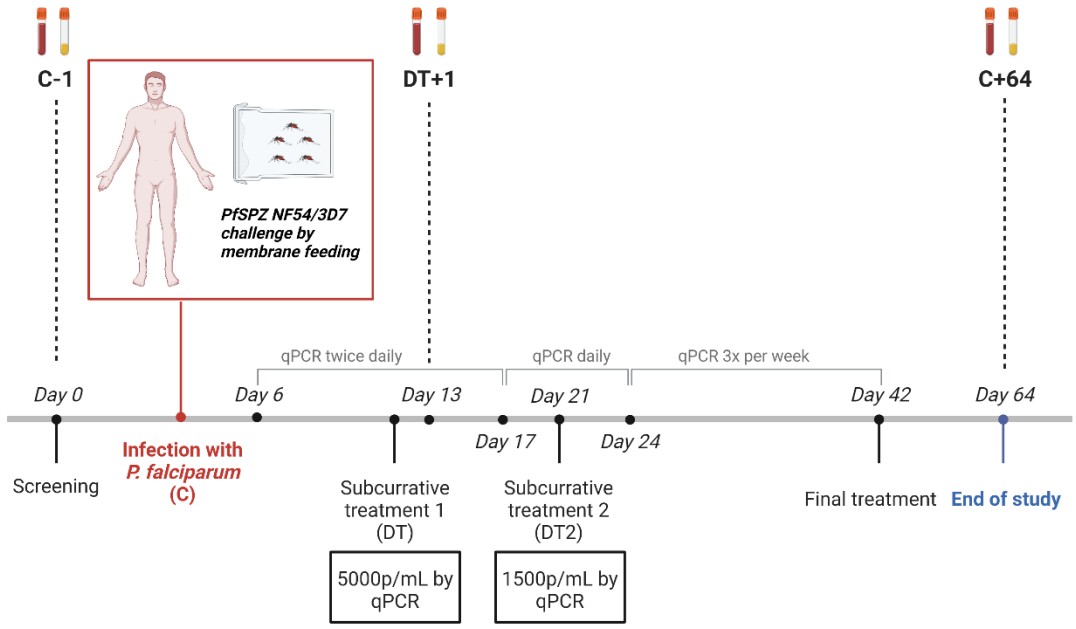

Figure 4. Controlled malaria infection outline and sampling time-points. *Sampling of blood and citrate-plasma is indicated by collection tubes above each time-point. (Figure by A. Miglar, designed in BioRender.com).*

3.3.1.1 Ethical approval

The CHMI was conducted at the Radboud University Medical Center, Nijmengen, the Netherlands. The trial was sponsored by the responsible party Radboud University Medical Center and lead by the principle investigator Prof. Robert Sauerwein and Dr. Isaie Reuling. The trial consortium consisted of the Radboud University Medical Center, The PATH Malaria Vaccine Initiative (MVI), and the QIMR Berghofer Medical Research Institute.

The ethical approval for this trial was granted by the Central Committee for Research Involving Human Subjects of The Netherlands CCMO (NL56659.091.16). The informed consent in this clinical research trial refers to a fully free decision or agreement for research participation following disclosure of relevant information (related to the value of participation, the

procedures to be performed, the potential risks and benefits of participation and the alternatives to participation, among others) and was given by all study participants. The ethical approval for the trail was approved by the Central Committee for Research involving human subjects (CCMO) located in the Netherlands, and the Western Institutional Review Board (WIRB) located in the USA.

The study procedure corresponds to the principles expressed in the Declaration of Helsinki and Good Clinical Practice standards, and all applied methods were carried out in accordance with relevant guidelines and regulations. The trial is registered on the clinicaltrials.gov registry under the identifier NCT02836002.

3.3.2 DNA extraction and quantification

DNA was extracted as total nucleic acid from blood samples from the 16 study participants and their respective 29–31 time-points at the collaborator's site, using an automated extraction system (MagNA Pure LC Total Nucleic Acid Isolation Kit, Roche Diagnostics).

3.3.3 RNA extraction and cDNA synthesis

RNA was isolated from total nucleic acid at Karolinska Institutet for all study participants at the three study time-points C-1, DT+1 and C+64, and converted to cDNA as described in section 2.3.6.

3.3.4 Telomere length measurement

Telomere length was measured in 481 whole blood samples collected from the 16 study participants and all their respective follow-up time-points, following the protocol described in section 2.3.2.2.

Telomere length in kb was calculated using a human genomic DNA reference of 515 kb (# 8918d; Science Cell), resulting in the final calculation of $((2^{-} \Delta\Delta C_T \times 151)/92)$. A human

genomic DNA reference sample was included in the qPCR run of 92 samples and extrapolated for all other samples based on the formula (T/S ratio 1 = 538 bp). Inclusion of gDNA sample on every qPCR plate (n = 24) resulted in non-significant variation in quantitative values. The qPCR runs demonstrated high intra- and inter-plate repeatability (ICC > 0.98).

3.3.5 Parasite detection

Samples were confirmed malaria parasite positive by qPCR targeting the highly conserved, multicopy 18S ribosomal RNA gene of the *P. falciparum* parasite in our collaborative laboratory in the Netherlands, following the protocol described in Hermsen et al.[85]. The sequence of primers and probe were 100% homologous with the sequence of the *P. falciparum* strain 3D7 that was used in the CHMI[85].

3.3.6 Expression of inflammatory cytokines, antioxidant enzymes and CDKN2A

Following the procedure described in section 2.3.7, gene expression analysis was performed for CDKN2A, TERT and the antioxidant enzymes SOD 1 and SOD2, NOS3, CAT, and GSTK-1 for all study participants at the three study time-points C-1, DT+1 and C+64. A list of the target genes and TaqMan™ Assay IDs is shown in **Table 4**. Each assay included the gene GAPDH labelled with JUN as endogenous control, and the gene of interest labelled with FAM.

Table 4. Commercial gene expression assays for antioxidant enzymes included in the study.

Gene	TaqMan™ Assay ID	Reference dye	Supplier
GAPDH	Hs02786624_g1	JUN	Thermo Fisher Scientific
TERT	Hs 00972650_m1	FAM	Thermo Fisher Scientific
CDKN2A	Hs 00923894_m1	FAM	Thermo Fisher Scientific
SOD 1	Hs 00533490_m1	FAM	Thermo Fisher Scientific
SOD 2	Hs 00167309_m1	FAM	Thermo Fisher Scientific
NOS 3	Hs01574665_m1	FAM	Thermo Fisher Scientific
CAT	Hs00156308_m1	FAM	Thermo Fisher Scientific
GSTK-1	Hs01114170_m1	FAM	Thermo Fisher Scientific

3.3.7 Statistical analysis

To investigate the relationship between TL and individual host factors in this study, a linear mixed-effect model with cubic regression splines was performed. Host factors including age, sex, and weight and treatment regimen were included when performing the models. To control for inter-individual variation and repeated measurements, individual ID was added as a random factor to the model. Time was modelled as independent variable and defined with 'knots' to stratify continuous data on TL into data-segments, constricted by linear data distribution before, and after each knot. To account for the effect of each host factor on TL and for the joint effect of host factors on TL, univariate and multivariate mixed models were performed separately.

Paired t-tests were performed to evaluate changes in telomere dynamics, cytokine levels and levels of antioxidant enzymes across the study time-points C-1, DT+1 and C+64. For this approach all values were log-transformed due to non-linearity.

Next, a Spearman's correlation model was applied to determine the inter-correlation of study variables and the direction of correlation.

A hierarchical clustering analysis was performed next to obtain a dendrogram that assembles variables based on similarities across the study time-points (C-1, DT+1 and C+64).

Further, a PCA was performed to form smaller subsets of linear combinations of study variables that explain most variation in the data. In this model, each linear combination corresponds to a principal component, with the component showing the highest Eigenvalue explaining the highest variance in the data. Our PCA resulted in three PC axes with Eigenvalues >1. These axes were further used to perform Factor analysis to use the individual Factor values on each of the three axes as dependent variable in a cubic spline mixed model to investigate how our values varied as a function (time, age and sex).

T-tests, mixed effect models and PCA were performed in the Stata statistic software, version 15 (StataCorp. 2017, Stata Statistical Software: Release 15. College Station, TX: StataCorp LLC).

Spearman's correlation models and visualization of the results were done in R statistic software, version 4.1.2 (R Core Team (2020). R Foundation for Statistical Computing, Vienna, Austria. URL: https://www.R-project.org/)[86].

3.4 RESULTS

This study was published in the open access journal *Scientific Reports* in 2021 (Miglar et al., Sci Rep. 2021 Sep 21; 11(1):18733. doi: 10.1038/s41598-021-97985-y) and is included in the Appendix of this thesis with the permission of the Nature Portfolio.

3.4.1 Characteristics of study population

All 16 previously malaria naïve volunteers who underwent CHMI were included for analysis. The participant characteristics are summarized in **Table 5** and details on the number of measurements per participant is described in **Table S1**.

Table 5. Characteristics of study population.

Characteristics	(n=16)
Sex - n (%)	
Male	4 (25)
Female	12 (75)
Age - years	
Median	22
Range	20 - 29
BMI - kg/m^2	
Median	23.6
Range	18 - 29.4

Telomere length was measured in peripheral blood collected on 29- 31 days per participant (**Table S1**). There was no significant effect of age, weight or anti-malaria regiment (**Table 6**). However, female participants had longer TL than male participants, which remained significant throughout the entire follow-up. Overall mean TL for females was 13.79 kb (SD 3.67; 95% CI 13.41–14.17) compared to males 10.88 kb (SD 2.84; 95% CI 10.37–11.39, two-sample t-test $_{t1,261} = 9.01$, $p < 0.001$).

Table 6. Association of host factors and TL during the CHMI.

	Univariate analysis				Multivariate analysis			
Parameters	**Coef.**	**SE**	**Z**	**p-value**	**Coef.**	**SE**	**Z**	**p-value**
Time	0.023	0.008	2.71	0.007				
Time Spline1					-0.053	0.024	-2.16	0.031
Time Spline 2					0.117	0.035	3.30	0.001
Age (Years)	-0.255	0.236	-1.08	0.281	-0.369	0.224	-1.65	0.099
Female	2.919	1.388	2.10	0.035	2.889	1.394	2.07	0.038
Weight (kg)	-0.064	0.067	-0.95	0.343	-0.05	0.074	-0.68	0.499
Treatment	-0.461	0.604	-0.76	0.446	-0.601	0.624	-0.96	0.335

Parasitaemia was measured by qPCR between day 6 (coinciding with *P. falciparum* entering the erythrocytic life cycle) until receiving the final treatment at day 42 post infection. The median time to day of the first sub-curative treatment +1 (DT+1) was 12 days (range: 9 – 13 days), with parasite levels reaching a median of 15650 p/mL blood (range: 2140 – 107000 p/mL). After administration of the second sub-curative treatment, a median of 21 days (range: 15 – 21), all study participants were qPCR negative (**Figure 5**). Peak parasiteamia was measured by qPCR after a median of 13 days (range: 10 - 13 days), reaching a median of 22092 p/mL blood (range: 2435 – 107000 p/mL), corresponding to a median of 0.0005% infected red blood cells (iRBC), which is much lower compared to clinical malaria, where the levels of iRBC usually reach >0.1%. No serious adverse events were reported during the entire study period[77].

3.4.2 Transient effect of *Plasmodium falciparum* malaria on telomere length

During the 64-day follow-up period post malaria infection, TL dynamics significantly changed over time (Wald $\chi2 = 26.13$, N = 139, $p<0.001$; **Figure 5A**). Concurrent with peak parasitaemia occurring roughly after 11.5 days post infection and a median of 22092 parasites per mL blood

(p/mL), corresponding to a median of 5.5E-05% infected red blood cells (iRBC), TL decreased on average 0.34-fold compared to the day before infection and was negatively correlated with parasite density (lme; p<0.006, **Figure 5B**). After parasite clearance 64 days post infection, TL restored in all study participants with an average of 0.91-fold increase compared to the day of peak parasitaemia (**Figure 5A**).

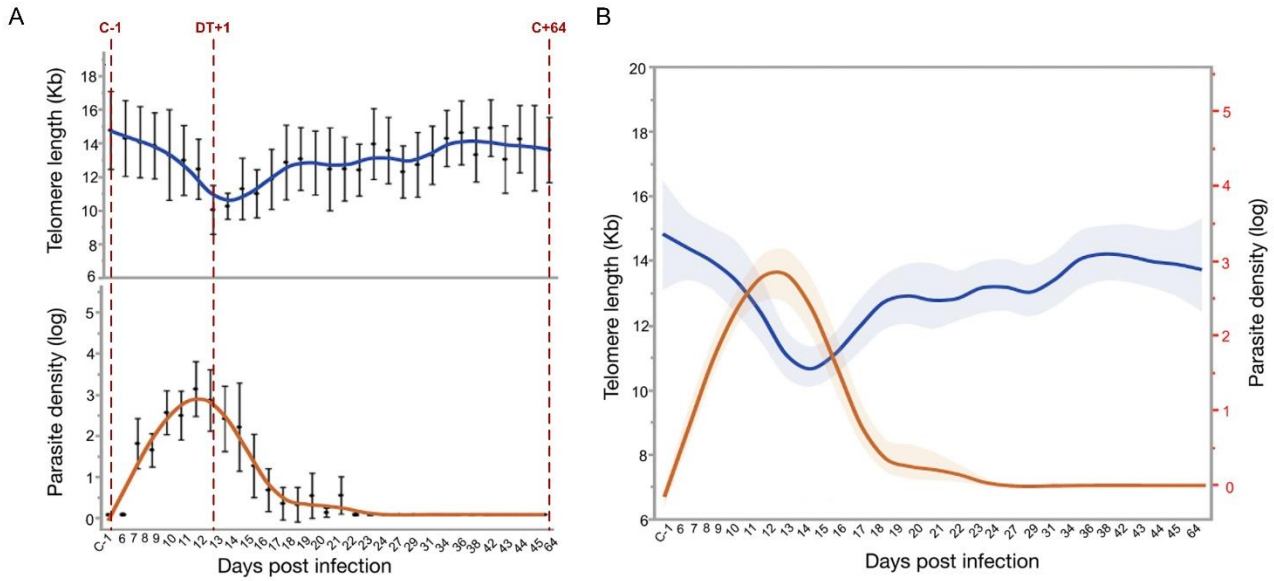

Figure 5. Dynamics of TL dynamics (kb) and parasite density during the CHMI. *A) Telomere length dynamics in kb during CHMI. Arrows indicate the study time point prior infection (C-1, base line sample), day post first sub-curative treatment (DT+1) and time of end treatment/ end of study (C+64). (B) Log values of P. falciparum parasite density (p/mL blood) during CHMI, peak parasite density was observed during day 11-12. Solid blue and orange lines represent predicted means, with black dots representing the detected mean value at each time point. Error bars denote the 95% CI. (C) Relationship between TL and parasite density (log) during CHMI. Solid blue line represents predicted mean of telomere length, solid orange line represents predicted mean of parasite, with shaded areas denoting the 95% CI of the mean, (N = 16, observations $_{TL}$ = 481, observations $_{parsitaemia}$= 278). Figure adapted from Miglar et al., Scientific Reports, 2021 with permission of the Nature Portfolio.*

3.4.3 Telomere length is inter-correlated with cellular senescence and aging related mechanisms

Results from the Spearman's correlation model are visualized in **Figure 6A**. Telomere length in whole blood was significantly correlated with CDKN2A, an indicator for cellular senescent levels (spearman's correlation; p= 3.1E-04, **Figure 6A, Table S2**). Concurrent with a decrease in TL, CDKN2A expression levels increased. There was no correlation between TL and the expression of TERT, the catalytic subunit of the telomerase (lme; Coef.= -2676.37m SE= 4003.68, z= -0.67, p= 0.50).

There was a negative correlation of TL and levels of inflammatory cytokines IL-8, IL-10, IL18 and INF-γ (spearman's correlation p-values: 1.1E-02; 2.2E-02; 1.9E-02; 4E-02), and a positive correlation of TL and the expression of the antioxidant enzymes MCP1, NOS3, CAT (spearman's correlation p-values: 1.01E-02; 4.6E-02; 4.83E-02, **Figure 6A, Table S2**).

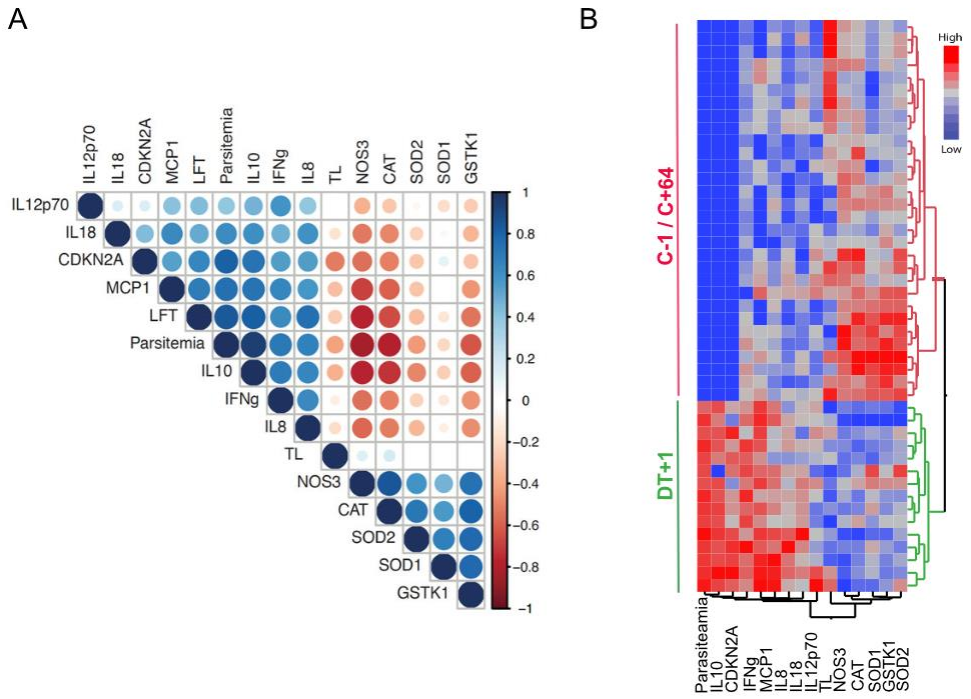

Figure 6. Changes in study markers before, during and after CHMI. *(A) Spearman's correlation of study variables with a significance level of p < 0.05. The size of the circles indicates the strength of correlation, while the colour of the scale bar denotes the nature of correlation. Dark blue (1) corresponds to positive correlation, and dark red (− 1) corresponds to negative correlation.(B)Hierarchical cluster analysis and differential expression of study variables at the study time-points C-1, DT+1 and C+64. Results show a clear distinction between the expression of study markers between DT+1 and C-1/C+64. TL = telomere length, CDKN2A = cyclin dependent kinase inhibitor 2A. Figure adapted from Miglar et al., Scientific Reports, 2021 with permission of the Nature Portfolio.*

3.4.4 Changes in aging markers, levels of inflammatory cytokines and antioxidant enzymes during CHMI

3.4.4.1 Accelerated cellular aging at DT+1 during CHMI

To evaluate changes in TL during the study period, a multivariate analysis was performed including data from all 29-30 time –points per study participant. Telomere length dynamics changed significantly over the course of the study (Wald $\chi 2 = 26.13$, N = 139, $p<0.001$). Differences in the expression levels at DT+1 compared to C+64 were observed in TL (t-test, p=0.004) and expression in CDKN2A (t-test, p<0.001; **Table 7A**, **Figure 7**). Notably, the changes in TL and CDKN2A levels fully reversed at day 64 post infection, showing no

significant difference between the time points C-1 and C+64 (t-test, all p>0.05, **Table 7A**). There was no difference in expression levels of TERT (**Table 7A**, **Figure 7**).

Table 7. Paired t-test significance levels (p-values) of mean difference of cellular aging markers, cytokine levels and antioxidant enzymes prior (C-1), during (DT+1) and post infection (C+64).

		C-1 /DT+1	C-1 /C+64	DT+1 /C+64
A	**TL**	**0.002**	0.343	**0.004**
	CDKN2A	**0.001**	0.98	**0.001**
	TERT	0.135	0.96	0.072
B	**IL-1β**			
	IFN-α2	0.95	**0.005**	**0.008**
	IFN-γ	**0.001**	**0.008**	**0.001**
	TNF-α			
	MCP-1	**0.001**	0.292	**0.001**
	IL-6			
	IL-8	**0.001**	**0.030**	**0.005**
	IL-10	**0.001**		**0.001**
	IL-12p70	0.023	0.057	0.141
	IL-17A	0.057	**0.031**	**0.008**
	IL-18	**0.001**	**0.017**	**0.001**
	IL-23			
	IL-33	0.090	0.201	**0.041**
C	**SOD1**	**0.017**	0.077	0.435
	SOD2	**0.001**	0.055	**0.027**
	GSTK	**0.001**	0.315	**0.001**
	NOS3	**0.001**	0.584	**0.001**
	CAT	**0.001**	0.088	**0.001**

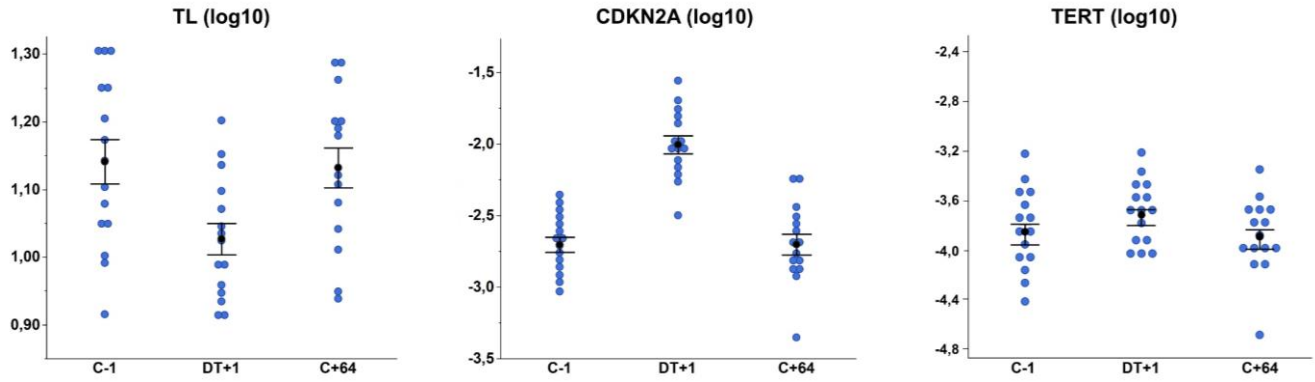

Figure 7. Expression profile of aging markers TL, CDKN2A and TERT during the CHMI.

3.4.4.2 Increased inflammatory cytokine levels during CHMI

The inflammatory response to CHMI on three study time-points was investigated using LEGENDplex assays to measure the plasma levels of 13 cytokines; 11 pro-inflammatory cytokines (INF-α2, INF-γ, IL-1β, IL-6, IL-8, IL12p70, IL-17A, IL-18, IL-23, IL-33 and TNFα) and two anti-inflammatory cytokines (IL-10 and MPC1). The levels of inflammatory cytokines in plasma at day prior to infection (C-1) were compared across the study time-points DT+1 and C+64 (**Figure 8, Table 7B**). Levels of inflammatory cytokines were significant higher at the study time-point DT+1 compared to C-1, yet, their expression profile was similar when comparing C-1 to C+64 (**Figure 6B**). The plasma expression levels of four pro-inflammatory cytokines, IL- 1β, IL-6, IL-23 and TNFα were not detectable in the majority of volunteers (IL-1β: 16/16 (100%); IL-6: 114/16 (87.5%); IL-23 16/16 (100%), TNFα: 16/16 (100%)). No differences in the expression levels during the study period were observed in the remaining cytokine levels when stratified by baseline (C-1) cytokine status.

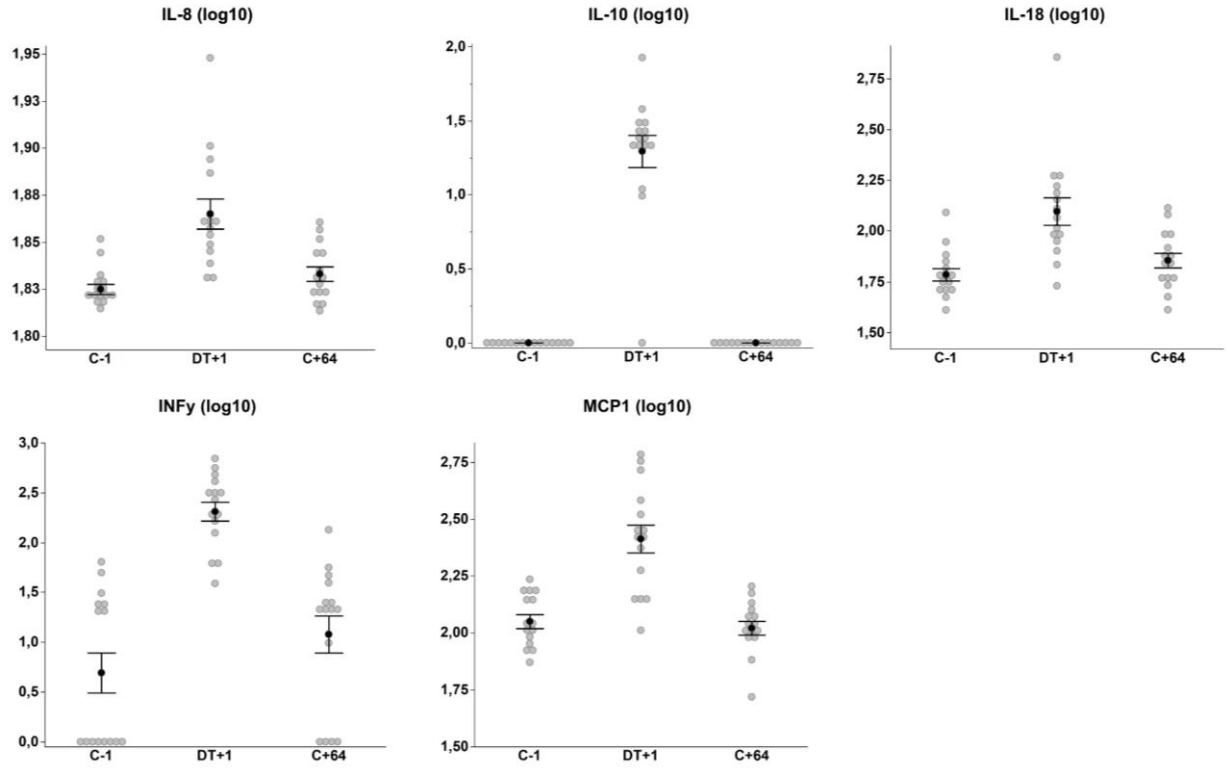

Figure 8. Inflammatory cytokine profile during the CHMI. *The mean values for peak-levels for cytokines in plasma at the study time-point DT+1 were: IFNγ 179.3 pg/mL; IL-8 72 pg/mL; IL-10 22.9 pg/mL; IL-12p70 44.1 pg/mL; IL-18 108.1 pg/mL; MPC1 263.3 pg/mL.*

3.4.4.3 Decreased levels of antioxidant enzymes during CHMI

Next, to evaluate the response of antioxidant enzymes at the three study time-points, gene expression assays were performed to determine the expression profile of SOD1, SOD2, NOS3, CAT and GSTK1. The gene expression profiles of antioxidant enzymes at day prior to infection (C-1) were compared across the study time-points DT+1 and C+64 (**Table 7C**). The gene expression of antioxidant enzymes was significantly decreased at the study time-point DT+1 compared to C-1, yet, their expression profile was similar when comparing C-1 to C+64 (**Figure 9**).

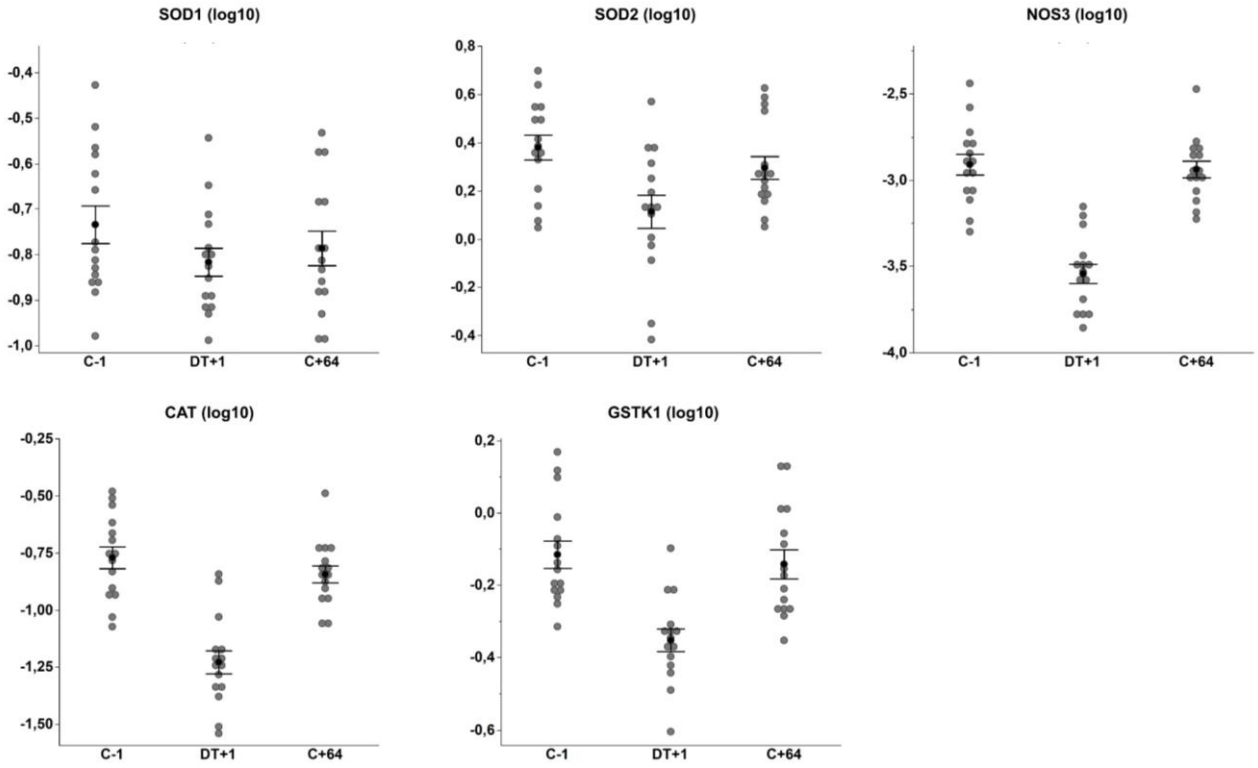

Figure 9. Profile of antioxidant enzymes during the CHMI.

3.4.4.4 PCA on combined datasets reveals clustering of cellular aging markers, inflammatory cytokines and antioxidant enzymes

Finally, PCA was used to combine all data sets in order to assess whether overall host responses and parasitaemia can be separated by their functional impact and by time. PCA was conducted using all available data at C-1, DT+1 and C+64. Clustering was observed between TL, inflammatory cytokines and antioxidant enzymes (**Figure 10A**), as well as by time-points (**Figure 10B**).

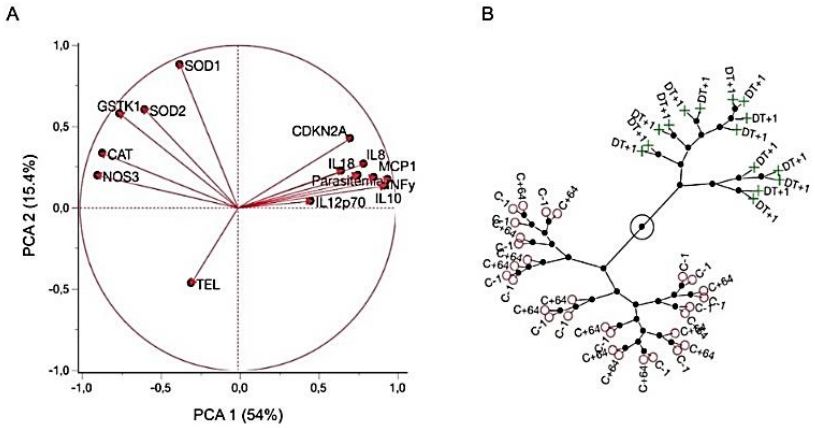

Figure 10. Principal component analysis (PCA) of all data at C-1, DT+1 and C+46. *PCA combining all TL data, pro-and anti-inflammatory cytokine levels and levels of antioxidant enzymes at the three study time-points. The first two principal components shown accounting for 69.4% of all variance.*

Factor analysis showed that CDKN2A and inflammatory cytokine levels (Factor 1), antioxidant enzymes (Factor 2) and TL (Factor 3) accounted for the greatest variance along the first principal component (**Table 8**).

Table 8. Relative contribution of each study marker in three significant factors.

	Factor 1	**Factor 2**	**Factor 3**
CDKN2A	69.18%	-8.76%	-54.36%
Parasitaemia	85.60%	-35.76%	-28.43%
LFT	84.21%	-25.53%	-11.23%
IFNγ	84.42%	-11.76%	16.25%
IL8	78.59%	-17.39%	-3.24%
IL10	84.33%	-35.99%	-19.95%
IL12p70	63.59%	-0.84%	57.59%
IL18	65.40%	-14.35%	-18.20%
MCP1	82.40%	-15.33%	-12.89%
TEL	-24.73%	-6.30%	80.66%
NOS3	-66.34%	61.89%	8.06%
SOD1	4.39%	89.85%	-32.45%
SOD2	-14.52%	88.19%	15.80%
CAT	-53.90%	75.04%	14.35%
GSTK1	-37.10%	87.29%	-4.53%

3.4.5 Summary of results

This chapter reveals significant changes in TL dynamics in volunteers with a mild malaria infection, followed over 64 days and confirms the complete recovery of TL after clearance of the parasites. The data further shows the significant correlation of TL and CDKN2A, and their association with inflammation and antioxidant enzymes during infection, which suggests an increased inflammatory cytokine production and an imbalanced oxidative stress response as potential mechanisms underlying accelerated cellular aging during malaria infection. These results provide a basic understanding of the interconnectedness of aging markers and aging-associated mechanisms before, during and after a *P. falciparum* infection.

4 CELL-SPECIFIC TELOMERE DYNAMICS IN ADULTS WITH NATURALLY ACQUIRED ACUTE MALARIA

4.1 AIM

The aim of this chapter was to explore whether infection driven telomere attrition is a synchronized process across immune cell types or if it is rather cell-type specific.

4.2 BACKGROUND

The majority of studies on TL are performed in whole blood. Accelerated telomere attrition and increased cellular senescence during malaria infection were confirmed in a study on human volunteers in **Chapter 3**, as well as, potential underlying mechanisms, including increased pro-inflammatory profile and a disrupted redox-homeostasis.

Nevertheless, TL was measured in whole blood, just as in the study in travellers with imported malaria[4] and the majority of other studies investigating telomere dynamics during infection and other conditions. Yet, it is known that infections and inflammation cause changes in the proportion and composition of PBMCs within whole blood [87-90] , which is another common trajectory of accelerated aging[91,92]. Therefore, studies using whole blood to investigate the impact of infections on TL may be affected by the change in composition of lymphocytes (T cells, B cells, and NK cells), monocytes, and dendritic cells in PBMCs and granulocytes, including neutrophils, basophils and eosinophils in response to infection.

The focus of this chapter was to investigate whether transient changes in the PBMC compartment affect TL measurements in whole blood, and to evaluate whether the effect of malaria on TL is synchronized across cell populations or rather cell-type specific.

The chapter investigates TL in total PBMC and six sorted cell types in PBMC, respectively, in travellers diagnosed with acute *P. falciparum* malaria infection and followed with repeated sampling over 12 months after successful treatment. PBMCs from three time points (Acute, 10-30 days and 6-12 months) were sorted into monocytes, NK cells, T cells, and naïve-,

memory- and atypical B cells. DNA was extracted from each cell population, and telomere length was measured by qPCR.

4.3 STUDY-SPECIFIC METHODS

4.3.1 Study population

A cohort of travellers diagnosed with malaria and followed over one year has been established at the Karolinska University Hospital in Stockholm, Sweden with the aim to assess the natural kinetics of immune responses without risk of re-exposure. The cohort consists of individuals of both, Swedish and African origin residing in Sweden that had travelled to malaria endemic countries and were diagnosed with a *Plasmodium falciparum* infection and successfully treated upon their return to Sweden. The country of origin and years of residency in Sweden is provided in Table S. These study participants were followed prospectively with repeated venous blood sampling over one year performed at the Karolinska University Hospital, providing an acute sample, a 10-day sample, a one-month, three-month, six-month and 12-month sample. The infections were successful cleared within a three-day course of artemether-lumefantrine (Riamet®).

For the purpose of this study, we included 13 individuals (aged 30-76 years) from this cohort and chose three sampling time points per study participant (acute, 10-30 days after treatment and convalescence at 6-12 months), based on results obtained from our previous study in the same cohort[4]. This study was approved by the Ethical Review Board and the Swedish Ethical Review Authority (Dnr 2006/893-31/4, 2013/550-32/4, 2015/2200-32, 2016/1940-32, 2018/2354-32, 2019/03436 and 2020-00859) in Stockholm and informed consent was given by all study participants.

4.3.2 PBMC isolation and preparation

Isolation of PBMC is described in section 2.3.4.1. All patient samples were processed shortly after collection and stored as PBMC in liquid nitrogen, until further use.

4.3.3 Cell sorting by flow-cytometry

PBMC from three time points were thawed as described in section 2.3.4.2, 2-7 years after sampling and sorted into T cells, naïve B cells, atypical B cells, memory B cells, NK cells and monocytes, using a BD influx 6-way sorter (BD Bioscience). Antibodies against cell-specific surface markers are described in **Table 9**. The gating strategy included gates for size (FSC) and granularity (SSC), and gates for singlets (Trigger pulse width low) and live cells (Aqua negative). Total $CD3^+$ T cells and $CD14^+$ monocytes were sorted, while $CD3^-CD14^-$ cells were gated for $CD56^+$ NK cells and $CD19^+$ B cells that were further gated for $CD20^+$CD38lo/int to remove plasma cells and immature B cells. Mature B cells were separated into $CD21^+CD27^+$ resting memory B cells and $CD21^+CD27^-$ naïve B cells. Atypical B cells were sorted from $CD21^-CD27^-FcRL5^+$ B cells (**Figure 11**).

Table 9. Staining cocktail for cell sorting

Marker	Clone	Antibody	Supplier
CD3	HIT3a	PE-CF594	BD Bioscience
CD14	M5E2	FITC	BD Bioscience
CD56	NCAM16.2	BV786	BD Bioscience
CD19	HIB19	PE-Cy7	BD Bioscience
CD21	B-ly4	BV421	BD Bioscience
CD27	M-T271	BV650	BD Bioscience
FcRL5	509f6	PE	Biolegend

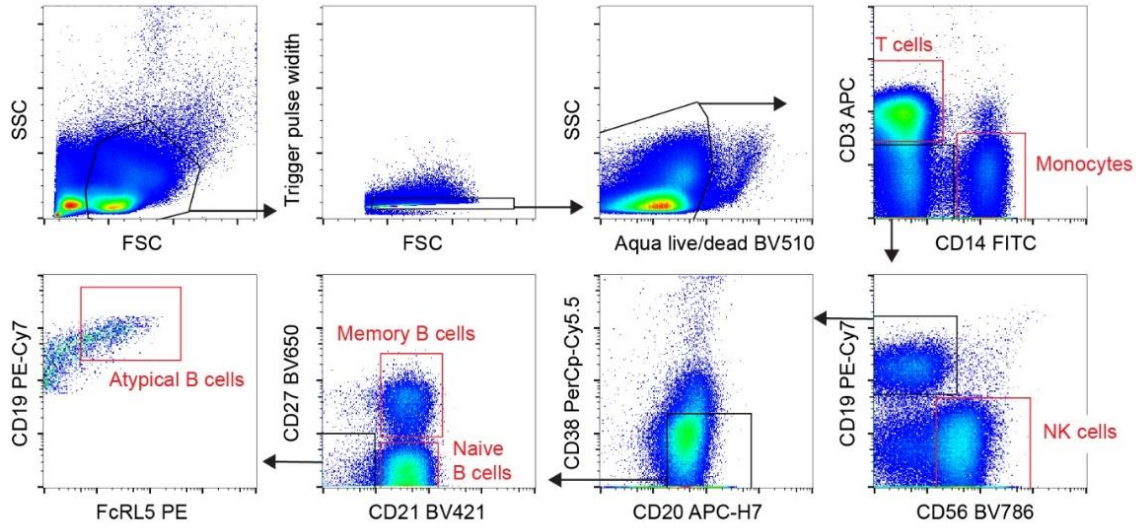

Figure 11. Gating strategy for cell sorting. *PBMCs were sorted into T cells, monocytes, NK cells, atypical B cells, memory B cells and naïve B cells.*

4.3.4 DNA extraction and quantification

DNA was extracted from 100 µL of total PBMCs and of each sorted PBMC sub- population using the QIAmp DNA Blood Mini™ Kit (Qiagen), according to the manufacturer instructions. Total DNA was quantified on a Qubit™ Fluorometer (Thermo Fisher Scientific Scientific, Baltics, UAB), using the Qubit™ dsDNA HS Assay Kit (cat # Q33230, Invitrogen, Thermo Fisher Scientific Scientific).

4.3.5 Telomere length measurement

Telomere length was measured in 215 samples from 13 study participants and their respective follow-up time-points collectively, following the protocol described in section 2.3.2.2. A detailed description of the number of samples analyzed is presented in **Table S3**.

Relative TL were calculated using the $\Delta\Delta C_T$ method after correcting for the PCR efficiency according to Pfaffl et al.[76]. Telomere length in kb was calculated using a human genomic DNA reference of 758 kb (# 8918d; Science Cell), resulting in the final calculation of ((2^− $\Delta\Delta C_T$ × 758)/92).

4.3.6 Statistical analysis

Linear mixed models were used to determine the expected change of TL in PBMCs and PBMC subpopulations across the one year follow-up, and to investigate the change of TL over time and between time-points for each cell sub-population separately. Host factors including age and sex were considered when performing the models, however, both adjusted and unadjusted models showed similar results, and the latter was used when presenting the results. To control for inter-individual variation and repeated measurements, individual ID was added as a random factor each model.

Partial correlations of TL within sorted cells were reported as the effect of each cell type on the corresponding cell type. Analysis of change in TL over time was calculated as TL at baseline (acute) subtracted from TL at the two follow-up time points (10-30 days post infection and at convalescence, 6-12 months). No analysis was performed on total cell counts, as total number of cells for each cell type was not accounted for in the sorted sample prior DNA extraction for TL measurement.

All analyses were performed in R statistic software, version 4.1.2 (R Core Team (2020). R Foundation for Statistical Computing, Vienna, Austria. URL: https://www.R-project.org/)[86].

4.4 RESULTS

4.4.1 Characteristics of study population

In total, 215 samples from 13 patients were included in the analysis. Characteristics about the study participants are summarized in **Table 10**. In total, the sample availability of overall PBMC across individuals and time points was 94.9% and sorting success resulted in the availability of 94.9% of the samples for monocytes, 84.6% of NK cells, 62% of naïve and memory B cells and 59% of atypical B cells.

Table 10. Characteristics of study individuals and time-points.

Study population	
Number of patients	13
Median age, years (range)	38 (30-76)
Sex, M/F	8/5
Patient origin, n (%)	
Sweden	6 (46)
Sub Saharan Africa	7 (54)
Number of time points per patient, mean (range)	2.8 (1-3)
Acute (T1)	13
10 days – 1 month (T2)	13
6 – 12 months (T3)	11
Time of residence in endemic country, years (range)*	24 (<0.5-35)
Mean parasitaemia, % infected erythrocytes (range)	1.3 (0.01-8.4)

*Number of years previously lived in the endemic country, including Uganda, Kenya, Tanzania, Cameroon, Sierra Leone and Nigeria

Telomere length in PBMCs was measured at three time points per individuals, with exception of two patients, who were missing a sample on the last study time-point. PBMC TL was correlated with age but not sex, however, the age effect was not significant when separating into the individual sorted cell subsets, except for monocytes, which might be limited by the broad age range and the limited sample size (**Table 11**).

4.4.2 Cell composition during infection and convalescence

The FACS-sorted cell populations represented on average 85.6% (range 70.4-95%) of all live PBMCs. The mean composition of cell frequencies at diagnosis was on average 14% monocytes, 11.4% NK cells, 4.4% naïve B cells, 1.1% memory B cells, 0.2% atypical B cells and 53.2% T cells (**Figure 12**).

Table 11. Change in telomere length over time. *Change in TL in overall PBMCs and cell sub-populations at time between acute and 10-30 days post infection (period 1) and between acute and convalescence (period 2). Linear mixed effect model adjusted for age and sex. A negative estimate indicates a reduction over time and a positive estimate indicates an increase over time.*

TL		Estimate	Std.	df	t	p
PBMC	(Intercept)	8.10	1.63	10.23	4.98	0.001
	Period 1	-0.57	0.32	22.09	-1.78	0.089
	Period 2	-0.46	0.34	22.30	-1.34	0.195
	Age	-0.09	0.04	9.94	-2.30	**0.044**
	Sex	-0.46	0.96	9.96	-0.48	0.643
Monocytes	(Intercept)	9.00	2.02	10.41	4.47	0.001
	Period 1	-0.96	0.47	22.22	-2.05	0.052
	Period 2	-0.67	0.50	22.50	-1.34	0.193
	Age	-0.11	0.05	10.02	-2.29	**0.045**
	Sex	-0.42	1.19	10.05	-0.35	0.733
NK cells	(Intercept)	4.87	1.34	11.83	3.64	0.003
	Period 1	-0.94	0.50	19.62	-1.89	0.074
	Period 2	-0.48	0.55	20.65	-0.88	0.391
	Age	-0.02	0.03	10.61	-0.67	0.519
	Sex	-1.45	0.72	9.05	-2.00	0.076
Naive B cells	(Intercept)	10.00	4.20	5.82	2.38	0.056
	Period 1	-1.11	0.87	13.08	-1.28	0.223
	Period 2	-0.41	1.00	13.67	-0.41	0.688
	Age	-0.13	0.11	5.62	-1.20	0.279
	Sex	-0.28	1.47	5.72	-0.19	0.853
Memory B cells	(Intercept)	8.53	4.44	6.12	1.92	0.102
	Period 1	-0.62	0.79	13.46	-0.79	0.445
	Period 2	-0.46	0.87	13.91	-0.53	0.606
	Age	-0.11	0.11	5.93	-1.00	0.356
	Sex	0.21	1.55	5.97	0.14	0.897
Atypical B cells	(Intercept)	8.68	3.20	5.90	2.72	0.035
	Period 1	-0.10	0.72	13.08	-0.13	0.896
	Period 2	-0.20	0.81	13.04	-0.24	0.813
	Age	-0.09	0.08	5.62	-1.06	0.333
	Sex	-0.66	1.17	5.85	-0.57	0.590
T cells	(Intercept)	6.24	1.53	10.02	4.08	0.002
	Period 1	-0.54	0.48	21.67	-1.12	0.274
	Period 2	0.02	0.51	22.17	0.05	0.964
	Age	-0.06	0.04	9.33	-1.72	0.118
	Sex	-0.82	0.89	9.37	-0.92	0.379

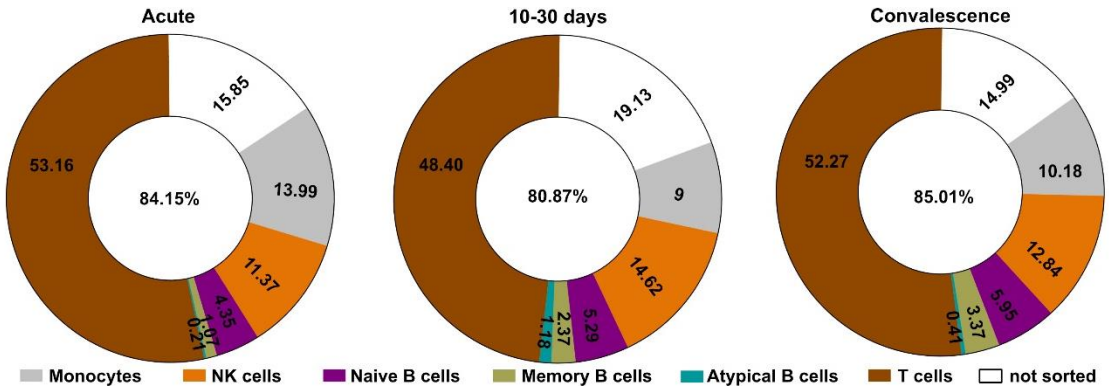

Figure 12. Frequency of sorted PBMC subtypes. *Mean cell frequency (%) of monocytes, NK cells, naïve B cells, memory B cells, atypical B cells and T cells of all live cells at diagnosis of acute infection, 10-30 days post diagnosis and after convalescence (6-12 months post diagnosis). Percentage in the centre of each graph represents the total frequency of live PBMCs that were sorted into the six different cell populations.*

At 10-30 days after treatment, the frequency of live NK cells, naïve B cells, memory B cells and atypical B cells increased with an average fold change of 33% (95% CI 9-75), while the frequency of monocytes, and T cells decreased with an average of 12% (95% CI 4-19) compared to the day of diagnosis. During convalescence, the frequency of live NK cells, naïve B cells, memory B cells and atypical B cells remained on average 24% higher than at diagnosis (95% CI 5-50), and frequencies of monocytes and T cells were on average 7% (95% CI 1-14) lower compared to the day of diagnosis.

4.4.3 Telomere dynamics during infection and convalescence

Telomere length at 10-30 days post infection tended to be shorter compared to TL at the acute time point in PBMCs, monocytes and NK cells (**Table 12**, **Figure 13**).

Table 12. Mean telomere length in kb ± SE across cell populations at study time points.

TL (kb)	Acute	10 -30 days	Convalescence
PBMC	4.03±0.59	3.45±0.46	3.37±0.64
Monocytes	4.04±0.70	3.08±0.66	3.17±0.75
NK cells	3.36±0.59	2.42±0.43	2.82±0.42
Naive B cells	4.94±0.81	3.83±0.80	4.63±1.13
Memory B cells	4.14±1.11	3.60±0.82	3.93±0.49
Atypical B cells	5.08±0.82	5.03±0.67	4.55±0.49
T cells	3.21±0.67	2.67±0.37	3.03±0.52

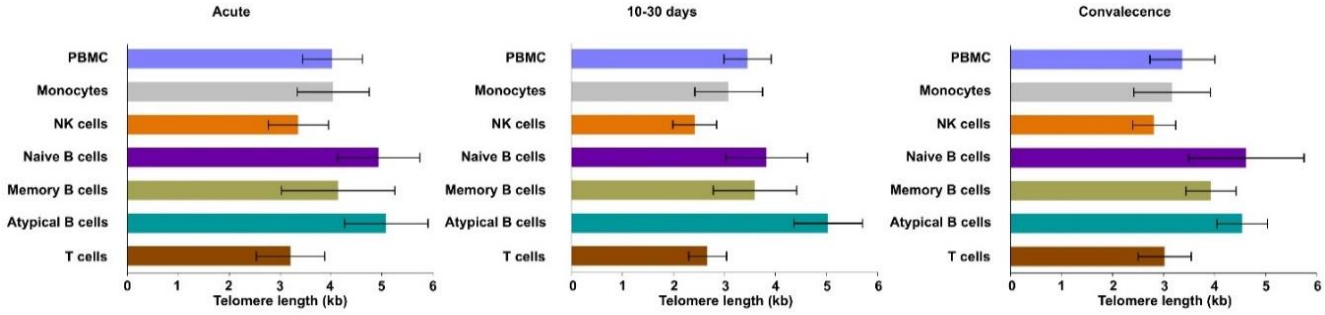

Figure 13. Mean telomere length (kb) in sorted cell populations at three time points during and after infection. *Acute; after treatment (10-30 days); and convalescence (6-12 months).*

No clear effect was seen of malaria infection on TL in total PBMCs. Similar results were observed when looking into the effect of malaria infection on TL in each sorted PBMC sub-population type (**Table 11**). Nevertheless, TL kinetics across cell types were similar in all individuals included in this study, with only a few exceptions (**Figure 14**).

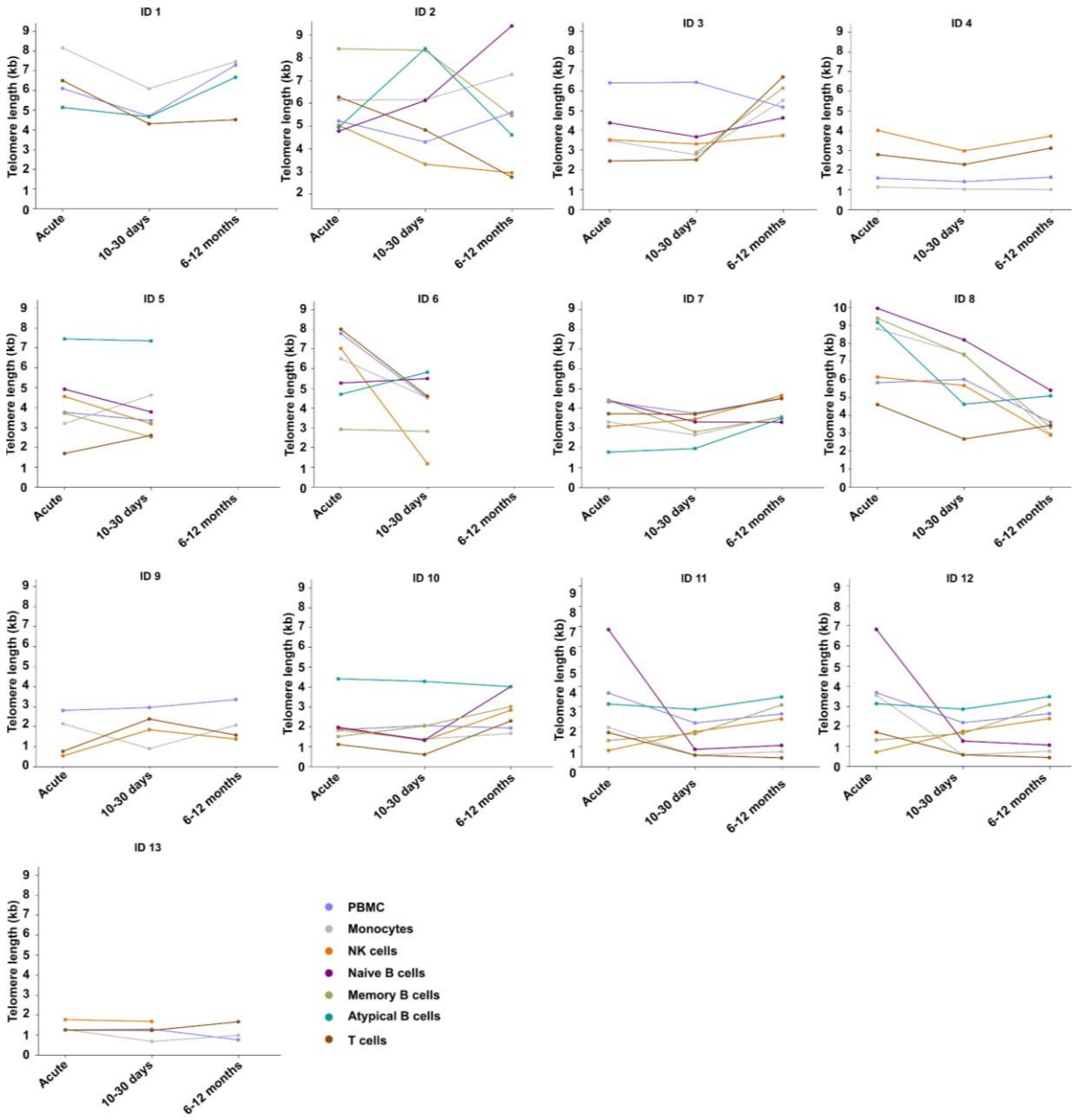

Figure 14. Individual telomere length kinetics across study time-points. *Telomere length (kb) of sorted PBMC sub populations. Each graph panel represents an individual. Measurements of TL in atypical B cells and memory B cells for three out of 13 individuals had to be excluded from analysis due to a limited amount of live cells obtained from the FACS-sort.*

At the time of diagnosis (Acute), naïve B cells exhibited the longest mean TL, followed by atypical B cells, memory B cells, monocytes, T cells and NK cells (**Table 12**, **Figure 13**). Similar cell-specific patterns in TL were observed at 10-30 days post diagnosis and during convalescence (6-12 months post diagnosis; **Table 12**, **Figure 13**).

4.4.4 TL was correlated across total PBMCs and sorted cell populations

Telomere length in total PBMCs was significantly correlated with the TL in each sorted cell sub-population, with the exception of memory B cells and atypical B cells (**Table 13**). However, when analyzing each follow-up time-point separately, TL in PBMCs was correlated with TL in monocytes, NK cells and T cells at the acute time-point and with monocytes, NK cells, naïve B cells and T cells 10-30 days post diagnosis. During convalescence, TL in PBMCs was correlated with TL in monocytes, memory B cells and T cells (**Table 13**). The results show that 10-30 days after treatment, one unit increase in TL of mostly NK cells and T cells, resulted in a 0.73 unit increase in PBMC TL, as described by the coefficient in **Table 13**, which indicates the high contribution of TL in NK cells and T cells to the overall TL when measured in PBMCs.

Table 13. Correlation between telomere length (TL) in total PBMCs and cell-sub populations, overall, and at three time points during and after infection. *Results from Linear mixed effect model (LME) with beta estimates of coefficients representing the expected unit change in TL, stratified for each time point.*

PBMC TL	**Overall[a]**		**Acute**		**After treatment 10-30 days**		**Convalescence 6-12 months**	
Cell subset TL	Coef.	p	Coef.	p	Coef.	p	Coef.	p
Monocytes	0.53	**<0.001**	0.67	**0.001**	0.52	**0.003**	0.78	**<0.001**
NK cells	0.46	**<0.001**	0.77	**0.005**	0.73	**0.026**	0.33	0.517
Naive B cells	0.31	**0.008**	0.44	0.138	0.53	**0.014**	0.34	0.17
Memory B cells	0.21	0.144	0.33	0.195	0.36	0.135	1.10	**0.031**
Atypical B cells	0.12	0.501	0.17	0.613	0.18	0.532	1.21	0.091
T cells	0.29	**0.032**	0.67	**0.002**	0.73	**0.03**	0.63	**0.047**

When comparing TL between the respective cell subtypes overall, TL was correlated between sorted cell subtypes, with the exception of atypical B cells and T cells, when controlling for repeated measurements (**Table 14**).

Table 14. Correlation of telomere length between cell sub populations*. Results from LME model accounting for repeated measurements. Coefficients are interpreted as unit increase of TL in PBMC with one unit change of cell-type specific TL.*

	Monocytes		**NK cells**		**Naive B cells**		**Memory B cells**		**Atypical B cells**		**T cells**	
	Coef.	p	Coef.	p	Coef.	p	Coef.	p	Coef.	p	Coef.	p
Monocytes	1		0.67	**0.001**	0.79	**<0.001**	0.74	**<0.001**	0.46	0.067	0.60	**0.001**
NK cells	0.67	**0.001**	1		0.74	**0.006**	0.63	**0.008**	0.22	0.356	0.63	0.153
Naive B cells	0.79	**<0.001**	0.74	**0.006**	1		0.69	**0.001**	0.46	0.125	0.17	0.541
Memory B cells	0.74	**<0.001**	0.63	**0.008**	0.69	**0.001**	1		0.59	**0.021**	0.58	**0.012**
Atypical B cells	0.46	0.067	0.22	0.36	0.46	0.125	0.59	**0.021**	1		0.19	0.419
T cells	0.60	**0.001**	0.64	0.153	0.166	0.541	0.58	**0.012**	0.19	0.419	1	

To receive more detailed information about telomere kinetics, the correlations were investigated at each follow-up time-point separately (**Table S4**). The correlation of TL between cell subtypes was similar at the acute time-point and during convalescence (10-12 months post diagnosis), with TL in monocytes being well correlated with the other cell-subtypes. During infection (10-30 days post diagnosis), TL between sorted cell subtypes were well correlated between all cell types, with exception of atypical B cells (**Table S4**).

4.4.5 Summary of results

This chapter provides individual cell type-specific TL kinetics during and after an acute malaria infection from individuals followed over one year as part of a larger clinical cohort study. The results show that TL of PBMC from whole blood is correlated with TL of monocytes, naïve B cells, T cells and NK cells, and reveals partial correlations within sorted cell subtypes. During infection, NK cells and T cells showed the shortest TL, which might suggest that telomere attrition following infection triggers partial cell-type specific responses. These results provide a base for further studies with in-depth analysis of cell-specific TL changes during infections.

5 THE EFFECT OF REPEATED SYMPTOMATIC AND ASYMPTOMATIC MALARIA INFECTIONS ON TELOMERE LENGTH IN LONGITUDINALLY FOLLOWED CHILDREN IN KENYA

5.1 AIM

The aim of this chapter was to determine whether telomere length dynamics are affected by the level of malaria exposure in children living in malaria endemic areas.

5.2 BACKGROUND

In malaria endemic countries in Sub-Saharan Africa, both, symptomatic episodes of malaria and asymptomatic infections are frequent in children[93]. Despite repeated infections leading to partial immunity, which reduces the severity of clinical manifestations of malaria, residents in endemic areas experience persistent and chronic asymptomatic infections throughout their life, which suggests that naturally acquired immunity is never complete[94]. In high to moderate transmission areas, incidence of severe, life-threatening malaria and related death is most pronounced in infants and young children [95,96]. Exposure to malaria is also associated with anemia, impaired neuro-cognitive and socio-economic development, poor school performance in children[52,97], and may have other long-term hidden costs for the host.

To what extent repeated clinical episodes of malaria and persistent asymptomatic infections may accelerate telomere shortening in children residing in malaria endemic areas is yet to be understood. However, to separate the impact of malaria from other environmental variables would require data from individuals with similar characteristics, such as environment, genetics and socio –economic level, but with different exposure to malaria.

Here, data is presented from two cohorts of children living on the coast of Kenya that share similar genetics and socio-economic structure, but differ in their exposure to malaria.

The focus of this chapter is to provide insights on the association of long-time malaria exposure and telomere shortening over time, using blood samples and weekly records of asymptomatic and symptomatic *P. falciparum* infections in children followed up to an average age of 10 years in two cohorts, one exposed to moderate malaria transmission and an unexposed control group.

The chapter first describes the study cohorts Junju and Ngerenya and the study design, followed by study-specific methods. An analysis is then presented on the correlation of TL and host factors, followed by the analysis on the correlation of TL and the number of symptomatic and asymptomatic malaria infections documented during yearly surveys and weekly surveillance for malaria. Analysis was performed for both cohorts in a join model and for both cohorts separately in a sub-group model.

5.3 STUDY-SPECIFIC METHODS

5.3.1 Study populations and study design

This study includes two study cohorts located in Junju and Ngerenya in Kilifi County, on the Indian Ocean coast of Kenya and are nested within the Kilifi Health and Demographic Surveillance System (**Figure 15A**) [98,99]. Despite their geographic proximity of approximately 40 km and similarities in ethnic make-up, social and economic structures, and culture, the populations living in Junju and Ngerenya are exposed to different levels of malaria. Malaria remains endemic in Junju with moderate transmission during the biannual rain seasons (May-July and October-December), and with an average of 27% prevalence of asexual *P. falciparum* parasitaemia during the dry season in the years 1998 -2016[100,101]. In contrast, in Ngerenya, malaria transmission is under complete control since the early 2000s, with no reported cases of clinical or asymptomatic *Plasmodium* infections, as determined through both passive surveillance and annual cross-sectional qPCR based surveys. Children from both cohorts are routinely recruited at birth into long-term longitudinal studies for malaria immunology. Ngerenya was under active weekly surveillance for malaria between 1998 and 2007, before

shifting to passive surveillance owing to the scarcity of malaria infections. Junju remains under active weekly surveillance for malaria since 2005 (**Figure 15B**). During the weekly visits, field workers measure axillary body temperature, *P. falciparum* positivity by rapid diagnostic test (RDT), and document history of fever. In the event of fever, or its recent history and a positive RDT, a venous blood sample is drawn, and the child is treated for malaria.

Annual cross-sectional surveys were conducted in both cohorts in March, following a three to four month dry period with minimal *P. falciparum* transmission, where anthropometric and parasitological data were collected, alongside with a 5 ml venous blood sample, which was collected if the child had fever (≥37.5˚C; **Figure 15A**). The samples were drawn at local facilities at the two respective study sites, following the same yearly procedure and are placed on ice until processed at the KEMRI. The blood was processed into PBMC and plasma within 4-6 hours from the time of collection and was stored in liquid nitrogen and -80˚C, respectively, until use. An additional whole blood pellet (0.3mL) in EDTA for DNA extraction was stored at -80˚C on the same day of the sample collection.

For the purpose of this study, samples from 218 children from Junju and 90 age-matched controls from Ngerenya were included, together with their data from active and passive follow-up. The inclusion criteria for the children selected for this study was the age of ≤1-9 years in 2007 (first study time-point) and a negative history of malaria exposure for controls from Ngerenya (**Figure 15**).

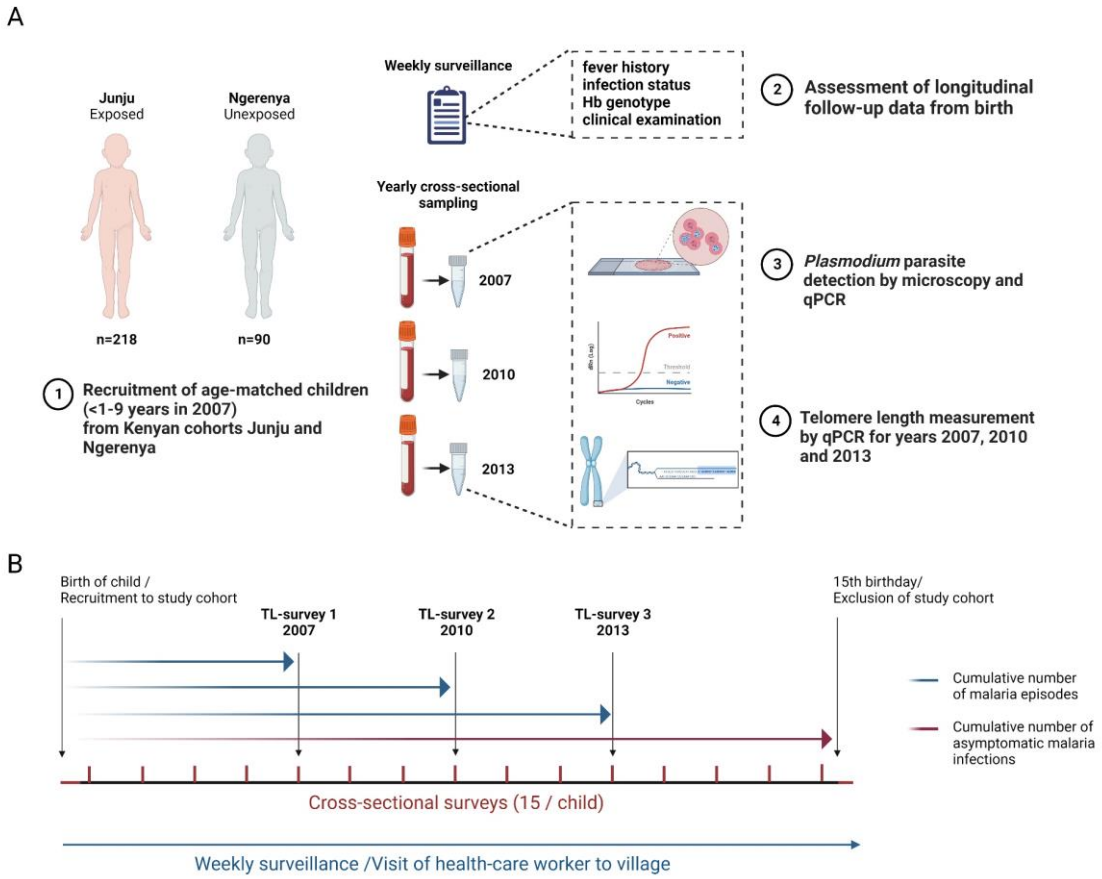

Figure 15. Study overview. *(A)The study includes data from 218 children from Junju that are exposed to moderate malaria transmission and 90 age-matched, malaria unexposed children from Ngerenya, followed from birth. Weekly surveillance data was available, providing information on fever history, infection status, hemoglobin genotype (Hb) and clinical examination, while data from yearly cross-sectional sampling in 2007, 2010 and 2013 provided additional data on parasite detection and individual TL. (B) Longitudinal follow-up data on the cumulative number of malaria episodes was measured from the child's entry into the cohort up to each of the respective study time-points and correlated to individual TL. Data from yearly cross-sectional surveys provided data on the cumulative number of asymptomatic malaria infections. (Figure by A. Miglar, designed in BioRender.com).*

5.3.1.1 Definitions of malaria

Symptomatic malaria was defined as fever (temperature ≥ 37.5°C) and parasite detection by microscopy or qPCR. A new episode of symptomatic malaria was defined as subsequent parasitaemic episode that occurred later than 7 days after the previous parasitaemic episode. Asymptomatic infections were defined as axillary temperature <37.5°C and *Plasmodium sp.* parasitaemia detected by RDT, microscopy and/or qPCR. Febrile children with axillary temperature ≥ 37.5°C and who were parasite negative by RDT, microscopy and/or qPCR are

referred to as non-malarial fever cases, while parasite negative individuals without fever are referred to as healthy.

5.3.1.2 Ethical approval

The study was approved by the KEMRI Scientific and Ethics Review Unit (Prot. no. KEMRI/SERU/CGMR-C/017/3149), and by the Swedish Ethical Review Authority (Dnr. 2008/998-31-3 and 2019-05746). Informed written consent was given by the parents of all the participants, or their guardians.

5.3.2 DNA extraction and quantification

DNA was extracted following the same procedure from approximately 30µL blood pellets from each sample using an automated Qiaxtractor (QIAcube®HT, Qiagen), and was stored at - 20 °C at KEMRI in Kenya. Quantification was performed on a NanoDrop™ 2000 Spectrophotometer.

5.3.3 Telomere length measurement

Telomere length measurements were performed on site at the KEMRI. Telomere length was measured in 886 samples from 308 children and their respective follow-up time-points on an ABI 7500 real-time PCR system (Applied Biosystems), following the protocol described in section 2.3.2.2. Detailed information about sample availability at the study time-points is provided in **Table S5**.

Relative TL were calculated using the $\Delta\Delta C_T$ method after correcting for the PCR efficiency according to Pfaffl et al.[76]. Telomere length in kb was calculated using a human genomic DNA reference of 515 kb (cat # 8918d; Science Cell), resulting in the final calculation of ((2^− $\Delta\Delta C_T$ × 515)/92).

5.3.4 Parasite detection

Parasite detection in active surveillance data (weekly surveys) was based on RDT and microscopy. Parasitaemia in samples from Junju was estimated based on actual leukocyte count measured for each blood smear, following the protocol in Olotu et al[99]. Asexual parasite density was counted against 200 WBCs, and symptomatic parasite density, measured as parasite/µl of whole blood, was calculated as follows: (number of parasites counted/WBC counted) × WBC count/µl of participant.

Parasitic assessment in passive surveillance data (yearly surveys) was based on performing a *Plasmodium* species-specific real-time PCR assay targeting the multi-copy 18S rRNA gene using an ABI TaqMan 7500 instrument (Applied Biosystems), following the protocol of Shokoples et al [74]. In the analysis, only *P. falciparum* species parasitaemia was included, due to very low prevalence of other *Plasmodium* species.

5.3.5 Genotyping for sickle cell trait and α^+thalassemia

DNA extracted in section 5.3.2 was genotyped for the sickle cell mutation by bi -directional allele -specific PCR amplifications, following the protocol in Waterfall et al.[102]. To detect single and/or double gene deletions leading to the α^+thalassemia, a single-tube multiplex-PCR assay was performed. The protocol and primer sequences for the analysis are outlined in Chong et al.[103].

5.3.6 Statistical analysis

To investigate telomere dynamics on a population and on an individual level, and to evaluate the association between TL and malaria, as well as the difference in change of TL between the two cohorts, linear mixed effect models (LME) with a random intercept and a random slope were performed, referring to TL in 2007 as reference. The models were adjusted for the potential confounders age, sex, hemoglobin genotype, survey year and cohort born into.

Data on malaria episodes experienced between the first individual data entrance (2005) and the date of the last TL-survey in 2013 was retrieved from the longitudinal active weekly surveillance in Junju to assess the effect of number of cumulative malaria episodes experienced on TL.

Next, a Cox-regression model was applied to test the association of TL in year 2007 and future symptomatic malaria infections until the last telomere measurement in year 2013.

Further, to evaluate differences in TL distribution in the cohorts, sub-group analysis was performed for each cohort separately, with age centred at the median (7 years).

Statistical analyses were performed in the R statistic software, version 4.1.2 (R Core Team (2020). R Foundation for Statistical Computing, Vienna, Austria. URL: https://www.R-project.org/) [86]. Graphical presentations were obtained in JMP, version 14.0.

5.4 RESULTS

5.4.1 Characteristics of study population

In total, 886 samples from three cross-sectional surveys for 308 children, and malaria records from longitudinal surveillance over an average of 11 years for Junju were included in the analysis. Data from all three cross-sectional surveys was available for 85.5% of the children in Junju and for 91.1% for children in Ngerenya. The participant characteristics and time-points for TL measurement are summarized in **Table 15**.

Table 15. Characteristics of study population.

	Junju Moderate transmission	**Ngerenya** No transmission
Number of children	218	90
Age in years at first TL-survey 2007, median (range)	5 (0-9)	3 (0-7)
Female, n (%)	114 (52.3)	46 (51.1)
Number of TL-surveys per child (2007, 2010, 2013), mean (range)	2.85 (1-3)	2.91 (2-3)
3 TL-surveys, n (%)	187 (85.8)	82 (91.1)
2 TL-surveys, n (%)	31 (14.2)	8 (8.9)
Total number of survey samples for telomere measurement	624	262
Sickle cell typing, n (%)		
HbAA	175 (80.7)	79 (87.8)
HbAS	42 (19.3)	11 (12.2)
HbSS	1 (0.005)	0
Thalassemia typing, n (%)		
Normal	77 (35.3)	32 (35.6)
Heterogenous	111 (50.9)	34 (37.8)
Homogenous	30 (13.8)	24 (26.7)
Malaria incidence rate (episodes/child/year)*	1.15	0
Cumulative number of non-malarial fevers until TL survey 2013 (weekly data), mean (range)	6.24 (0-21)	7.4 (1-16)
Cumulative number of symptomatic malaria episodes until TL survey 2013 (weekly data), mean (range)	6 (0-21)	0
Cumulative number of asymptomatic infections until TL survey 2013 (yearly surveys), mean (range)	2 (0-6)	0

5.4.1.1 Prevalence of Plasmodium falciparum and non-malaria fevers

The majority of children in Junju were asymptomatic at the cross-sectional surveys in 2007, 2010 and 2013. In Junju, there were a total of seven non-malarial fevers, eight symptomatic *P. falciparum* infections and 208 asymptomatic *P. falciparum* infections, collectively, at the time of cross-sectional surveys. At the time of cross-sectional sample collection in Junju, asymptomatic parasitaemia was detected in 36% of the children in 2007, in 47% of the children in 2010 and in 32% of the children in 2013. In Ngerenya, a total of 11 non-malaria fevers were

reported at the time of cross-sectional sample collection and none of the children had detected parasites by qPCR throughout the follow-up.

Longitudinal active surveillance data (weekly case detection) on malaria in the children from Junju reported a total of 3278 *P. falciparum* infections during the study period 2005 to the survey in 2013. Malaria infections were invariably caused by *P. falciparum*, and parasite density measured by qPCR ranged from 1- 162 868 p/ µL blood (median= 45). During the surveillance period in Junju, the mean number of malaria fevers between 2005 and the survey in 2013 was 7 (range 1-57) per child and for non-malarial fevers was of 5.3 (range 0-16) per child. In Ngerenya, the mean number of non-malarial fevers was 5.5 (range 0-17) per child.

5.4.2 Telomere length decreased both, on an individual and population level

Telomere length was measured in 624 samples from Junju and in 262 samples from Ngerenya (**Figure 16**). On an individual level, TL decreased with age in 85% of all individuals, while the effect of age on TL was less pronounced in individuals with initially shorter telomeres, which was interpreted as lower TL shortening rate with time. TL also decreased with age on a population level (lme, Est.= -0.11, SE=0.04, t= -2.93, p=0.004), independent of sex (lme, Est.= 0.29, SE=0.15, t= 1.84, p=0.067) or cohort (lme; Est.= 0.13; SE=0.20; t= 0.65, p=0.52). The interaction between age and sex was tested non-significant in a separate LME analysis (lme, Est.= -0.01; SE=0.02; t= -0.07, p=0.94; **Table S6**) and thus, was excluded from the main model. Out of the cross-sectional surveys in 2007, 2010 and 2013, population TL was shortest during the survey in 2010 (lme, Est.= -1.38, SE=0.14; t= -9.84, p<0.001).

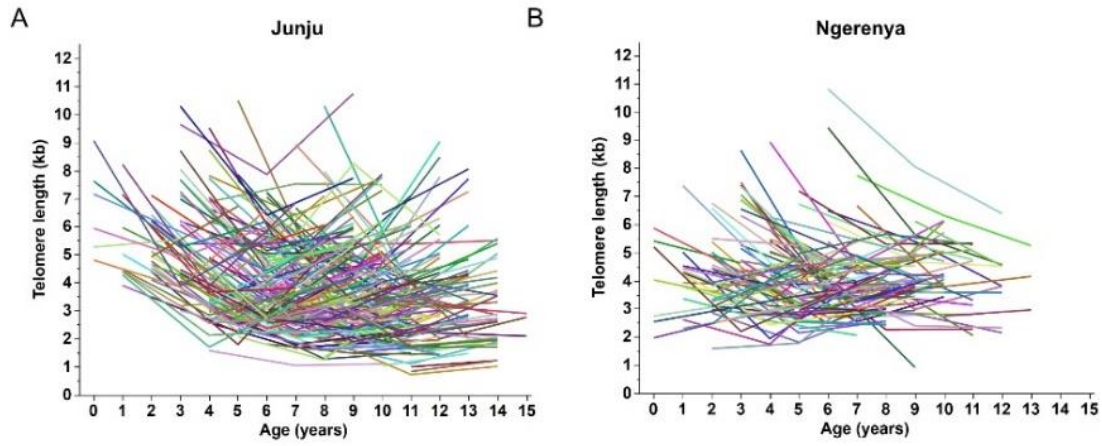

Figure 16. Individual telomere kinetics. *A) In malaria exposed Junju children and (B) in unexposed Ngerenya children.*

5.4.3 Non-malaria fever and *Plasmodium falciparum* infection at survey did not affect TL

Non-malarial fever at the time of cross-sectional survey did not affect TL when analyzing the cohorts jointly (lme, Est.= -0.11, SE= 0.25, t= -0.43, p= 0.66). A similar result was received when performing a sub-group analysis on each cohort separately (lme, Junju: Est.= -0.24, SE= 0.40, t= -0.61, p=0.54; Ngerenya: Est.= 0.02, SE= 0.30, t= 0.08, p=0.94).

At the time of cross-sectional survey, TL was not correlated with an ongoing febrile malaria episode (lme, Est.=-0.17, SE=0.37, t= -0.48, p=0.63), however, it seemed to be associated with asymptomatic *Plasmodium* infection (lme, Est.=0.22, SE=0.10, t=2.14, p=0.03). Yet, although significant, the effect of asymptomatic infection was small, hence, clinical relevance is uncertain.

5.4.4 Cumulative number of febrile episodes did not affect TL when adjusted for age

During the follow-up period from 2005 to the survey in 2013, an average of six cumulative febrile episodes per child was reported (7 in Junju, and 5.5 in Ngerenya; **Table 15**). The cumulative number of *P. falciparum* episodes (fever and parasitaemia >0) during the period 2005 - 2013 did not affect TL (lme, Est.=0.02, SE=0.01, t=1.23, p=0.22; **Table S6**), when

adjusting for age. A similar outcome was obtained when including only malaria episodes with parasitaemia > 2500 p/µl blood (lme, Est.=0.02, SE=0.02, t=1.23, p=0.22).

5.4.5 TL could not predict future symptomatic malaria infections

Cox-regression analysis on the association of TL in 2013 with the time to the first episode after the survey in 2013 revealed that TL in 2013 did not predict future symptomatic *P. falciparum* infection when adjusting for age (Cox regression, HRadj=1.05, p=0.21). A similar outcome was obtained when performing the model for TL in 2007 and 2010 and time to the first episode after the cross-sectional survey in 2007/2010 (Cox regression, 2007: HRadj= 0.94, p=0.13; 2010: HRadj= 1.03, p=0.66).

5.4.6 TL was longer in children with homozygous α –thalassaemia compared to children with a normal –haemoglobin genotype, but no differences in TL between the sickle and normal genotype

There was no difference between TL in children with a normal haemoglobin type, and carriers of the sickle trait (lme, genotype AS: Est.= -0.05, SE=0.21, t= -0.22, p=0.83; SS: Est.= -1.64, SE= 1.46, t= -1.13, p=0.26). However, children with homozygous α-thalassaemia had longer telomeres, compared to children with a normal haemoglobin genotype (lme, Est.= 0.45, SE=0.23, t=1.95, p=0.05).

5.4.7 Cohort specific analysis

Telomere length in Ngerenya was differently distributed over age compared to Junju, with more children presenting a smaller age effect on TL, and was further associated with sex (**Table 16**). Telomere length in Ngerenya children carrying the genotype for thalassaemia was longer compared to children with a normal haemoglobin genotype (**Table 16**). Furthermore, both survey years, 2010 and 2013 were negatively linked to TL in Ngerenya, which indicates the decrease in TL over time. Results from the Junju-specific analysis were similar to results from the main LME, which are presented in the result sections above. Nevertheless, TL in children

of both cohorts was shorter in the survey year 2010, with a more pronounced effect in Ngerenya.

Table 16. Sub -group analysis of exposed (Junju) and unexposed (Ngerenya) children.

	Junju					**Ngerenya**				
	Est.	SE	df	t	p	Est.	SE	df	t	p
Intercept	4.07	0.36	228	11.24	**<0.001**	4.96	0.45	88	11.06	**<0.001**
Age	-0.21	0.046	216	-4.63	**<0.001**	0.20	0.06	92	3.48	**<0.001**
Sex	0.16	0.20	210	0.81	0.418	0.45	0.20	84	2.21	**0.029**
Survey year 2010	-1.13	0.17	441	-6-53	**<0.001**	-2.15	0.20	160	-10.63	**<0.001**
Survey year 2013	0.34	0.31	310	1.1	0.276	-2.40	0.36	106	-6.77	**<0.001**
Cumulative malaria episodes	0.01	0.02	388	0.26	0.799	-	-	-	-	-
Status at survey										
Non-malarial fever	-0.24	0.40	431	-0.61	0.54	0.02	0.30	156	0.08	0.938
Symptomatic malaria	-0.07	0.38	440	-0.20	0.845	-	-	-	-	-
Asymptomatic infection	0.27	0.11	495	2.59	**0.01**	-	-	-	-	-
Sickle cell trait										
AS	-0.04	0.25	212	-0.17	0.87	-0.23	0.31	80	-0.74	0.465
SS	-1.91	1.49	135	-1.29	0.20	*NA*	*NA*	*NA*	*NA*	*NA*
Thalassemia										
Heterozygous	0.13	0.21	210	0.61	0.543	0.47	0.23	84	2.00	**0.049**
Homozygous	0.25	0.31	205	0.81	0.421	0.75	0.26	84	2.86	**0.005**

5.4.8 Summary of results

Taken together, this study chapter reveals that TL in children living in a malaria endemic area shortens with age on an individual and on a population level. TL was not affected by repeated febrile malaria and chronic malaria in exposed children, however, TL seems to be shorter in 2010 in children of both cohorts, with a more pronounced effect in Ngerenya, which might suggest other, non-malaria related factors affecting TL. A small effect of asymptomatic infection on TL was detected, however, future studies with larger study populations are needed to confirm this effect.

6 LONG-TERM CONSEQUENCES OF SYMPTOMATIC AND ASYMPTOMATIC MALARIA ON CELLULAR AGING IN A THREE-DECADE LONGITUDINAL COHORT STUDY IN TANZANIA

6.1 AIM

The aim of this chapter was to study TL dynamics across all aged individuals in a population living in a malaria endemic area and to assess whether repeated exposure to malaria causes long-term consequences on cellular aging.

6.2 BACKGROUND

People living in malaria endemic areas are repeatedly exposed to infectious mosquito bites and suffer multiple malaria episodes, which can lead to detrimental consequences on their life. Children in Sub-Saharan Africa are at particularly high risk of severe and fatal outcome before acquiring immunity that prevents symptoms and severe disease[104]. Partial immunity is gradually acquired after repeated *Plasmodium spp.* infections, but is largely inefficient at preventing and clearing asymptomatic low level parasitaemia [94]. These persistent low density asymptomatic infections are therefore highly prevalent in endemic areas, especially across large parts of Sub-Saharan Africa. Continuous exposure or persistent infections can lead to chronic activation of immune responses and low-grade inflammation, which might lead to long-term consequences such as inflamm-aging (an aging-associated inflammatory state) and senescence[105].

Results from our CHMI study (**Chapter 3**), including a pre-infection baseline sample confirmed that a single low density *P. falciparum* infection induced accelerated telomere shortening, with telomere dynamics being completely restored upon final treatment and clearance of infection[83]. However, whether repeated and persistent asymptomatic infections

have any long-term consequences on cellular aging in populations living in endemic malaria areas has not been studied.

Here, using a well characterized longitudinal population cohort from a rural village followed over three decades (since 1985), in Nyamisati in the Rufiji Delta Region, in Tanzania [106], we investigated the effect of malaria, both, symptomatic and asymptomatic infections on cellular aging by characterizing telomere length in yearly blood samples across different life stages within the same population. This chapter further aims to provide insights into TL dynamics in all-aged individuals across time.

6.3 STUDY-SPECIFIC METHODS

6.3.1 Study population

Nyamisati is a small rural fishing village, situated in the Rufiji River Delta on the East African coast, 150 km south of Dar es Salaam, Tanzania. The population in Nyamisati has been part of a longitudinal study on malaria epidemiology since 1985. Malaria transmission has been reported as high and perennial with seasonal fluctuations[107], however, a gradual decline in transmission intensity was reported after the establishment of a primary healthcare unit and a passive malaria case detection system during, and after providing anti-malarials and insecticide-treated bed nets (ITNs) free of charge[107]. The passive malaria case detection system was introduced and operated in 1985 and 1993-1999. Furthermore, yearly cross-sectional surveys were conducted in the years 1986-1989, 1993-1999, 2010 and 2016. These surveys consisted of blood sampling and a general health assessment including axillary body temperature, auscultation of lung and heart, and spleen examination in children. Optional HIV testing was performed during the years 1993-99, 2003 and 2010 in all ages, as described elsewhere[107]. Venous blood was collected in EDTA tubes at the research facility in Nyamisati. The samples were centrifuged and stored frozen as plasma and packed cells separately the same day, and stored at -20˚C. The samples were shipped frozen to Karolinska Institutet within 2-4 months after collection and stored at -80˚C, until further use. All villagers were invited to

participate in the yearly surveys starting from year 1986, except for 2016, where only children were included.

For the purpose of this study, 1002 individuals of all ages living in the village with cross-sectional surveys between the years 1986, 1993-1999, 2010 were randomly selected, as well as children (<11 years) in 2016. Available samples collected at the cross-sectional surveys were selected for analysis for the presence of malaria parasites by *Plasmodium*-specific qPCR. Clinical data and infection history from the clinical follow-up period in 1993-1999 was included in the analysis. The study design is outlined in **Figure 17**.

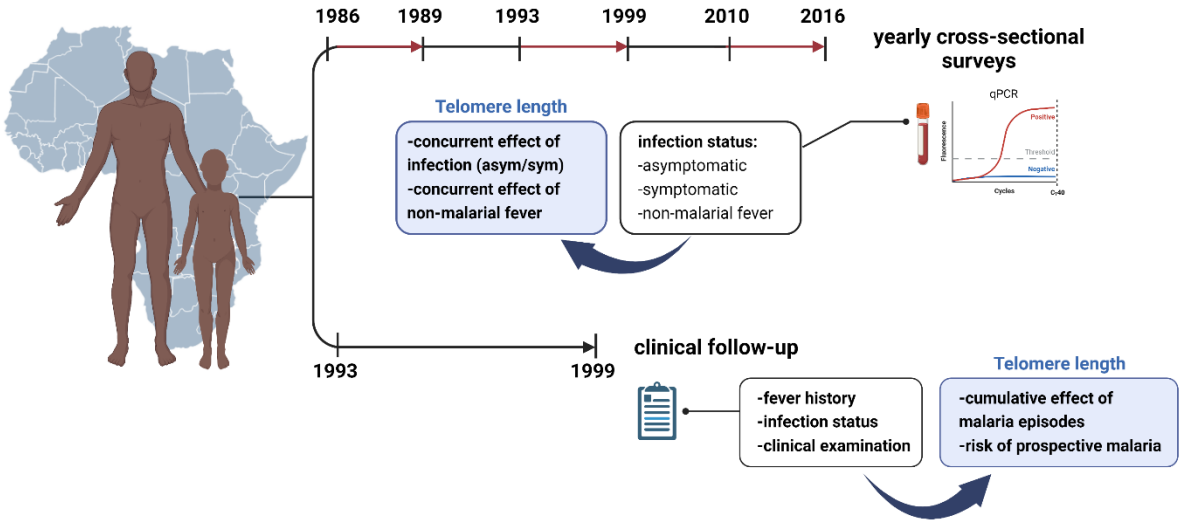

Figure 17. Study design. *All aged individuals from the cohort are followed longitudinally over time. Follow-up data is available from passive malaria case detection during 1986-1989, 1993-1999 and 2010-2016 and from a clinical follow-up period 1993-1999. (Figure by A. Miglar, designed in BioRender.com).*

6.3.1.1 Definitions of malaria

For the purpose of this study, a clinical episode of malaria was defined as detection of *Plasmodium sp.* parasites by microscopy and/or qPCR together with fever (axillary temperature >37.5°C) or reported hot body within the last 24 hours. Asymptomatic infections were defined

as detection of *Plasmodium sp.* parasites by microscopy and/or qPCR together with an axillary temperature <37.5°C and no history of fever within the last 24 hours. Individuals with fever (axillary temperature ≥ 37.5°C or reported hot body and no detection of parasites were referred to as having non-malarial fever. Parasite negative individuals without elevated body temperature were referred to as asymptomatic non-infected.

6.3.1.2 Ethical approval

The study was approved by the Nyamisati Village Board, the Ethical Review Board of National Institute for Medical Research in Tanzania, and the Central Ethical Review Board in Stockholm (Dnr 00-084, 2012/1151-32, 2015/2199-32 and 2016/1688-32). Informed written consent was given by all participants or their guardians.

6.3.2 DNA extraction and quantification

DNA was purified from frozen packed cells using QIAamp® DNA Blood Mini Kit (Qiagen), and a BioRobot Universal System (Qiagen), at Karolinska Institutet. Phenol-chloroform extraction was performed for a subset of samples (year 1999). DNA quantification was carried out on NanoDrop™ 2000 Spectrophotometer to verify the DNA quantity of all samples.

6.3.3 Telomere length measurement

Telomere length was measured in 2604 whole blood samples collected from 1002 study participants and their respective follow-up time-points, following the protocol described in section 2.3.2.2. Telomere length in kb was calculated using a human genomic DNA reference of 515 kb (# 8918d; Science Cell), resulting in the final calculation of $((2^{-} \Delta\Delta C_T \times 151)/92)$. Similar to the study described in **Chapter 3**, the human genomic DNA reference sample was included in the qPCR run of 92 samples on the single copy and telomere run and extrapolated for all other samples.

6.3.4 Parasite detection and species identification

The detection of malaria parasites and estimation of parasite density was determined by the examination of blood smears stained with 2% Giemsa using conventional light microscopy. Parasite density was calculated as the number of parasites per microliter blood (p/µL), presuming $5x10^6$ erythrocytes per microliter whole blood or 200 fields in thick films, as described elsewhere[107].

Parasite prevalence was confirmed by a *Plasmodium* species-specific real time PCR, following the protocol described in section 2.3.2.1, which further contributed with the more accurate identification of the *Plasmodium* species causing the infection.

6.3.5 Statistical analysis

The statistical analyses of this chapter are restricted to descriptive statistics, describing TL dynamics and the prevalence of *Plasmodium* infections over time. Further multivariate analyses accounting also for changes in malaria transmission over time will be performed.

Statistical analyses were performed in the Stata statistic software, version 16 (StataCorp. 2019. Stata Statistical Software: Release 16. College Station, TX: StataCorp LLC).

To assess changes in TL over time in the study population, a LME model was performed, with ID as random factor and potential cofounders (age, sex, survey year, hemoglobin level and fever at survey, microscopy and qPCR positivity, parasite density, cumulative number of malaria) as fixed factors.

Next, a linear spline mixed model was applied, dividing the study population into four age categories including childhood (0-11 years), adolescence (12-20 years), adulthood (21-60 years) and old age (61-100 years) that were included as age-splines in the model to receive a more detailed analysis of TL dynamics across age.

6.3.5.1 Prospective data analysis

Prospective approaches for this study include the assessment of the concurrent effect of symptomatic and asymptomatic malaria infection, and non-malaria fever on TL, using data retrieved from yearly cross-sectional surveys.

The next step will be to establish the cumulative effect of malaria episodes across years on TL, using data from the clinical follow-up period 1993-1999, which includes detailed information about fever history, infection status and clinical examination.

Finally, using these data, a Poisson regression model will be applied to determine the association of TL and the risk of prospective malaria.

6.4 RESULTS

The result section of this chapter includes preliminary descriptive analysis of the study population and telomere dynamics over time in all-aged individuals. Further statistical analyses of the effect of repeated symptomatic and asymptomatic malaria infections on TL need to account for changes in malaria transmission during the three decade long study period.

6.4.1 Characteristics of study population

In total, 2604 samples from cross-sectional surveys for 1002 study participants (mean = 2.6 samples per individual, range 1-10, **Figure S1**), and malaria records at these surveys were included in the analysis. Among these, 425 (42.4%) individuals contributed with a single cross-sectional survey, and 577 (57.6%) individuals contributed with multiple annual surveys (median= 3, range 2-10, **Table 17**). Age at individual baseline ranged between <1 and 96 years (median=18), and 524 (52.3%) individuals were female.

Table 17. Characteristics of study population.

		Age groups			
	All	**Childhood (<1 -11y)**	**Adolescence (12-20y)**	**Adulthood (21-60y)**	**Old age (61-96y)**
Number of individuals	1002	478	239	265	20
Age at inclusion, median (range)	18 (0 – 96)	8 (<1-11)	14 (12-20)	36 (21-60)	68 (61-96)
Sex ratio (M/F)	0.82 (1175/1429)	1 (239/239)	1 (120/119)	0.87 (104/161)	3 (15/5)
Mean number of TL-surveys/ individual (range)	2.6 (1-10)	2.3 (1-8)	2 (1-9)	3.7 (1-10)	3 (1-7)
Asymptomatic infection at survey*, n (%)	1241/2427 (51.1)	397/ 721 (55.1)	337/550 (61.3)	464/ 1059 (43.8)	43/97 (44.3)
Fever at survey, n (%)	205/2427 (8.4)	126 (61.4)	46 (22.4)	32 (15.6)	1 (0.5)
Malaria, n (%)	151 (73.7)	104 (82.5)	29 (63)	17 (53.1)	1 (100)
Non-malarial fever, n (%)	54 (26.3)	22 (17.5)	17 (37)	15 (46.9)	0
Parasites at survey (symptomatic and asymptomatic, %)	1392 (57.4)	501 (69.5)	366 (48.4)	481 (45.4)	44 (44.4)
Parasite density, parasites per µl, median (range)	400 (8-660000)	560 (8-660000)	320 (8-21280)	80 (8-4080)	8 (8)
Real-time PCR positive°, n (%)	1442/2548 (56.6)	510/761 (67)	391/584 (67)	496/1120 (44.3)	45/110 (40.9)
Microscopy positive°, n (%)	495/1549 (32)	285 /615 (46.3)	127/371 (34.2)	80/519 (15.4)	3/43 (0.7)
Microscopy and/or qPCR positive°, n (%)	1392/2427 (57.4)	501/721 (69.5)	366/550 (66.5)	481/1059 (45.4)	44/97 (45.4)
HIV positive/tested, (%)	14/458 (3.1)	1 (0.2)	1 (0.4)	12 (4.5)	ND

At the time of the cross-sectional surveys, 205 (8.4%) individuals had fever and 151 (74%) of the febrile individuals were parasite positive. Data on HIV status was available for 458 individuals, out of which 14 (3.1%) individuals had been tested HIV positive (**Table 17**).

To investigate TL dynamics across life, the study individuals were grouped into four age categories: childhood, 0-11 years (n=478; 47.7%); adolescence, 12-20 years (n=239; 23.9%); adulthood 21-60 years (265; 26.4%), and old age, 60-96 years (20; 2%; **Table 17**). Demographic characteristic of the study cohort across passive surveillance are outlined in **Table S7**.

6.4.2 Telomere length across ages

Telomere length decreased with age in the study population (**Figure 18A**, **B**, **C**, **D** and **Figure S2**). Results from our linear spline mixed model show that the rate of telomere shortening was highest during childhood (lme, coef.=-0.37 ± 0.023 SE, Z = -15.77, p< 0.001), followed by adolescence (lme, coef.=-0.11 ± 0.021 SE; Z= -5.18; p<0.001) and adulthood (lme, coef.=-0.06 ± 0.007 SE, Z= -8.16, p<0.001), while no significant change was observed during old age (lme, coef.= -0.01 ± 0.031, Z= -0.46, p= 0.649; **Figure 18C** and **Figure S2**).

In addition, TL differed between sexes (**Figure 18D** and **Figure S3**). More detailed age stratified analysis revealed no sex-specific difference in TL during childhood (lme, coef.= -0.03 ± 0.29 SE, Z = -0.11, p=0.912; **Figure 18E**), while females had longer telomeres during adolescence (lme, coef.= 0.59 ± 0.13 SE, Z = 4.62, p<0.001) and adulthood (lme, coef.= 0.48 ± 0.14 SE, Z = 3.41, p=0.001), however, this difference was not significant during old age (lme, lme, coef.= 0.41 ± 0.27 SE, Z = 1.51; p=0.13; **Figure 18E**).

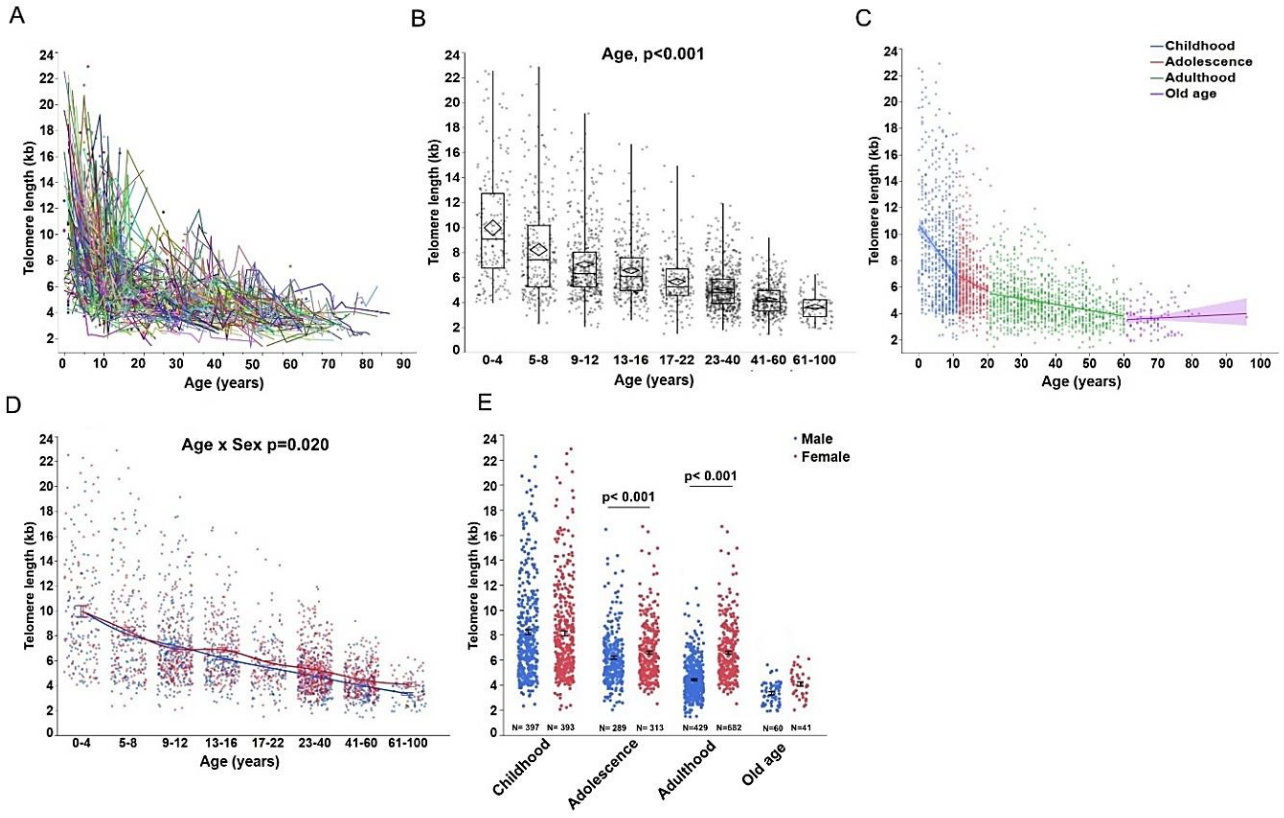

Figure 18. Telomere length dynamics with age in 1002 individuals residing in Nyamisati, Tanzania. *(A) Telomere dynamics with age; each line represents an individual. (B) Age-stratified analysis of the correlation of TL and age, based on multivariate analysis of longitudinal data; boxplots represent quantiles and median of the data, diamonds denote the 95% CI of the mean. (C) Linear splines showing the decrease of TL with age. Solid line represents the predicted mean, the shaded area denotes the 95% CI interval of the mean. (D) Sex-specific telomere dynamics of males (blue) and females (red) with age; dots represent the detected mean value ± standard error. (E) Age-stratified analysis of TL and age in males (blue) and females (red). Dots represent the mean value ± standard error.*

6.4.3 The effect of ongoing *Plasmodium* infection on telomere length

Plasmodium parasites were detected by microscopy and/or qPCR in 1392 (57.4%) of all samples (**Table 17**). Malaria parasite prevalence decreased across survey years in the study village, as previously described[107]. No microscopy data was available for years 1997 and 2010. Due to the interest of time and the complexity of data, including changes in malaria transmission and multiple time points per individual, the results are limited to descriptive

statistics and statistical analysis on the effect of malaria on TL is currently performed with the support of the Biostatistics Department at Karolinska Institutet.

7 DISCUSSION

The studies presented within this thesis investigate the effect of acute, chronic and repeated *Plasmodium* infection on cellular aging in humans. By analyzing data from longitudinal cohorts, including children, adults and elderly individuals, this work provides further insights into telomere length across life and discusses potential molecular mechanisms underlying the effect of malaria infection on telomere shortening. The combination of experimental infection and single-infection models with studies in populations living in endemic malaria areas contributes to a more comprehensive understanding on the impact of malaria on telomere dynamics, and provides insights into detailed dynamics, as well as potentially associated long-term consequences of infection.

7.1 TELOMERE DYMANICS BEFORE, DURING AND AFTER INFECTION

In **Chapter 3**, data is presented from a CHMI study that was performed at the Radboud University in the Netherlands. The study provides data on previously malaria naïve individuals that were experimentally infected with *P. falciparum*, strictly monitored, treated and followed over 64 days to study infection driven changes in TL dynamics and potential underlying mechanisms involved. Compared to previous study approaches, including individuals naturally infected with malaria[4], this approach included a sample prior to infection, enabling the detailed study of aging markers before, during and after infection.

This experimental approach minimizes the heterogeneity inherent in studies on natural infections, including history of malaria exposure and environmental factors such as co-infections; key factors that are well-known to influence TL and other cellular aging processes [4,46]. The benefit of the CHMI approach was the highly controlled setting and daily sampling

before and during infection, which facilitated the detailed study of the association of parasiteamia on TL.

Results from this CHMI study show a transient effect of malaria infection on TL. These results confirm findings in the travellers with a fulminant clinical *P. falciparum* infection, where the effect on cellular aging (accelerated telomere shortening and increased CDKN2A levels) was more pronounced, especially one month after diagnosis and treatment, and then appeared to be almost reversed after 12 months post diagnosis in the absence of reinfection[4]. Here, the results from the CHMI study reveal that TL fully restored to its pre-infection status after curative treatment. Concurrent with parasite levels peaking 10-13 days post CHMI, telomere shortening was accelerated in all 16 study individuals and reversed 64 days after the CHMI and after clearance of parasite levels. In contrast to the study in travellers with natural acquired infection, parasite levels in this study were extremely low and strictly controlled by low doses of subcurative treatment, which prevented clinical manifestations in all participants and provided an extended infection period. No effect was seen of the subcurative treatment on TL, which might be explained by the low, single doses administered (480 – 525mg).

Despite complete restoration of TL post CHMI, there was no significant change in telomerase TERT expression levels over the study period. However, TERT expression levels were slightly elevated upon time-point DT+1, which might have been enough to restore TL. These results are in line with the previous study in travellers that did not detect a significant correlation between increasing TL and TERT expression levels, despite a moderate increase of TERT expression over time[4]. One explanation underlying TL restoration could be the activation and differentiation of T lymphocytes as part of humoral immune response, which has been a long discussed hypothesis[18]. In response to immune activation or drug treatment, the majority of activated cells turn into apoptosis, while memory T and B cells with longer telomeres remain in circulation for longer time, which could partially explain telomere restoration in whole blood. Another plausible explanation could be the fact that infection leads to an increased cell

turn-over upon activated immune response or drug treatment, in which case TL measured in whole blood would reflect DNA dynamics of recently divided cells with shorter telomeres.

Another possible explanation for accelerated telomere shortening and increased CDKN2A levels in peripheral blood could be a change in cell composition during infection. However, in the travellers with natural infections, no significant correlation between TL and changes in overall cell compositions was found[4]. Yet, TL was not measured within the respective cell types, which was therefore performed in the study **Chapter 4** and is further discussed below.

7.2 ASSOCIATION OF AGING MARKERS AND AGING-ASSOCIATED MECHANISMS DURING INFECTION

The CHMI study further evaluates the relation between the aging markers TL and CDKN2A, as well as their interaction with inflammatory cytokine expression and antioxidant enzymes during infection. The concurrent attrition of TL with peak parasiteamia is most likely due to increased cytokine levels and reduced antioxidant defence that was observed in our study.

Reactive oxygen species (ROS) and inflammation are well characterized host responses to *Plasmodium* infection[108], which have further been described as potential contributors to age-related loss of homeostasis and health[24]. The production of ROS by host phagocytes is an essential part in the process of parasite clearance, nevertheless, excessive amounts of pro-oxygen compounds can mediate the production of chemokines and other inflammatory mediators[109], which can contribute to cellular injuries and aging in the absence of efficient anti-inflammatory defence systems[105]. In terms of cellular aging, an increase in pro-inflammatory cytokines has been shown to induce a reinforced senescence status, known as the SASP, which impacts the cell's plasticity and metabolic activity, as described in section 1.2.2 in this thesis[110].

The host immunologic response to acute malaria typically involves increased levels of the pro-inflammatory cytokines TNF-α, IL-1β, IL-6, IL-10, IL-12 and IL-18 levels[111-113]. The

Legendplex assays used here did detect significant increases in the plasma of several inflammatory cytokines during the CHMI compared to the time point before infection, including two of the above mentioned cytokines. However, levels of IL-1β and IL-6, key players in clinical malaria[114], together with TNFα were not detected. A similar effect has been reported in other CHMI studies[115,116]. The lack of detectable pro-inflammatory cytokines observed could reflect the strictly controlled study setting and suppression of parasite levels in the host already at low levels and study participants even rarely developed fever, as compared to severe clinical pathology in natural malaria infection where these cytokines are highly abundant. A more technical explanation could be the use of citrate plasma for cytokine measurement, which has been reported to compromise the IL-6 detection as described in Jager et al.[117].

Besides the host's production of ROS to counteract infection, the parasite itself aggravates the oxidative burden on the host by releasing free heme (a side product of the parasitic degradation of hemoglobin) at the end of its replication cycle in the blood, which might be an additional causative of accelerated telomere shortening observed in this CHMI. Oxidative stress has been linked to aging and pronounced DNA damage[118]. Telomeric DNA is particularly susceptible to ROS cleavage due to the high intrinsic sensitivity of the triplet G repeat sequences leading to single strand breaks and increased accumulation of critically short telomeres[119]. Critically short telomeres or damage in telomeric sequences are known mechanisms to induce cellular senescence[120], which might explain the increased CDKN2A levels detected during the CHMI and the previous study in travellers[4].

The accumulation of senescent cells in turn, leads to the acquisition of the SASP, which has a deleterious effect on the tissue microenvironment and further increases the levels of pro-inflammatory cytokines, including IL-6, IL-8 and INF-γ [121,122,123]. The pro-inflammatory phenotype consequently leads to an imbalance of the cellular redox state, generating even higher amounts of oxidative stress. It is well established that deprivation of antioxidant defence

mechanisms along with oxidative damage play a major role in several pathways leading to cellular senescence [124], mainly reasoned by declining levels of IL-10 causing inflamm-aging (an aging-associated inflammation state)[118,125].

Results from our CHMI study revealed the down-regulation of the antioxidant enzymes SOD1, SOD2, NOS3, CAT and GSTK during infection, which is in line with findings published from the same CHMI model by Reuling et al.[77]. These findings indicate an imbalanced oxidative stress homeostasis, which has been a relatively frequent finding in severe malaria infections[126,127]. As partially mentioned before, oxidative stress is commonly observed during malaria pathogenesis as a consequence of i) inflammatory processes initiated by the host's response to infection [126,127], ii) reactive species produced directly by the parasite [126], iii) *Plasmodium* infected erythrocytes producing twice as much hydroxyl radicals compared to uninfected erythrocytes [128] and vi) antimalarial treatment [129-131].

The association of cytokine levels, antioxidant enzymes, CDKN2A expression and TL in this CHMI study suggests that even a low density *Plasmodium* infection increases cytokine production and lowers the expression of antioxidant enzymes in the human host. Yet, all study markers were assessed in whole blood and it remains elusive, whether the observed effect is synchronized or rather cell-type specific.

In conclusion, using a CHMI approach with samples collected daily, **Chapter 3** characterized the impact of low-density malaria infection on cellular aging markers, and their complete restoration after clearing the infection. Results from our study present an integrative model of hallmarks of aging during infection, combining data of aging marker dynamics with inflammation and oxidative stress, generated by extremely low levels of malaria parasiteamia. Findings from this study revealed that even a short term exposure to *Plasmodium* affects markers of cellular aging with transient shortening of telomeres and increasing cellular senescence. These results urged the need to explore the impact of malaria in endemic areas,

considering the continuous exposure to the parasite, repeated clinical episodes, and chronic asymptomatic infections could potentially lead to permanent long-term consequences on cellular aging.

7.3 CELL-SPECIFIC CHANGES IN TELOMERE LENGTH DYNAMICS DURING INFECTION

Telomere length is usually measured in whole blood, thus peripheral leukocytes. Nonetheless, TL kinetics may be different in cell populations as a result of the immune response to infection. In a study in travellers with acute malaria, TL was shown to be shortened and later restored several months after infection when studied in peripheral blood[4], which was confirmed by results from our CHMI study presented in **Chapter 3** of this thesis. Yet, it is uncertain if the shorter TL is an overall effect in all cells or appears due to reduced TL in specific cell-subtypes.

To address this question in **Chapter 4**, we isolated PBMCs and sorted six different cell subsets, corresponding to approximately 85% of all cells constituting PBMCs at three time-points, during and after natural malaria infection in adults. We found that TL in PBMC and cell subtypes were correlated within each individual, and generally well correlated between cell subtypes, suggesting no apparent cell specific effect on TL within the PBMC compartment.

Only a few studies have examined TL in different cell subtypes over time. Lin et al., investigated TL in human B and T cell populations over time during steady state [132], while Olsson et al. evaluated TL in overall lymphocytes in reptiles [133].

A study by Sundling et al., investigating immune reactions in the traveller cohort, applied an exploratory approach with mass cytometry, followed by targeted flow cytometry to study cell-specific responses to natural acquired *P. falciparum* malaria[89]. Results from that study revealed an expansion of T helper cells and memory B cells, suggesting them as the most abundant cell

type changes, which further contributed to our interest in including B-cell subsets (naïve, memory and atypical B cells) in the experimental design of the study presented in **Chapter 4**.

In **Chapter 4**, changes in TL were studied during and after infection to assess whether TL attrition is a systematic effect or if it is rather cell-type specific. In the one-year prospective immunology study in travellers, Asghar et al. reported a decrease in peripheral blood TL until three months post diagnosis, with a gradual increase in TL reaching almost back to baseline after 12 months post diagnosis[4]. These results might to some extend represent lymphocyte TL and thus, it is relevant to further study TL in overall PBMC, and PBMC sub-sets.

Longitudinal changes in whole blood TL have further been shown in a study by Spurgin et al., reporting considerable fluctuations within individuals, including both decreased TL, triggered by age or external stressors, and also increased TL over periods of time [79]. Such temporary increases in TL are sporadic and might occur due to changes in the cellular composition of the blood or due to telomere elongation mechanisms [79,134]. The most commonly referred telomere maintenance mechanism is performed by the holoenzyme telomerase [135]. However, in a previous longitudinal study, there was no correlation between TL restoration and telomerase expression [4]. Alternatively, studies have further highlighted the importance of alternative lengthening of telomeres, including cellular mechanisms, such as homologous recombination mediated repair [136], or nuclear peripheral mechanisms, including the nuclear envelope in the maintenance process [137]. However, the mechanisms underlying TL restoration are not yet fully understood and further studies are needed.

Accelerated TL shortening in T cells has previously been described in vitro and in vivo in adults with chronic viral infection, including CMV, HIV, EBV and HCV [138]. Also, a study performed in HIV positive children reported accelerated telomere shortening in overall PBMCs, which seemed to be driven by CD8+ / CD28- differentiated T cells [139]. Shorter TL in T cells was further observed in another study on CMV infection, mentioning abundance of highly

differentiated T cell subsets [140]. The primary underlying mechanism of accelerated telomere shortening during chronic infection, but also cancer and autoimmunity was suggested to be persistent immune activation and cellular exhaustion mediated by replicative stress [141]. In the case of malaria, molecular mechanisms underlying telomere shortening in whole blood included increased oxidative stress and consistent low-grade inflammation [83].

Results from our study show an overall correlation of TL between PBMC and sorted cell sub-populations. It could be hypothesized that cell populations constituting PBMCs the most, also contribute the most to TL in PBMCs. However, the most abundant cell type constituting PBMCs are T cells and one could hypothesise that they are less responsive to external stressors (e.g. disease/ infection) as compared to innate immune cells (including NK cells and monocytes), considering the differences in their activation and response mechanisms, as well as antigen-specificity. Our results are contradictive to the results of the previously mentioned studies in T-cells, nevertheless, those studies did not study T cell TL within the context of other PBMC sub-populations. NK cells and monocytes are highly dynamic and responsive cell types during malaria infection, which could explain the stronger correlation of TL in NK cells and monocytes with TL in PBMCs, compared to TL in T cells in this study. Nevertheless, these cell types have previously not been investigated much in the context of TL and infection.

Furthermore, the overall TL change in the six cell subtypes was largely correlated between cell subtypes, but seems to be dependent on time of TL measurement and activation of the immune compartment. Our results further suggest somewhat different TL between immune cell-types, however, without reaching the significance level. Telomere length among all cell subtypes was longest in naïve B and atypical B cells, which might indicate cell-type specific responses to infection. These results are in line with the study by Lin et al., reporting that B cells have the longest TL out of total PBMC, B cells and three T-cell subtypes[132], and could have implications for our understanding of change in cell compositions during disease exposure.

Telomere length of total PBMC was partially correlated with TL in the sorted cell-populations when analyzing each time-point individually, similar to results reported in sorted cell populations in healthy pre-menopausal women followed over 18 months, by Lin et al., suggesting an overall TL shortening effect, rather than cell-type specific responses. Yet, despite a similar overall pattern within individuals, our results show inter-individual variation with no clear pattern, indicating that further studies including a bigger sample size are required to confirm our observations.

A limitation of this study is the low number of study individuals (n=13) and the broad age range (30-76 years). Nonetheless, the aim was to study the correlation of TL across PBMC sub-types within individuals, and not the effect of age on TL. Moreover, our study was based on stored PBMCs available from the cohort and as such, neutrophils constituting a large part of the leukocyte compartment in peripheral blood could not be included in the study. Hence, changes in TL measured in peripheral whole blood during and after infection that we previously observed could be contingent also to changes in TL of neutrophils rather than just PBMCs. This might explain why there was no as clear effect of infection on TL in total PBMCs, as compared to the overall effect shown in the previous study on TL in whole blood in these travellers with malaria[4].

7.4 THE EFFECT OF REPEATED SYMPTOMATIC AND ASYMPTOMATIC MALARIA ON TELOMERE LENGTH IN EXPOSED VERSUS UNEXPOSED CHILDREN

Studies in birds have shown that malaria affects cellular aging by accelerating TL shortening in whole blood and multiple body tissues[47], and that chronic malaria infection results in reduced host fitness and reduced lifespan[46]. In human, two studies in adults with acute malaria, one in travellers[4] and one in volunteers with induced malaria infection (**Chapter 3**), respectively, showed a transient effect of malaria on TL that was fully restored upon clearance of the parasite[4,83]. These results further urge the need to explore the impact of malaria in endemic

areas. Continuous exposure to the parasite with repeated clinical episodes, and chronic asymptomatic infections could potentially lead to permanent long-term consequences on cellular aging and immune function, which may cause irreversible health consequences in human.

Chapter 5 of this thesis assessed the effect of repeated exposure to malaria on TL in children (aged <1-15 years) from two culturally and socio-economic similar cohorts in Kenya, living with and without malaria transmission. Results from the study show that TL in malaria exposed children did not differ from TL in unexposed children. Moreover, children carrying asymptomatic parasitaemia at the time of survey did not have shorter telomeres but rather appeared to have slightly longer telomeres than uninfected children, although the effect was very small with the coefficient estimate reaching only 0.22. These results suggest that repeated exposure to malaria does not have any apparent consequences on cellular aging by driving accelerated telomere shortening in children of these two Kenyan cohorts.

Neither symptomatic *Plasmodium* malaria nor non-malarial fevers at the time of survey affected the TL in children in the two cohorts. These findings are in contrast to the previous studies in travellers with a single acute naturally acquired malaria infection, and volunteers with a CHMI that reported accelerated telomere shortening[4,83]. However, here only eight children had a symptomatic *Plasmodium* infection at the time of survey and TL was only measured at the time of infection, whereas the shortest TL in the travellers was detected one month after the infection was treated.

The infection effect on TL might, hence, not have been detected due to the high variation in telomere dynamics[79]. Both previous studies in adults report a malaria effect on TL after approximately 10-30 days post infection and an apparently complete TL restoration after successful treatment and 12 months in the traveller cohort, and 64 days in the CHMI cohort, respectively[4,83]. This indicates that infection with *P. falciparum* parasites might cause a

temporary change in TL kinetics, which can be fully restored by the host. Here, in the Kenyan children, changes in telomere kinetics might have therefore been missed as TL was measured at annual cross-sectional surveys three years apart.

The level of immunity might be another important contributing factor to consider when comparing the results from Kenyan children with travellers and infected volunteers. Study participants in the CHMI study[83], as well as in the travellers cohort[4] were malaria naïve, and the infection caused inflammation and reactive oxygen stress, which has recently been linked to accelerated telomere shortening[83]. Furthermore, a study by Lautenbach et al. revealed that the inflammatory response due to infection in the travellers was higher in primary-infected individuals, compared to previously exposed individuals with African origin[142].

Chapter 5 presents data on telomere kinetics in a malaria endemic area and long-term exposure to the *P. falciparum* parasite. This exposure has previously been shown to trigger adaptive immune responses that give rise to short-lived, low-affinity antibodies[143] and consequently a less severe parasite-host reaction [94]. Infants in endemic areas are relatively protected from early symptomatic malaria through the transfer of maternal antimalarial antibodies during pregnancy[144]. These antimalarial antibodies decrease around the age of 6 months leaving the infant more vulnerable to malaria[144], nonetheless these infections might still cause less inflammation and oxidative stress than in previously naïve adults.

Here, TL was measured at three annual surveys (2007, 2010 and 2013) and when stratifying our data by survey year, results revealed that the overall population TL was significantly shorter in children during the survey year 2010. Weekly surveillance data show that parasite prevalence was higher in 2010 compared to the other TL-surveys, however we observed a positive effect (i.e. longer TL) of asymptomatic parasiteamia on TL at the time of survey. We could not identify the reason for this finding, but one could speculate that an asymptomatic infection does not greatly affect TL due to malaria specific tolerance mechanisms of the human immune

system. This strategy might be common in endemic countries to keep the immune responses low and minimizing the pathogen damage to the host[145].

A recent study by Frimpong et al., evaluating senescence markers in T cell populations in children from Ghana, living in malaria endemic areas showed that the senescence phenotype of T cells in children with asymptomatic *Plasmodium* infection did not differ from the one in healthy children[146]. These results confirm our findings, as cellular senescence and telomere shortening are well correlated markers[147].

The shorter TL dynamics in 2010 for both cohorts, and additional in the years 2007 and 2013 for Ngerenya could not be explained by spatio-temporal changes that might differ between the cohorts, despite sharing similarities in culture, genetics and socio-economic structure, as described in a study by Spurgin et al.[79]. Another study in birds including cross-sectional and longitudinal data on Seychelles warblers of 22 different cohorts, further points out that TL variation is associated with temporal variation and availability of nourishment[79]. The same study reports a high variation of individual TL dynamics over life, including TL increases, and the statistical support that the increases are unlikely to be explained solely by qPCR measurement errors, which might further explain the telomere dynamics of both cohorts in this study.

Furthermore, if malaria had a major impact on TL, we would have expected to see an effect of sickle hemoglobin on TL, as sickle cell trait is well recognized to protect against malaria[148]. According to the hypothesis that malaria leads to accelerated TL attrition, children with a normal hemoglobin genotype should have had shorter TL than children carrying the sickle cell trait. Nevertheless, despite active weekly surveillance, capturing all malaria morbidity, there was no effect of sickle trait on TL in this study. Moreover, we cannot explain the tendency of increased TL in children with thalassemia trait in Ngerenya. It has been reported that α-thalassemia, both homozygous and heterozygous, is associated with significant reductions in

the rate of hospital admission due to malaria, and lower rates of severe disease outcome and anemia in Kenyan children[149]. Nevertheless, the effect of thalassemia heamoglobinpathy is more pronounced in Ngerenya, the malaria-free control group. However, this was detected in only few individuals, hence the effect on TL remains uncertain.

The limitations of the study are that TL was measured only at three time-points, each three years apart, which could have led to limitations on detecting detailed changes in telomere kinetics. Nonetheless the strength of this study is the availability of weekly active and passive surveillance data, including detailed information about cumulative malaria infection in children living under different malaria transmission, longitudinally followed over an average of 11 years.

Findings from the study in **Chapter 5** are thus not consistent to results from a study in birds chronically infected with malaria, which demonstrated that chronic malaria accelerates telomere shortening and reduces individual lifespan[46,47]. Besides the correlation of reduced telomere length and lifespan[46], studies revealed that also the rate of telomere loss is linked to the individuals' life expectancy, and potentially predicts its lifespan[150-152]. Nevertheless, avian malaria pathophysiology differs from the one in humans, considering that birds have nucleated erythrocytes and are infected by a different parasite species and mosquito vector. Moreover, birds have much shorter lifespan than humans. Yet, the implication of our findings on the lifespan of malaria exposed human populations is unclear and it has been well established that the immune system in children is immature and still develops throughout life, raising the question, whether the observed effect may have effects later in life, as the individuals reach adulthood and old age.

In Sub-Saharan Africa, malaria has a considerable impact on mortality, especially in children under the age of five. Results from a longitudinal demographic analysis in Ghana, applying single-decrement life-table methods suggest that life expectancy at birth could be expected to

increase by more than 6 years if malaria was eliminated[153]. Data published by the International Network for the Demographic Evaluation of Populations and Their Health (INDEPTH) network further provides insights into malaria age-group-specific death rates and revealed a U-shaped mortality curve for populations living in high transmission areas in Africa, indicating higher case-of death rates owed to malaria in adults and elderly[154]. Similar results were obtained from 'The 2010 Million Death Study' based on data obtained in high malaria transmission areas in India[155].

Taken together, this is the first study assessing the effect of repeated and chronic malaria infection on telomere dynamics in endemic settings. Our study reveals that TL shortens with age, but is not affected by repeated exposure to malaria infection in children, which could further be caused by consequences of infection (i.e. anemia), which was not studied here. A study including more consecutive measurements of TL in larger populations with a longer follow-up time and across all ages, including adults, could further contribute to understanding the impact of repeated and chronic malaria exposure on cellular aging and its long-term impact on host fitness.

7.5 LONG-TERM CONSEQUENCES OF REPEATED SYMPTOMATIC AND ASYMPTOMATIC MALARIA ON CELLULAR AGING IN A THREE-DECADE LONGITUDINAL COHORT STUDY IN TANZANIA

Comprehension of telomere dynamics in human is mainly based on single time-points and only a few longitudinal studies with limited number of time points that suggest that TL is determined by genetics and shaped by environmental factors[156-158]. As previously mentioned, in humans, both, natural and experimental acute malaria infection outside malaria endemic areas have shown to affect cellular aging markers in whole blood[4,83]. Results from these studies provide insights into the natural telomere kinetics after a single cured malaria episode. Contrarily, results from **Chapter 5** revealed that repeated malaria infection did not affect telomere kinetics

in Kenyan children (<1-15 years) that were exposed to *P. falciparum* compared to age-matched unexposed children, with no difference in the rate of telomere shortening between the two groups.

Preliminary data presented in **Chapter 6**, includes more consecutive measurements of TL in a larger population with a longer follow-up time and across all ages, including adults. The study applies 34-year longitudinal data from a rural fishing village in Nyamisati, Tanzania to investigate the effect of repeated clinical episodes of malaria and asymptomatic *Plasmodium* infections on cellular aging by accelerating telomere shortening. Preliminary results introduce longitudinal telomere dynamics across all life stages within the same population, which has never been shown before.

In the past decades, TL was recognized as one of the most relevant biomarkers of aging, due to the fact that telomeres are known to be critically implicated in cellular aging [150,159,160]. Furthermore, in an epidemiological point of view, TL has shown to reflect the risk for age-related chronic pathological conditions[161]. Confirming previous studies, this study reports age-dependent telomere shortening, and further shows the high variability in the rate of telomere shortening at different life stages. Existing studies, including a Swedish twin study, showed that the rate of telomere loss varies between early life and adulthood [150,159,160,162] and suggest that it is highest in early life [13]. Yet, to fully understand the dynamics of TL and rate of telomere loss during different life stages, requires longitudinal data from all aged individuals of the same cohort, which is scarce. Results from our 34-year longitudinal data show that the highest telomere shortening-rate was observed in childhood, followed by adulthood, adolescence and old age, respectively.

Further, dissecting the effect of infection from the pervasive age effect in this study, results reveal that after fluctuant telomere shortening rate during childhood, telomeres shortening rate remains consistent once reaching adolescence. These results are contrarily to existing studies,

claiming that telomere loss stabilizes not earlier than in adulthood [163]. However, the age effect on telomere shortening seems to be redundant in individuals of old age, which might be due to low sample size of individuals older than 60 years. An alternative explanation could be natural selection, promoting individuals with longer telomeres to live longer, which in turn leads to an elderly population represented with longer telomeres, the so-called centenarians. This hypothesis is supported by Benetos et al., suggesting that individuals who enter adulthood with longer telomeres are likely to maintain this status during the remaining lifetime[164]. Furthermore, TL in whole blood has been linked to mortality in elderly patients (<60 years)[37].

Furthermore, our study shows that average telomere attrition rate in children is approximately three to four-fold higher than in adults, as further extrapolated in previous studies[165,166]. One explanation could be the drastic increase in cell replication and turnover rates during early somatic development that leads to a rapid and intermitted loss of telomeres[167], nevertheless, in this study setting, malaria infection might be an additional contributor.

The data further characterize a sex-specific difference in TL, with females having longer telomeres than males. Similar results have been reported in previous studies by Barrett et al., and others[168-170]. Yet, as TL at birth does not differ between sexes[171,172], it has been unknown at what stage in life women attain longer telomeres than men. To estimate and evaluate inter-sex changes in TL during lifetime, consistent follow-up data from all age individuals are required. Here, the longitudinal data over three decades including all-age individuals (<1 to 96 years) are provided, and reveal no sex difference in TL during childhood (1-11 years age), while girls seem to have longer telomeres during adolescence (12-20 years) and maintain this difference throughout adulthood and old age. Results obtained from these longitudinal data are the first to provide longitudinally measured telomere dynamics within closely monitored individuals of the same cohort and adds novelty to the field of telomere research.

The exact mechanism behind this observation is yet to be understood, however, it has long time been hypothesized that biological factors, such as steroid hormones are an explanation for females having longer telomeres than males. The sex steroid hormone estrogen is found at higher levels in females and is thought to activate the holoenzyme telomerase[173]. Additionally, compared to the male sex hormone testosterone, estrogen exhibits antioxidant property, protecting telomeres from extensive oxidative damage [172,174]. In contrast, a cross-sectional study in children during early adolescence (8-14 years) reported that sex differences in TL are not mediated by sex steroid hormones[175]. Alternatively, it has been suggested that basic genetic and physiological differences are involved[168]. Some telomere maintenance genes reside on the X chromosome, and while females benefit from the preservation of chromosomes with longer telomeres due to X-inactivation, males have a natural disadvantage of having only one X chromosome, increasing the risk of mutations or malfunction in those genes[176,177]. Nevertheless, we hypothesize that also steroid sex hormones may play a role in telomere dynamic changes, considering their effect on redox balance and telomere maintenance, noticing that the sex difference appears simultaneously with entering puberty.

Collectively, preliminary data presented in **Chapter 6** confirms TL as pronounced marker to estimate population lifespan, when controlling for external stimuli, as proposed in multiple other studies[13,178]. Remaining analyses will further provide insights on whether repeated symptomatic and asymptomatic malaria contribute to long-term consequences in the host, by accelerating cellular aging. Over the course of this study, malaria transmission in the Nyamisati village has changes substantially from very high transmission between the years 1985-1993, followed by a significant decline in transmission between the years 1993-2010 and consistent low-moderate transmission to the present day[106,107]. Results from our analyses will provide substantial knowledge on how these changes affect telomere dynamics in the population of this village. Despite the significant value of longitudinal cohort studies in the interdisciplinary field of aging and infectious disease research, analyses on the retrieved data are challenging as

multiple co-factors need to be considered on a population and on an individual level, including changes in disease transmission over time, co-infections, socio-economic factors, as well as host genetics.

Despite the longitudinal value the study will add to the telomere work, an important factor to consider when interpreting the results are the conditions of sample collection and long-term storage, which has previously been critically evaluated in telomere studies, as further discussed in section 9.1. The sample collection for this study was performed in a remote village in rural Tanzania under simple conditions, and freezing conditions in the early years of the study were limited, which might be a limitation that we are aware of.

8 MAIN FINDINGS

- A single *Plasmodium falciparum* infection causes a transient effect on TL and cellular senescence, which is restored after sucessful treatment and clearance of the parasite.

- The aging markers TL and CDKN2A are significantly inter-correlated with inflammation and an inbalanced redox-homeostasis during acute malaria infection.

- Telomere length dynamics in peripheral whole blood are largely synchronized across immune cells during infection, and changes in TL in PBMCs seem not to be associated with changes in cell compositions.

- Telomere length shortens on an individual and population level across all ages and is longer in females upon reaching adolescence.

- Telomere length dynamics are similar in malaria exposed and non-exposed children in endemic areas, and the cumulative number of malaria episodes or ongoing asymptomatic infection did not have an apparent effect on TL shortening.

Taken together, results from this thesis imply that acute malaria infection causes transient accelerated telomere shortening in humans, driven by increased inflammation and oxidative stress caused by the parasite and the host immune response. Nevertheless, in the analyses so far, we did not find any evidence of malaria affecting TL in populations living in endemic areas that are chronically exposed to malaria.

8.1 STUDY CONSIDERATIONS

First and foremost, it is worth to mention that the integrity of TL as biological aging marker has long been debated, yet, extensive research within the past years and latest reviews have contributed to the establishment of TL as cellular marker of aging [179-183], justified by its role of

DNA stability and integrity[184] (one of the hallmarks of aging), its association with individual life-span[46] , morbidity and the risk for mortality[37,185] and various age-related pathologies[186-189], which provides further support for its intrinsic property of cellular aging.

An overall aspect to consider when interpreting results presented in this thesis is the heterogeneity in sample collection and storage. For the majority of our studies, the samples were collected and stored long time before analysis and we are aware that this might be a limitation to the work.

Reviews on longitudinal telomere studies addressed that heterogeneity in sample storage potentially impacts telomere measurement[190,191]. Precioso et al. reported storage-dependent degradation of TL that caused TL shortening during the first four years of storage of blood in ethanol, while after that the degradation stops[192]. Nevertheless, I would like to add that none of the samples included in this thesis were preserved in ethanol. A study in birds evaluated the impact of storage methods similar to the ones applied in this work and revealed significant correlations between TL measurements in samples stored as whole blood at −80 °C or stored as extracted DNA at −80 °C [191].

In order to reduce the number of factors impacting our TL measurements, we followed the recommended protocols on sample collection and storage published by the Blackburn Telomere Research Core and the Telomere Research Network, as far as practicable, to maintain consistency of sample storage and DNA extraction.

In conclusion, the limitation with long term storage of archived samples is inherent in longitudinal studies in the field of aging. On the one hand, longitudinal data on TL provide more robust information on aging dynamics and are fundamental for predictive studies, while on the other hand, it cannot be ruled out that multiple samples per individual, collected at different time points introduce measurement errors.

9 CONCLUDING REMARKS AND FUTURE PERSPECTIVES

This thesis aimed to better understand the causal link between *Plasmodium* infection and cellular aging in humans. Despite from being far from understanding the complex relationship between biological aging and infection, the findings herein help us to understand telomere dynamics across life and to counteract the complexity and the inter-relation of aging markers and aging-associated mechanisms during infection, and further help us to comprehend the impact of malaria infectious on African populations. This thesis has described some findings, which to some extend contradict earlier studies in birds, revealing an effect of repeated and chronic malaria infection on TL. Here, we find transient TL shortening during and after an infection in non-immune individuals, but could not find that repeated febrile malaria episodes or asymptomatic infections in Kenyan children resulted in persistent telomere shortening.

An important aspect to consider when interpreting results from animal and human studies is that telomere dynamics and telomere maintenance mechanisms behave differently across species[150,193,194]. Despite mice, birds and humans sharing identical telomeric sequences, differences are found in the initial TL (*Mus musculus* 50kb; Audouin's gull 35kb, *Homo sapiens* 15kb), in the yearly rate of telomere shortening (*Mus musculus* 7000bp/y; Audouin's gull 771bp/y, *Homo sapiens* 71bp/y) and telomerase expression[150]. While TL in mice is 5-10 times longer, their life expectancy is 30 times shorter compared to humans. Birds additionally share haematological differences by having nucleated erythrocytes in contrast to humans and mice, which further needs to be considered when comparing blood TL across animal and human studies. Nevertheless, research across species is important and contributes to a basic understanding of the determinants of longevity, as well as to the interdisciplinary relationship of cellular aging and environmental factors, including infections.

This thesis provides novel insights into the dynamics across life and elaborates the impact of acute and repeated malaria infection on cellular aging in humans. The findings contribute to the understanding of the relationship between infectious diseases and cellular aging in humans. However, caution needs to be exercised when interpreting our results from chapters 3, 5 and 6, as TL in the respective studies is measured in whole blood. Study results from Chapter 4 emphasize the significant change in immune cell populations during infection and to fully understand the associated changes in telomere dynamics, the research on immune responses during aging needs to be expanded. Further, differences in changes in TL might also occur between tissues[47], which also needs to be accounted for in future studies.

The complexity of aging dynamics during infection is challenging, as many potential co-founding variables need to be accounted for. Besides oxidative stress and low-grade persistent inflammation, several other factors were shown to influence cellular aging, including not only genomic factors characterizing aging on a cellular and molecular level (hallmarks of aging), but also epigenetic modifications[195] and the impact of the exposome, which captures all environmental exposures across lifetime, both abiotic[196,197] and biotic stimuli[198,199]. The modulation of the interplay of (epi-) genomic and environmental influences on aging urgently requires to determine whether the hallmarks of aging function simultaneously, cumulatively, or independently with the exposome[199]. Moreover, building on our results, it will be exciting to conduct longitudinal studies combining the parallel research of multiple aging markers, including mitochondrial dysfunction and epigenetic alterations. Also, in depth analysis of aging associated mechanisms, including the implementation of inflammatory versus non-inflammatory infection models, could further contribute on the interplay of the aging paradigm during infection.

On an overall perspective, future analyses on cellular and molecular aging-mechanism should estimate aging dynamics not only in cells, but on an organismal level. In an interview about

human longevity, Ilia Stambler, senior scientist and author of the book ‘Longevity Promotion: Multidisciplinary Perspectives’, raised the issue of researchers being committed to the ‘molecular gaze’, rather than considering the entire human organism when studying aging mechanisms. He further emphasized the lacking collaboration between clinicians and scientists that would benefit the fundamental science in the aging field.

This thesis further provides implications on our understanding of host-pathogen. Our results did not find evidence that repeated malaria exposure cause long-term consequences, however, there was a trend of asymptomatic infection affecting telomere length. These results imply the urgency to continue carrying out studies in malaria-endemic areas to better understand the impact of asymptomatic infections on cellular aging and the interplay of immunology, and further to evaluate the role of TL as predictive marker for immunity and risk for prospective malaria infection.

In the future, it will also be exciting to see how advanced methods of investigating aging dynamics in human, such as heterochronic parabiosis experiments, studies on DNA fidelity and hematopoietic stem cell (HSC) rejuvenation can be utilised to provide answers to outstanding questions in the relationship between infectious diseases and aging in this context of upscaling and promoting a healthier lifespan.

10 ACKNOWLEDGEMENTS

First and foremost, I would like to thank all the study participants of the cohorts presented in the chapters of this thesis. I further would like to acknowledge all funding sources that have supported this work, including the Ragnar Söderberg Foundation, the Swedish Research Council, Karolinska Institutet Funds and Foundation, including the KI-internal doctoral student (KID) funding; as well as all the people and collaborators who have provided the groundwork, infrastructure and the scientific expertise for my studies.

I would like to express my great appreciation to **Anna Färnert** for taking over as my main supervisor and for providing continuous support and knowledge during the writing process of this thesis. Anna, your outstanding support and expertise in the field of malaria has significantly contributed to the work presented here. Throughout the years you have given me the opportunity to not only develop my scientific interests, but further let me explore the world outside academia. Anna, your door has always been open, regardless of what time of the day and no matter how small the problem seemed to be. Thank you for your vast support. Thank you also to my co-supervisor, **Eduardo Villablanca**, for sharing his inspiring insights on the projects and for being a supportive part of my supervisor team.

I wish to acknowledge my former supervisor **Muhammad Asghar** for introducing me to the field of aging research and for the financial support.

I further want to thank **Matteo Bottai** and his team at the Department of Biostatistics, Karolinska Institutet for statistics support, and **Sara Hägg** for the critical evaluation of the study design and applied statistics in this work. My appreciation also goes to **Univ.-Prof. Mag. Dr. Karl-Heinz Wagner** und **Prof. Akira Kaneko**, for the thorough assessment of my thesis work.

My gratitude further goes to our collaborator **Dr. Francis Ndungu** – Francis, despite not being officially part of my supervisor team, you have substantially contributed to the highlights of my PhD. Thank you for welcoming me to your laboratory at the KEMRI Wellcome Trust Institute in Kenya and for making me feel like home during my 5-month research stay. *Asanti sana* for all the late night scientific discussions, your extensive knowledge on malaria immunology and last but not least, my birthday *mbuzi*. I would further like to thank **Jedidah Mwacharo**, **Jennifer Musyoki**, **Barnes Kitsao** and **David Amadi** for their assistance during my project at KEMRI and **Philip Bejon** and **Tom Williams** for their relevant input on the manuscript. Special thanks also to **Brian Bartilol**, **Charles Kolombo**, **Rinter Kimathi**, **David Lavu**, **Diana Nyabundi**, **Charles Kevin Kamau (CKK)**, **Alex Macharia**, **Johnstone Makale**, **Eunice Chege**, **Hilda Wacuka, Emily** and **Timothy Kuria** for making my time in Kilifi remarkably memorable - I will always think back to these days with joy and euphoria.

Thank you to all the present and previous members of the **Färnert lab** and **Broliden lab** for the daily company and celebrations of the small successes. To **Chris**, **David** and **Julius** for making the MAM conference in Australia so special, and for putting up a portable speaker once the DJ stopped the music. To my 'hard-core' scientists **Julia**, **Ioanna**, **Matthias**, **Vilde**, **Alan, Zaynab, Rebecca** and **Lin** for always having each other's back. To **Gabi** and **Frideborg**, who I looked up to the first days I joined the lab. **Doreen**, for our joint journey from a summer internship to the PhD – interrupted, not only, by a monkey breaking into our bathroom. To **Sahra Bunner** for helping out with the administration. A special thanks to **Fariba**, who is an absolutely indispensable member of our lab. Fariba, you are one of the most caring and loving people I met, thank you for everything during the past years. I am particularly thankful for **Amani** having joined the lab, even if just for a short time. Amani, working with you has given me so much strength, love and countless reasons to laugh about. I would have never accomplished this without having you by my side.

My appreciation further goes to **Michael Fored**, **Bob Harris**, **Ingeborg Van De Ploeg**, **Claes Frostell**, **Åsa Samuelsson Ökmengil, Ninna Oom** and **Nazira Hammoud Shahwan**, for their advice and support in conquering challenges that seemed far from being feasible.

Love and gratitude to all the beautiful people I met on the way (in no particular order): **Rico&Rebeca**, **Dr. Rub** (we ruled the CMM dancefloor!), **Sanna**, **Jill**, **Kasra**, **Sissi**, **Makpal**, **Jens**, **Felix**, **Captain J., Alessandro**, **Lucia**, **Ulla**, **Malvina**, **Isi**, **Lena**, **Vahid**, **Flavio**, **Matthias**, **Tesi**, **Akua**, **Omid**, **Astrid, Patrick** and **Marco**.

I thank all my friends from **Run Collective** (prev. SSideline City) for the best Tuesday and Saturday runs, sauna sessions, crayfish parties, adventures – and for running my first half-marathon with me. I made friends for life.

I am also thankful for all the support I received from back home, including letters, WhatsApp calls and visits from **Nina**, **Melissa, Johanna** und **Hanna**. Danke Mädels, dass ihr immer fuer mich da seid und es immer wieder schafft mir ein Lächels aufs Gesicht zu zaubern! **Thomas** - egal ob in Krems oder in Wien – die richtige Mischung aus Abenteur und Bier stimmt immer!

Finally and most importantly my vast gratitude goes to my beloved parents. **Mami**, **Papi**, without your enormous love and support I would have never gotten this far in life. I was once asked what my parents could have possibly done better when raising me. I could not think of a single thing. Thank you for always believing in me and for the tremendous support throughout the past five years. It was you who kept me going. Ich hab euch lieb.

The past years have taught me independence, resilience, and enormous strength – which will take me far in life.

Memories of meeting Prof. Elizabeth Blackburn, winner of The Nobel Prize in Physiology or Medicine 2009, “for the discovery of how chromosomes are protected by telomeres and the enzyme telomerase”, at the Nobel Week Dialogues in Stockholm, 2016. Her discoveries lay the foundation for my work and passion for science.

11 REFERENCES

1 Yoshikawa, T. T. Epidemiology and unique aspects of aging and infectious diseases. *Clin Infect Dis* **30**, 931-933, doi:10.1086/313792 (2000).

2 Gavazzi, G. & Krause, K. H. Ageing and infection. *Lancet Infect Dis* **2**, 659-666 (2002).

3 Durso, D. F. *et al.* Living in endemic area for infectious diseases accelerates epigenetic age. *Mech Ageing Dev* **207**, 111713, doi:10.1016/j.mad.2022.111713 (2022).

4 Asghar, M. *et al.* Cellular aging dynamics after acute malaria infection: A 12-month longitudinal study. *Aging Cell* **17**, doi:10.1111/acel.12702 (2018).

5 Lopez-Otin, C., Blasco, M. A., Partridge, L., Serrano, M. & Kroemer, G. The hallmarks of aging. *Cell* **153**, 1194-1217, doi:10.1016/j.cell.2013.05.039 (2013).

6 Daniali, L. *et al.* Telomeres shorten at equivalent rates in somatic tissues of adults. *Nature Communications* **4**, doi:ARTN 1597, DOI 10.1038/ncomms2602 (2013).

7 Zhao, Y., Shay, J. W. & Wright, W. E. Telomere G-overhang length measurement method 1: the DSN method. *Methods Mol Biol* **735**, 47-54, doi:10.1007/978-1-61779-092-8_5 (2011).

8 Blackburn, E. H., Epel, E. S. & Lin, J. Human telomere biology: A contributory and interactive factor in aging, disease risks, and protection. *Science* **350**, 1193-1198, doi:10.1126/science.aab3389 (2015).

9 Gu, B. W. & Mason, P. Telomere 3' overhang and disease. *Leuk Lymphoma* **54**, 1347-1348, doi:10.3109/10428194.2013.769538 (2013).

10 de Lange, T. T-loops and the origin of telomeres. *Nat Rev Mol Cell Biol* **5**, 323-329, doi:10.1038/nrm1359 (2004).

11 Diotti, R. & Loayza, D. Shelterin complex and associated factors at human telomeres. *Nucleus* **2**, 119-135, doi:10.4161/nucl.2.2.15135 (2011).

12 Wynford-Thomas, D. & Kipling, D. The end-replication problem. *Nature* **389**, 551-551, doi:10.1038/39210 (1997).

13 Heidinger, B. J. *et al.* Telomere length in early life predicts lifespan. *Proc Natl Acad Sci U S A* **109**, 1743-1748, doi:10.1073/pnas.1113306109 (2012).

14 Monaghan, P. Telomeres and life histories: the long and the short of it. *Ann N Y Acad Sci* **1206**, 130-142, doi:10.1111/j.1749-6632.2010.05705.x (2010).

15 Okuda, K. *et al.* Telomere length in the newborn. *Pediatr Res* **52**, 377-381, doi:10.1203/01.Pdr.0000022341.72856.72 (2002).

16 Niccoli, T. & Partridge, L. Ageing as a Risk Factor for Disease. *Curr Biol* **22**, R741-R752, doi:10.1016/j.cub.2012.07.024 (2012).

17 Ben-Porath, I. & Weinberg, R. A. The signals and pathways activating cellular senescence. *Int J Biochem Cell Biol* **37**, 961-976, doi:10.1016/j.biocel.2004.10.013 (2005).

18 Weng, N. P. Telomere and adaptive immunity. *Mech Ageing Dev* **129**, 60-66, doi:10.1016/j.mad.2007.11.005 (2008).

19 Atzmon, G. *et al.* Evolution in health and medicine Sackler colloquium: Genetic variation in human telomerase is associated with telomere length in Ashkenazi centenarians. *Proc Natl Acad Sci U S A* **107 Suppl 1**, 1710-1717, doi:10.1073/pnas.0906191106 (2010).

20 Victorelli, S. & Passos, J. F. Telomeres and Cell Senescence - Size Matters Not. *Ebiomedicine* **21**, 14-20, doi:10.1016/j.ebiom.2017.03.027 (2017).

21 Hayflick, L. & Moorhead, P. S. The serial cultivation of human diploid cell strains. *Exp Cell Res* **25**, 585-621 (1961).

22 McHugh, D. & Gil, J. Senescence and aging: Causes, consequences, and therapeutic avenues. *J Cell Biol* **217**, 65-77, doi:10.1083/jcb.201708092 (2018).

23 Ray, D. & Yung, R. Immune senescence, epigenetics and autoimmunity. *Clin Immunol* **196**, 59-63, doi:10.1016/j.clim.2018.04.002 (2018).

24 Xu, M. *et al.* Senolytics improve physical function and increase lifespan in old age. *Nat Med* **24**, 1246-1256, doi:10.1038/s41591-018-0092-9 (2018).

25 Sheppard, K. E. & McArthur, G. A. The cell-cycle regulator CDK4: an emerging therapeutic target in melanoma. *Clin Cancer Res* **19**, 5320-5328, doi:10.1158/1078-0432.CCR-13-0259 (2013).

26 Vallejo, A. N., Weyand, C. M. & Goronzy, J. J. T-cell senescence: a culprit of immune abnormalities in chronic inflammation and persistent infection. *Trends Mol Med* **10**, 119-124, doi:10.1016/j.molmed.2004.01.002 (2004).

27 Solana, R. *et al.* Innate immunosenescence: effect of aging on cells and receptors of the innate immune system in humans. *Semin Immunol* **24**, 331-341, doi:10.1016/j.smim.2012.04.008 (2012).

28 Fulop, T. *et al.* Signal transduction and functional changes in neutrophils with aging. *Aging Cell* **3**, 217-226, doi:10.1111/j.1474-9728.2004.00110.x (2004).

29 Sebastian, C., Espia, M., Serra, M., Celada, A. & Lloberas, J. MacrophAging: a cellular and molecular review. *Immunobiology* **210**, 121-126, doi:10.1016/j.imbio.2005.05.006 (2005).

30 Dorshkind, K., Montecino-Rodriguez, E. & Signer, R. A. J. The ageing immune system: is it ever too old to become young again? *Nature Reviews Immunology* **9**, 57-62, doi:10.1038/nri2471 (2009).

31 Eaton, S. M., Maue, A. C., Swain, S. L. & Haynes, L. Bone marrow precursor cells from aged mice generate CD4 T cells that function well in primary and memory responses. *J Immunol* **181**, 4825-4831 (2008).

32 Czesnikiewicz-Guzik, M. *et al.* T cell subset-specific susceptibility to aging. *Clin Immunol* **127**, 107-118, doi:10.1016/j.clim.2007.12.002 (2008).

33 Miller, J. P. & Cancro, M. P. B cells and aging: balancing the homeostatic equation. *Exp Gerontol* **42**, 396-399, doi:10.1016/j.exger.2007.01.010 (2007).

34 Weksler, M. E. Changes in the B-cell repertoire with age. *Vaccine* **18**, 1624-1628, doi:Doi 10.1016/S0264-410x(99)00497-1 (2000).

35 Harley, C. B., Futcher, A. B. & Greider, C. W. Telomeres shorten during ageing of human fibroblasts. *Nature* **345**, 458-460, doi:10.1038/345458a0 (1990).

36 Kong, C. M., Lee, X. W. & Wang, X. Y. Telomere shortening in human diseases. *Febs J* **280**, 3180-3193, doi:10.1111/febs.12326 (2013).

37 Cawthon, R. M., Smith, K. R., O'Brien, E., Sivatchenko, A. & Kerber, R. A. Association between telomere length in blood and mortality in people aged 60 years or older. *Lancet* **361**, 393-395, doi:10.1016/S0140-6736(03)12384-7 (2003).

38 Wolthers, K. C. *et al.* T cell telomere length in HIV-1 infection: no evidence for increased CD4+ T cell turnover. *Science* **274**, 1543-1547, doi:10.1126/science.274.5292.1543 (1996).

39 Plunkett, F. J. *et al.* The flow cytometric analysis of telomere length in antigen-specific CD8+ T cells during acute Epstein-Barr virus infection. *Blood* **97**, 700-707, doi:10.1182/blood.v97.3.700 (2001).

40 Kitay-Cohen, Y., Goldberg-Bittman, L., Hadary, R., Fejgin, M. D. & Amiel, A. Telomere length in Hepatitis C. *Cancer Genet Cytogen* **187**, 34-38, doi:10.1016/j.cancergencyto.2008.08.006 (2008).

41 van de Berg, P. J. *et al.* Cytomegalovirus infection reduces telomere length of the circulating T cell pool. *J Immunol* **184**, 3417-3423, doi:10.4049/jimmunol.0903442 (2010).

42 Zannetti, C. *et al.* The expression of p16INK4a tumor suppressor is upregulated by human cytomegalovirus infection and required for optimal viral replication. *Virology* **349**, 79-86, doi:10.1016/j.virol.2006.01.042 (2006).

43 Robinson, M. W. *et al.* Non cell autonomous upregulation of CDKN2 transcription linked to progression of chronic hepatitis C disease. *Aging Cell* **12**, 1141-1143, doi:10.1111/acel.12125 (2013).

44 Ilmonen, P., Kotrschal, A. & Penn, D. J. Telomere attrition due to infection. *Plos One* **3**, e2143, doi:10.1371/journal.pone.0002143 (2008).

45 Cohen, S. *et al.* Association between telomere length and experimentally induced upper respiratory viral infection in healthy adults. *JAMA* **309**, 699-705, doi:10.1001/jama.2013.613 (2013).

46 Asghar, M. *et al.* Chronic infection. Hidden costs of infection: chronic malaria accelerates telomere degradation and senescence in wild birds. *Science* **347**, 436-438, doi:10.1126/science.1261121 (2015).

47 Asghar, M. *et al.* Parallel telomere shortening in multiple body tissues owing to malaria infection. *Proc Biol Sci* **283**, doi:10.1098/rspb.2016.1184 (2016).

48 Organization, G. W. H. World malaria report 2022. Report No. CC BY-NC-SA 3.0 IGO, (2022).

49 WHO. 232 (World Health Organisation WHO, 2019).

50 Midekisa, A., Beyene, B., Mihretie, A., Bayabil, E. & Wimberly, M. C. Seasonal associations of climatic drivers and malaria in the highlands of Ethiopia. *Parasit Vectors* **8**, 339, doi:10.1186/s13071-015-0954-7 (2015).

51 Okafor CN, F. N. Malaria (Plasmodium Ovale). (2019). <https://www.ncbi.nlm.nih.gov/books/NBK519021/>.

52 Vitor-Silva, S., Reyes-Lecca, R. C., Pinheiro, T. R. & Lacerda, M. V. Malaria is associated with poor school performance in an endemic area of the Brazilian Amazon. *Malar J* **8**, 230, doi:10.1186/1475-2875-8-230 (2009).

53 Idro, R., Marsh, K., John, C. C. & Newton, C. R. Cerebral malaria: mechanisms of brain injury and strategies for improved neurocognitive outcome. *Pediatr Res* **68**, 267-274, doi:10.1203/00006450-201011001-00524, DOI 10.1203/PDR.0b013e3181eee738 (2010).

54 Richardson, E. D., Varney, N. R., Roberts, R. J., Springer, J. A. & Wood, P. S. Long-Term Cognitive Sequelae of Cerebral Malaria in Vietnam Veterans. *Applied Neuropsychology* **4**, 238-243, doi:10.1207/s15324826an0404_5 (1997).

55 Wyss, K. *et al.* Malaria and risk of lymphoid neoplasms and other cancer: a nationwide population-based cohort study. *BMC Med* **18**, 296, doi:10.1186/s12916-020-01759-8 (2020).

56 Chen, I. *et al.* "Asymptomatic" Malaria: A Chronic and Debilitating Infection That Should Be Treated. *PLoS Med* **13**, e1001942, doi:10.1371/journal.pmed.1001942 (2016).

57 Feleke, D. G. *et al.* Asymptomatic malaria infection among pregnant women attending antenatal care in malaria endemic areas of North-Shoa, Ethiopia: a cross-sectional study. *Malaria J* **19**, doi:10.1186/s12936-020-3152-9 (2020).

58 Press, N. A. in *Malaria: Obstacles and Opportunities* (1991).

59 WHO. *Malaria diagnosis*, <https://www.who.int/malaria/areas/diagnosis/microscopy/en/> (2019).

60 Krampa, F. D., Aniweh, Y., Awandare, G. A. & Kanyong, P. Recent Progress in the Development of Diagnostic Tests for Malaria. *Diagnostics* **7**, doi:ARTN 54, DOI 10.3390/diagnostics7030054 (2017).

61 Organization, W. H. (World Health Organization, Geneva, 2022).

62 Sidhu, A. B., Verdier-Pinard, D. & Fidock, D. A. Chloroquine resistance in Plasmodium falciparum malaria parasites conferred by pfcrt mutations. *Science* **298**, 210-213, doi:10.1126/science.1074045 (2002).

63 Doolan, D. L., Dobano, C. & Baird, J. K. Acquired immunity to malaria. *Clin Microbiol Rev* **22**, 13-36, Table of Contents, doi:10.1128/CMR.00025-08 (2009).

64 Snow, R. W. *et al.* Relation between severe malaria morbidity in children and level of Plasmodium falciparum transmission in Africa. *Lancet* **349**, 1650-1654, doi:10.1016/S0140-6736(97)02038-2 (1997).

65 Reynaldi, A. *et al.* Interaction between maternally derived antibodies and heterogeneity in exposure combined to determine time-to-first Plasmodium falciparum infection in Kenyan infants. *Malaria J* **18**, doi:ARTN 19, DOI 10.1186/s12936-019-2657-6 (2019).

66 Marsh, K. & Snow, R. W. Host-parasite interaction and morbidity in malaria endemic areas. *Philos Trans R Soc Lond B Biol Sci* **352**, 1385-1394, doi:10.1098/rstb.1997.0124 (1997).

67 Sturrock, H. J. *et al.* Targeting asymptomatic malaria infections: active surveillance in control and elimination. *PLoS Med* **10**, e1001467, doi:10.1371/journal.pmed.1001467 (2013).

68 Mbogo, C. N. *et al.* Low-level Plasmodium falciparum transmission and the incidence of severe malaria infections on the Kenyan coast. *Am J Trop Med Hyg* **49**, 245-253, doi:10.4269/ajtmh.1993.49.245 (1993).

69 Williams, T. N. *et al.* An immune basis for malaria protection by the sickle cell trait. *PLoS Med* **2**, e128, doi:10.1371/journal.pmed.0020128 (2005).

70 Ashburn, P. M., Craig, C. F. & Diseases, U. S. A. B. f. t. S. o. T. Experimental investigations regarding the etiology of dengue fever. 1907. *J Infect Dis* **189**, 1747-1783; discussion 1744-1746, doi:10.1086/383418 (2004).

71 Roestenberg, M. *et al.* The frontline of controlled human malaria infections: A report from the controlled human infection models Workshop in Leiden University Medical Centre 5 May 2016. *Vaccine* **35**, 7065-7069, doi:10.1016/j.vaccine.2017.10.093 (2017).

72 Snounou, G. & Perignon, J. L. Malariotherapy - Insanity at the Service of Malariology. *Adv Parasit* **81**, 223-255, doi:10.1016/B978-0-12-407826-0.00006-0 (2013).

73 WHO. WHO guidance on the ethical conduct of controlled human infection studies. 106 (2022).

74 Shokoples, S. E., Ndao, M., Kowalewska-Grochowska, K. & Yanow, S. K. Multiplexed real-time PCR assay for discrimination of Plasmodium species with improved sensitivity for mixed infections. *J Clin Microbiol* **47**, 975-980, doi:10.1128/JCM.01858-08 (2009).

75 Cawthon, R. M. Telomere measurement by quantitative PCR. *Nucleic Acids Res* **30**, e47 (2002).

76 Pfaffl, M. W. A new mathematical model for relative quantification in real-time RT-PCR. *Nucleic Acids Res* **29**, doi:ARTN e45, DOI 10.1093/nar/29.9.e45 (2001).

77 Reuling, I. J. *et al.* Liver Injury in Uncomplicated Malaria is an Overlooked Phenomenon: An Observational Study. *Ebiomedicine* **36**, 131-139, doi:10.1016/j.ebiom.2018.09.018 (2018).

78 O'Meara, W. P. *et al.* Relationship between exposure, clinical malaria, and age in an area of changing transmission intensity. *Am J Trop Med Hyg* **79**, 185-191, doi:DOI 10.4269/ajtmh.2008.79.185 (2008).

79 Spurgin, L. G. *et al.* Spatio-temporal variation in lifelong telomere dynamics in a long-term ecological study. *J Anim Ecol* **87**, 187-198, doi:10.1111/1365-2656.12741 (2018).

80 Walk, J. *et al.* Modest heterologous protection after Plasmodium falciparum sporozoite immunization: a double-blind randomized controlled clinical trial. *Bmc Medicine* **15**, doi:ARTN 168, DOI 10.1186/s12916-017-0923-4 (2017).

81 Sauerwein, R. W., Roestenberg, M. & Moorthy, V. S. Experimental human challenge infections can accelerate clinical malaria vaccine development. *Nat Rev Immunol* **11**, 57-64, doi:10.1038/nri2902 (2011).

82 Cheng, Q. *et al.* Measurement of Plasmodium falciparum growth rates in vivo: a test of malaria vaccines. *Am J Trop Med Hyg* **57**, 495-500 (1997).

83 Miglar, A. *et al.* Biomarkers of cellular aging during a controlled human malaria infection. *Sci Rep* **11**, 18733, doi:10.1038/s41598-021-97985-y (2021).

84 Reuling, I. J. *et al.* A randomized feasibility trial comparing four antimalarial drug regimens to induce Plasmodium falciparum gametocytemia in the controlled human malaria infection model. *Elife* **7**, doi:10.7554/eLife.31549 (2018).

85 Hermsen, C. C. *et al.* Detection of Plasmodium falciparum malaria parasites in vivo by real-time quantitative PCR. *Mol Biochem Parasitol* **118**, 247-251 (2001).

86 R: A Language and Environment for Statistical Computing v. 1.1.442 (R Foundation for Statistical Computing, 2018).

87 Pulko, V. *et al.* Human memory T cells with a naive phenotype accumulate with aging and respond to persistent viruses. *Nat Immunol* **17**, 966-975, doi:10.1038/ni.3483 (2016).

88 Roos, M. T. *et al.* Changes in the composition of circulating CD8+ T cell subsets during acute epstein-barr and human immunodeficiency virus infections in humans. *J Infect Dis* **182**, 451-458, doi:10.1086/315737 (2000).

89 Sundling, C. *et al.* B cell profiling in malaria reveals expansion and remodeling of CD11c(+) B cell subsets. *Jci Insight* **4**, doi:ARTN e126492, DOI 10.1172/jci.insight.126492 (2019).

90 Kleiveland, C. R. in *The Impact of Food Bioactives on Health* Ch. 15, (Springer, Cham, 2015).

91 Lin, Y. *et al.* Changes in blood lymphocyte numbers with age in vivo and their association with the levels of cytokines/cytokine receptors. *Immun Ageing* **13**, doi:ARTN 24, DOI 10.1186/s12979-016-0079-7 (2016).

92 Le Garff-Tavernier, M. *et al.* Human NK cells display major phenotypic and functional changes over the life span. *Aging Cell* **9**, 527-535, doi:10.1111/j.1474-9726.2010.00584.x (2010).

93 Botwe, A. K. *et al.* Dynamics in multiplicity of Plasmodium falciparum infection among children with asymptomatic malaria in central Ghana. *Bmc Genet* **18**, doi:ARTN 67, DOI 10.1186/s12863-017-0536-0 (2017).

94 Langhorne, J., Ndungu, F. M., Sponaas, A. M. & Marsh, K. Immunity to malaria: more questions than answers. *Nat Immunol* **9**, 725-732, doi:10.1038/ni.f.205 (2008).

95 Simon J Brooker, S. C., Deepika Fernando, Caroline W Gitonga, Joaniter Nankabirwa, David Schellenberg, and Brian Greenwood. *Child and Adolescent Health and Development*. 3 edn, Vol. 8 (Worldbank, 2017).

96 Sons, J. W. *Severe Malaria*. Vol. 19, Supplement material 1 (WHO, 2014).

97 Fink, G., Olgiati, A., Hawela, M., Miller, J. M. & Matafwali, B. Association between early childhood exposure to malaria and children's pre-school development: evidence from the Zambia early childhood development project. *Malar J* **12**, 12, doi:10.1186/1475-2875-12-12 (2013).

98 Cowgill, K. D. *et al.* Effectiveness of Haemophilus influenzae type b conjugate vaccine introduction into routine childhood immunization in Kenya. *Jama-Journal of the American Medical Association* **296**, 671-678, doi:DOI 10.1001/jama.296.6.671 (2006).

99 Olotu, A. *et al.* Defining Clinical Malaria: The Specificity and Incidence of Endpoints from Active and Passive Surveillance of Children in Rural Kenya. *Plos One* **5**, doi:ARTN e15569, DOI 10.1371/journal.pone.0015569 (2010).

100 Mwangi, T. W., Ross, A., Snow, R. W. & Marsh, K. Case definitions of clinical malaria under different transmission conditions in Kilifi District, Kenya. *J Infect Dis* **191**, 1932-1939, doi:10.1086/430006 (2005).

101 Muthui, M. K. *et al.* Gametocyte carriage in an era of changing malaria epidemiology: A 19-year analysis of a malaria longitudinal cohort. *Wellcome Open Res* **4**, 66, doi:10.12688/wellcomeopenres.15186.2 (2019).

102 Waterfall, C. M. & Cobb, B. D. Single tube genotyping of sickle cell anaemia using PCR-based SNP analysis. *Nucleic Acids Res* **29**, doi:ARTN e119, DOI 10.1093/nar/29.23.e119 (2001).

103 Chong, S. S., Boehm, C. D., Higgs, D. R. & Cutting, G. R. Single-tube multiplex-PCR screen for common deletional determinants of alpha-thalassemia. *Blood* **95**, 360-362 (2000).

104 Manego, R. Z. *et al.* Description of Plasmodium falciparum infections in central Gabon demonstrating high parasite densities among symptomatic adolescents and adults. *Malaria J* **18**, doi:ARTN 371, DOI 10.1186/s12936-019-3002-9 (2019).

105 Bauer, M. E. & Fuente Mde, L. The role of oxidative and inflammatory stress and persistent viral infections in immunosenescence. *Mech Ageing Dev* **158**, 27-37, doi:10.1016/j.mad.2016.01.001 (2016).

106 Yman, V. *et al.* Persistent transmission of Plasmodium malariae and Plasmodium ovale species in an area of declining Plasmodium falciparum transmission in eastern Tanzania. *PLoS Negl Trop Dis* **13**, e0007414, doi:10.1371/journal.pntd.0007414 (2019).

107 Farnert, A. *et al.* Epidemiology of malaria in a village in the Rufiji River Delta, Tanzania: declining transmission over 25 years revealed by different parasitological metrics. *Malar J* **13**, 459, doi:10.1186/1475-2875-13-459 (2014).

108 Vasquez, M., Zuniga, M. & Rodriguez, A. Oxidative Stress and Pathogenesis in Malaria. *Front Cell Infect Microbiol* **11**, 768182, doi:10.3389/fcimb.2021.768182 (2021).

109 Lee, I. T. & Yang, C. M. Role of NADPH oxidase/ROS in pro-inflammatory mediators-induced airway and pulmonary diseases. *Biochem Pharmacol* **84**, 581-590, doi:10.1016/j.bcp.2012.05.005 (2012).

110 Ortiz-Montero, P., Londono-Vallejo, A. & Vernot, J. P. Senescence-associated IL-6 and IL-8 cytokines induce a self- and cross-reinforced senescence/inflammatory milieu strengthening tumorigenic capabilities in the MCF-7 breast cancer cell line. *Cell Commun Signal* **15**, 17, doi:10.1186/s12964-017-0172-3 (2017).

111 Stevenson, M. M., Tam, M. F., Wolf, S. F. & Sher, A. Il-12-Induced Protection against Blood-Stage Plasmodium-Chabaudi as Requires Ifn-Gamma and Tnf-Alpha and Occurs Via a Nitric Oxide-Dependent Mechanism. *J Immunol* **155**, 2545-2556 (1995).

112 Weiss, W. R., Sedegah, M., Berzofsky, J. A. & Hoffman, S. L. The Role of Cd4(+) T-Cells in Immunity to Malaria Sporozoites. *J Immunol* **151**, 2690-2698 (1993).

113 Kurup, S. P., Butler, N. S. & Harty, J. T. T cell-mediated immunity to malaria. *Nat Rev Immunol* **19**, 457-471, doi:10.1038/s41577-019-0158-z (2019).

114 Lyke, K. E. *et al.* Serum levels of the proinflammatory cytokines interleukin-1 beta (IL-1beta), IL-6, IL-8, IL-10, tumor necrosis factor alpha, and IL-12(p70) in Malian

children with severe Plasmodium falciparum malaria and matched uncomplicated malaria or healthy controls. *Infect Immun* **72**, 5630-5637, doi:10.1128/IAI.72.10.5630-5637.2004 (2004).

115 De Mast, Q. *et al.* A decrease of plasma macrophage migration inhibitory factor concentration is associated with lower numbers of circulating lymphocytes in experimental Plasmodium falciparum malaria. *Parasite Immunol* **30**, 133-138, doi:10.1111/j.1365-3024.2007.01008.x (2008).

116 Harpaz, R. *et al.* Serum Cytokine Profiles in Experimental Human Malaria - Relationship to Protection and Disease Course after Challenge. *Journal of Clinical Investigation* **90**, 515-523, doi:Doi 10.1172/Jci115889 (1992).

117 de Jager, W., Bourcier, K., Rijkers, G. T., Prakken, B. J. & Seyfert-Margolis, V. Prerequisites for cytokine measurements in clinical trials with multiplex immunoassays. *BMC Immunol* **10**, 52, doi:10.1186/1471-2172-10-52 (2009).

118 Postma, N. S., Mommers, E. C., Eling, W. M. & Zuidema, J. Oxidative stress in malaria; implications for prevention and therapy. *Pharm World Sci* **18**, 121-129 (1996).

119 Ahmed, W. & Lingner, J. Impact of oxidative stress on telomere biology. *Differentiation* **99**, 21-27, doi:10.1016/j.diff.2017.12.002 (2018).

120 von Zglinicki, T. Role of oxidative stress in telomere length regulation and replicative senescence. *Ann N Y Acad Sci* **908**, 99-110, doi:10.1111/j.1749-6632.2000.tb06639.x (2000).

121 Oikawa, S. & Kawanishi, S. Site-specific DNA damage at GGG sequence by oxidative stress may accelerate telomere shortening. *Febs Lett* **453**, 365-368, doi:Doi 10.1016/S0014-5793(99)00748-6 (1999).

122 Davalos, A. R., Coppe, J. P., Campisi, J. & Desprez, P. Y. Senescent cells as a source of inflammatory factors for tumor progression. *Cancer Metastasis Rev* **29**, 273-283, doi:10.1007/s10555-010-9220-9 (2010).

123 Coppe, J. P., Desprez, P. Y., Krtolica, A. & Campisi, J. The senescence-associated secretory phenotype: the dark side of tumor suppression. *Annu Rev Pathol* **5**, 99-118, doi:10.1146/annurev-pathol-121808-102144 (2010).

124 Davies, K. J. The Oxygen Paradox, oxidative stress, and ageing. *Arch Biochem Biophys* **595**, 28-32, doi:10.1016/j.abb.2015.11.015 (2016).

125 Meador, B. M., Krzyszton, C. P., Johnson, R. W. & Huey, K. A. Effects of IL-10 and age on IL-6, IL-1beta, and TNF-alpha responses in mouse skeletal and cardiac muscle to an acute inflammatory insult. *J Appl Physiol (1985)* **104**, 991-997, doi:10.1152/japplphysiol.01079.2007 (2008).

126 Percario, S. *et al.* Oxidative stress in malaria. *Int J Mol Sci* **13**, 16346-16372, doi:10.3390/ijms131216346 (2012).

127 Becker, K. *et al.* Oxidative stress in malaria parasite-infected erythrocytes: host-parasite interactions. *Int J Parasitol* **34**, 163-189, doi:10.1016/j.ijpara.2003.09.011 (2004).

128 Atamna, H. & Ginsburg, H. Origin of reactive oxygen species in erythrocytes infected with Plasmodium falciparum. *Mol Biochem Parasitol* **61**, 231-241, doi:10.1016/0166-6851(93)90069-a (1993).

129 Pandey, A. V. *et al.* Mechanism of malarial haem detoxification inhibition by chloroquine. *Biochem J* **355**, 333-338, doi:10.1042/0264-6021:3550333 (2001).

130 Bolchoz, L. J., Gelasco, A. K., Jollow, D. J. & McMillan, D. C. Primaquine-induced hemolytic anemia: formation of free radicals in rat erythrocytes exposed to 6-methoxy-8-hydroxylaminoquinoline. *J Pharmacol Exp Ther* **303**, 1121-1129, doi:10.1124/jpet.102.041459 (2002).

131 Haynes, R. K. & Krishna, S. Artemisinins: activities and actions. *Microbes Infect* **6**, 1339-1346, doi:10.1016/j.micinf.2004.09.002 (2004).

132 Lin, J. *et al.* Systematic and Cell Type-Specific Telomere Length Changes in Subsets of Lymphocytes. *J Immunol Res* **2016**, 5371050, doi:10.1155/2016/5371050 (2016).

133 Olsson, M., Geraghty, N. J., Wapstra, E. & Wilson, M. Telomere length varies substantially between blood cell types in a reptile. *Roy Soc Open Sci* **7**, doi:10.1098/rsos.192136 (2020).

134 Blackburn, E. H. *et al.* Recognition and elongation of telomeres by telomerase. *Genome* **31**, 553-560, doi:10.1139/g89-104 (1989).

135 Hornsby, P. J. Telomerase and the aging process. *Exp Gerontol* **42**, 575-581, doi:10.1016/j.exger.2007.03.007 (2007).

136 Dave, A. *et al.* Homologous recombination repair intermediates promote efficient de novo telomere addition at DNA double-strand breaks. *Nucleic Acids Res* **48**, 1271-1284, doi:10.1093/nar/gkz1109 (2020).

137 Jurikova, K., De Wulf, P. & Cusanelli, E. Nuclear Periphery and Telomere Maintenance: TERRA Joins the Stage. *Trends Genet* **37**, 608-611, doi:10.1016/j.tig.2021.02.003 (2021).

138 Bellon, M. & Nicot, C. Telomere Dynamics in Immune Senescence and Exhaustion Triggered by Chronic Viral Infection. *Viruses* **9**, doi:10.3390/v9100289 (2017).

139 Gianesin, K. *et al.* Premature aging and immune senescence in HIV-infected children. *AIDS* **30**, 1363-1373, doi:10.1097/QAD.0000000000001093 (2016).

140 Solana, C., Pereira, D. & Tarazona, R. Early Senescence and Leukocyte Telomere Shortening in SCHIZOPHRENIA: A Role for Cytomegalovirus Infection? *Brain Sci* **8**, doi:10.3390/brainsci8100188 (2018).

141 McKinney, E. F. & Smith, K. G. T-cell exhaustion: understanding the interface of chronic viral and autoinflammatory diseases. *Immunol Cell Biol* **94**, 935-942, doi:10.1038/icb.2016.81 (2016).

142 Lautenbach, M. J. *et al.* Systems analysis shows a role of cytophilic antibodies in shaping innate tolerance to malaria. *Cell Reports* **39**, doi:ARTN 110709, 10.1016/j.celrep.2022.110709 (2022).

143 Portugal, S., Pierce, S. K. & Crompton, P. D. Young Lives Lost as B Cells Falter: What We Are Learning About Antibody Responses in Malaria. *J Immunol* **190**, 3039-3046, doi:10.4049/jimmunol.1203067 (2013).

144 Dobbs, K. R. & Dent, A. E. Plasmodium malaria and antimalarial antibodies in the first year of life. *Parasitology* **143**, 129-138, doi:10.1017/S0031182015001626 (2016).

145 Nahrendorf, W., Ivens, A. & Spence, P. J. Inducible mechanisms of disease tolerance provide an alternative strategy of acquired immunity to malaria. *Elife* **10**, doi:10.7554/eLife.63838 (2021).

146 Frimpong, A. *et al.* Phenotypic Evidence of T Cell Exhaustion and Senescence During Symptomatic Plasmodium falciparum Malaria. *Front Immunol* **10**, 1345, doi:10.3389/fimmu.2019.01345 (2019).

147 Bernadotte, A., Mikhelson, V. M. & Spivak, I. M. Markers of cellular senescence. Telomere shortening as a marker of cellular senescence. *Aging-Us* **8**, 3-11, doi:DOI 10.18632/aging.100871 (2016).

148 Gong, L., Parikh, S., Rosenthal, P. J. & Greenhouse, B. Biochemical and immunological mechanisms by which sickle cell trait protects against malaria. *Malaria J* **12**, doi:Artn 317, 10.1186/1475-2875-12-317 (2013).

149 Wambua, S. *et al.* The effect of alpha+-thalassaemia on the incidence of malaria and other diseases in children living on the coast of Kenya. *PLoS Med* **3**, e158, doi:10.1371/journal.pmed.0030158 (2006).

150 Whittemore, K., Vera, E., Martinez-Nevado, E., Sanpera, C. & Blasco, M. A. Telomere shortening rate predicts species life span. *Proc Natl Acad Sci U S A* **116**, 15122-15127, doi:10.1073/pnas.1902452116 (2019).

151 Vera, E., Bernardes de Jesus, B., Foronda, M., Flores, J. M. & Blasco, M. A. The rate of increase of short telomeres predicts longevity in mammals. *Cell Rep* **2**, 732-737, doi:10.1016/j.celrep.2012.08.023 (2012).

152 Haussmann, M. F. *et al.* Telomeres shorten more slowly in long-lived birds and mammals than in short-lived ones. *Proc Biol Sci* **270**, 1387-1392, doi:10.1098/rspb.2003.2385 (2003).

153 Bawah, A. A. & Binka, F. N. How many years of life could be saved if malaria were eliminated from a hyperendemic area of northern Ghana? *Am J Trop Med Hyg* **77**, 145-152, doi:DOI 10.4269/ajtmh.2007.77.145 (2007).

154 Gelband, H. *et al.* Is Malaria an Important Cause of Death among Adults? *Am J Trop Med Hyg* **103**, 41-47, doi:10.4269/ajtmh.20-0036 (2020).

155 Dhingra, N. *et al.* Adult and child malaria mortality in India: a nationally representative mortality survey. *Lancet* **376**, 1768-1774, doi:10.1016/S0140-6736(10)60831-8 (2010).

156 Codd, V. *et al.* Identification of seven loci affecting mean telomere length and their association with disease. *Nat Genet* **45**, 422-427, doi:10.1038/ng.2528 (2013).

157 Mangino, M. *et al.* Genome-wide meta-analysis points to CTC1 and ZNF676 as genes regulating telomere homeostasis in humans. *Hum Mol Genet* **21**, 5385-5394, doi:10.1093/hmg/dds382 (2012).

158 Dugdale, H. L. & Richardson, D. S. Heritability of telomere variation: it is all about the environment! *Philos T R Soc B* **373**, doi:ARTN 20160450, 10.1098/rstb.2016.0450 (2018).

159 Frenck, R. W., Jr., Blackburn, E. H. & Shannon, K. M. The rate of telomere sequence loss in human leukocytes varies with age. *Proc Natl Acad Sci U S A* **95**, 5607-5610, doi:10.1073/pnas.95.10.5607 (1998).

160 Martin-Ruiz, C. *et al.* Stochastic variation in telomere shortening rate causes heterogeneity of human fibroblast replicative life span. *J Biol Chem* **279**, 17826-17833, doi:10.1074/jbc.M311980200 (2004).

161 Franceschi, C. *et al.* The Continuum of Aging and Age-Related Diseases: Common Mechanisms but Different Rates. *Front Med (Lausanne)* **5**, 61, doi:10.3389/fmed.2018.00061 (2018).

162 Wang, Q., Zhan, Y., Pedersen, N. L., Fang, F. & Hagg, S. Telomere Length and All-Cause Mortality: A Meta-analysis. *Ageing Res Rev* **48**, 11-20, doi:10.1016/j.arr.2018.09.002 (2018).

163 Gorenjak, V., Petrelis, A. M., Stathopoulou, M. G. & Visvikis-Siest, S. Telomere length determinants in childhood. *Clin Chem Lab Med* **58**, 162-177, doi:10.1515/cclm-2019-0235 (2020).

164 Benetos, A. *et al.* Tracking and fixed ranking of leukocyte telomere length across the adult life course. *Aging Cell* **12**, 615-621, doi:10.1111/acel.12086 (2013).

165 Zeichner, S. L. *et al.* Rapid telomere shortening in children. *Blood* **93**, 2824-2830 (1999).

166 Lulkiewicz, M., Bajsert, J., Kopczynski, P., Barczak, W. & Rubis, B. Telomere length: how the length makes a difference. *Mol Biol Rep* **47**, 7181-7188, doi:10.1007/s11033-020-05551-y (2020).

167 Tomasetti, C. *et al.* Cell division rates decrease with age, providing a potential explanation for the age-dependent deceleration in cancer incidence. *P Natl Acad Sci USA* **116**, 20482-20488, doi:10.1073/pnas.1905722116 (2019).

168 Barrett, E. L. & Richardson, D. S. Sex differences in telomeres and lifespan. *Aging Cell* **10**, 913-921, doi:10.1111/j.1474-9726.2011.00741.x (2011).

169 Moller, P. *et al.* Sex-related differences in length and erosion dynamics of human telomeres favor females. *Aging (Albany NY)* **1**, 733-739, doi:10.18632/aging.100068 (2009).

170 Lapham, K. *et al.* Automated Assay of Telomere Length Measurement and Informatics for 100,000 Subjects in the Genetic Epidemiology Research on Adult Health and Aging (GERA) Cohort. *Genetics* **200**, 1061-1072, doi:10.1534/genetics.115.178624 (2015).

171 Youngren, K. *et al.* Synchrony in telomere length of the human fetus. *Hum Genet* **102**, 640-643, doi:DOI 10.1007/s004390050755 (1998).

172 Aviv, A., Shay, J., Christensen, K. & Wright, W. The longevity gender gap: are telomeres the explanation? *Sci Aging Knowledge Environ* **2005**, pe16, doi:10.1126/sageke.2005.23.pe16 (2005).

173 Kyo, S. *et al.* Estrogen activates telomerase. *Cancer Res* **59**, 5917-5921 (1999).

174 Vina, J., Borras, C., Gambini, J., Sastre, J. & Pallardo, F. V. Why females live longer than males? Importance of the upregulation of longevity-associated genes by oestrogenic compounds. *Febs Lett* **579**, 2541-2545, doi:10.1016/j.febslet.2005.03.090 (2005).

175 Eleanor L. Axson, K. E. P., Martha M. Tellez-Rojo, Jaclyn M. Goodrich, John Meeker, Adriana Mercado-Garc´ıa, & Needham, M. S. a. B. L. Sex Differences in Telomere Length Are Not Mediated by Sex Steroid Hormones or Body Size in Early Adolescence. *Gender and the Genome* **1-8**, doi:10.1177/2470289718795177 (2018).

176 Bessler, M., Wilson, D. B. & Mason, P. J. Dyskeratosis congenita and telomerase. *Curr Opin Pediatr* **16**, 23-28, doi:Doi 10.1097/00008480-200402000-00006 (2004).

177 Surralles, J., Hande, M. P., Marcos, R. & Lansdorp, P. M. Accelerated telomere shortening in the human inactive X chromosome. *Am J Hum Genet* **65**, 1617-1622, doi:Doi 10.1086/302665 (1999).

178 Bodnar, A. G. *et al.* Extension of life-span by introduction of telomerase into normal human cells. *Science* **279**, 349-352, doi:10.1126/science.279.5349.349 (1998).

179 Khan, S. S., Singer, B. D. & Vaughan, D. E. Molecular and physiological manifestations and measurement of aging in humans. *Aging Cell* **16**, 624-633, doi:10.1111/acel.12601 (2017).

180 Xia, X., Chen, W., McDermott, J. & Han, J. J. Molecular and phenotypic biomarkers of aging. *F1000Res* **6**, 860, doi:10.12688/f1000research.10692.1 (2017).

181 Kudryashova, K. S., Burka, K., Kulaga, A. Y., Vorobyeva, N. S. & Kennedy, B. K. Aging Biomarkers: From Functional Tests to Multi-Omics Approaches. *Proteomics* **20**, e1900408, doi:10.1002/pmic.201900408 (2020).

182 Vaiserman, A. & Krasnienkov, D. Telomere Length as a Marker of Biological Age: State-of-the-Art, Open Issues, and Future Perspectives. *Front Genet* **11**, doi:ARTN 630186, 10.3389/fgene.2020.630186 (2021).

183 Pearce, E. E. *et al.* Telomere length and epigenetic clocks as markers of cellular aging: a comparative study. *Geroscience* **44**, 1861-1869, doi:10.1007/s11357-022-00586-4 (2022).

184 O'Sullivan, R. J. & Karlseder, J. Telomeres: protecting chromosomes against genome instability. *Nat Rev Mol Cell Biol* **11**, 171-181, doi:10.1038/nrm2848 (2010).

185 Epel, E. How "Reversible" Is Telomeric Aging? *Cancer Prev Res* **5**, 1163-1168, doi:10.1158/1940-6207.Capr-12-0370 (2012).

186 Honig, L. S., Kang, M. S., Schupf, N., Lee, J. H. & Mayeux, R. Association of shorter leukocyte telomere repeat length with dementia and mortality. *Arch Neurol* **69**, 1332-1339, doi:10.1001/archneurol.2012.1541 (2012).

187 Nilsson, P. M., Tufvesson, H., Leosdottir, M. & Melander, O. Telomeres and cardiovascular disease risk: an update 2013. *Transl Res* **162**, 371-380, doi:10.1016/j.trsl.2013.05.004 (2013).

188 Wu, X. F. *et al.* Telomere dysfunction: A potential cancer predisposition factor. *J Natl Cancer I* **95**, 1211-1218, doi:10.1093/jnci/djg011 (2003).

189 Panossian, L. A. *et al.* Telomere shortening in T cells correlates with Alzheimer's disease status. *Neurobiol Aging* **24**, 77-84, doi:Pii S0197-4580(02)00043-X, Doi 10.1016/S0197-4580(02)00043-X (2003).

190 Morinha, F., Magalhaes, P. & Blanco, G. Standard guidelines for the publication of telomere qPCR results in evolutionary ecology. *Mol Ecol Resour* **20**, doi:10.1111/1755-0998.13152 (2020).

191 Reichert, S. *et al.* Telomere length measurement by qPCR in birds is affected by storage method of blood samples. *Oecologia* **184**, 341-350, doi:10.1007/s00442-017-3887-3 (2017).

192 Precioso, M., Molina-Morales, M., Dawson, D. A., Burke, T. A. & Martinez, J. G. Effects of long-term ethanol storage of blood samples on the estimation of telomere length. *Evol Ecol* **36**, 915-931, doi:10.1007/s10682-022-10198-1 (2022).

193 Calado, R. T. & Dumitriu, B. Telomere dynamics in mice and humans. *Semin Hematol* **50**, 165-174, doi:10.1053/j.seminhematol.2013.03.030 (2013).

194 Gomes, N. M. *et al.* Comparative biology of mammalian telomeres: hypotheses on ancestral states and the roles of telomeres in longevity determination. *Aging Cell* **10**, 761-768, doi:10.1111/j.1474-9726.2011.00718.x (2011).

195 Shiels, P. G., McGuinness, D., Eriksson, M., Kooman, J. P. & Stenvinkel, P. The role of epigenetics in renal ageing. *Nat Rev Nephrol* **13**, 471-482, doi:10.1038/nrneph.2017.78 (2017).

196 Ellaway, A., Dundas, R., Robertson, T. & Shiels, P. G. More miles on the clock: Neighbourhood stressors are associated with telomere length in a longitudinal study. *Plos One* **14**, e0214380, doi:10.1371/journal.pone.0214380 (2019).

197 Shiels, P. G. *et al.* Accelerated Telomere Attrition Is Associated with Relative Household Income, Diet and Inflammation in the pSoBid Cohort. *Plos One* **6**, doi:ARTN e22521,10.1371/journal.pone.0022521 (2011).

198 Epel, E. S. *et al.* Accelerated telomere shortening in response to life stress. *Proc Natl Acad Sci U S A* **101**, 17312-17315, doi:10.1073/pnas.0407162101 (2004).

199 Shiels, P. G., Buchanan, S., Selman, C. & Stenvinkel, P. Allostatic load and ageing: linking the microbiome and nutrition with age-related health. *Biochem Soc Trans* **47**, 1165-1172, doi:10.1042/BST20190110 (2019).

SUPPLEMENTARY MATERIAL

Table S1. Study overview (Chapter 3): total number of measurements and analyzed markers per study individual (n= 16). *In total, 16 healthy volunteers were enrolled in the CHMI study. Study individuals account for 29-31 time points each, for which continuous data on telomere dynamic is available (N= 481). Cellular markers were measured on three time points for each individual respectively, with exclusion of one individual lacking one time point (C+64). One individual was dropped for gene expression analysis, due to errors in cDNA synthesis. Total number of analyzed markers N= 919.*

ID (n=16)	D.F. 1960	D.L. 1970	E.A. 2257	D.S. 2878	E.K. 2921	D.N. 3146	D.B. 3259	D.O. 3270	D.V. 3366	E.B. 3368	D.K. 3382	E.D. 3899	D.X. 3903	D.Y. 3911	E.N. 3934	E.F. 3963	$N_{individuals}$	$N_{samples}$
$N_{time\text{-}points}$	30	30	30	31	30	30	31	31	31	31	30	31	30	31	30	29		
TL	30	30	30	31	30	30	30	31	31	30	29	30	29	31	30	29	16	481
IL-1β	3	3	3	3	3	3	3	3	3	3	2	3	3	3	3	3	16	47
IFNα2	3	3	3	3	3	3	3	3	3	3	2	3	3	3	3	3	16	47
IFNγ	3	3	3	3	3	3	3	3	3	3	2	3	3	3	3	3	16	47
TNFα	3	3	3	3	3	3	3	3	3	3	2	3	3	3	3	3	16	47
MCP-1	3	3	3	3	3	3	3	3	3	3	2	3	3	3	3	3	16	47
IL-6	3	3	3	3	3	3	3	3	3	3	2	3	3	3	3	3	16	47
IL-8	3	3	3	3	3	3	3	3	3	3	2	3	3	3	3	3	16	47
IL-10	3	3	3	3	3	3	3	3	3	3	2	3	3	3	3	3	16	47
IL-12p70	3	3	3	3	3	3	3	3	3	3	2	3	3	3	3	3	16	47
IL-17A	3	3	3	3	3	3	3	3	3	3	2	3	3	3	3	3	16	47
IL-18	3	3	3	3	3	3	3	3	3	3	2	3	3	3	3	3	16	47
IL-23	3	3	3	3	3	3	3	3	3	3	2	3	3	3	3	3	16	47
IL-33	3	3	3	3	3	3	3	3	3	3	2	3	3	3	3	3	16	47
CDKN2A	3	3	3	3	3	3	3	-	3	3	2	3	3	3	3	3	15	44
TERT	3	3	3	3	3	3	3	-	3	3	2	3	3	3	3	3	15	44
SOD1	3	3	3	3	3	3	3	-	3	3	2	3	3	3	3	3	15	44
SOD2	3	3	3	3	3	3	3	-	3	3	2	3	3	3	3	3	15	44
GSTK	3	3	3	3	3	3	3	-	3	3	2	3	3	3	3	3	15	44
NOS3	3	3	3	3	3	3	3	-	3	3	2	3	3	3	3	3	15	44
CAT	3	3	3	3	3	3	3	-	3	3	2	3	3	3	3	3	15	44

Table S2. Spearmen correlation Matrix of response variables showing significant correlations with significance value p <0.05 (Chapter 3).

	TL	**INFγ**	**IL-8**	**IL-10**	**IL12p70**	**IL-18**	**MCP1**	**NOS3**	**SOD1**	**SOD2**	**CAT**	**GSTK1**	**CDKN2A**
Parasite density	7.4E-03	5.3E-09	3.7E-09	9.5E-17	7.6E-04	2.3E-07	1.7E-10	5.1E-11	2.1E-03	8.2E-07	1.8E-10	2.3E-07	1.3E-08
TL	0.0E+00	4.0E-02	2.2E-02	1.1E-02		1.9E-02	1.0E-02	4.6E-02			4.8E-02		3.1E-04
INFγ		0.0E+00	1.8E-08	2.7E-09	3.0E-05	6.1E-06	2.0E-08	5.9E-09	6.0E-04	2.1E-06	1.1E-08	1.1E-07	9.0E-06
IL-8			0.0E+00	3.7E-09	6.0E-04	2.6E-07	3.2E-08	5.6E-09	1.4E-03	9.5E-07	1.1E-08	2.2E-07	2.5E-06
IL-10				0.0E+00	4.0E-04	3.3E-07	2.8E-10	1.3E-11	1.1E-03	2.3E-07	2.9E-11	6.1E-08	8.5E-08
IL12p70					0.00E+00	3.15E-01	1.04E-02	1.93E-03	3.50E-03	3.59E-01	3.37E-02	2.56E-02	1.77E-05
IL-18						0.00E+00	2.19E-01	4.97E-01	5.40E-01	1.09E-01	1.23E-01	1.48E-01	5.12E-01
MCP1							0.00E+00	8.57E-06		3.86E-02	8.60E-04	3.88E-04	2.50E-02
NOS3								0.00E+00	1.44E-03	4.31E-02	9.96E-06	8.11E-06	1.38E-02
SOD1									0.00E+00	1.72E-03	1.70E-05	1.45E-05	4.83E-02
SOD2										0.00E+00	4.20E-04	1.10E-04	7.52E-01
CAT											0.00E+00	8.10E-12	1.57E-01
GSTK1												0.00E+00	1.05E-01
CDKN2A													0.00E+00

Table S3. Study overview (Chapter 4): total number of telomere measurements and study time-points per patient (n= 13). *In total, 13 malaria infected patients were enrolled in the study. Study individuals account for three time points each, with exception of two patients that were unavailable during their follow-up appointment at the hospital. On each of the individual time points, TL was measured in PBMCs and six PBMC sub-populations. The number of B cell populations was affected by the FACS sort, due to adhesive nature of the cells, in particular atypical B cells and the very low number of such cells for each donor. Total number of telomere length measurements N= 215.*

ID (n=13)	**1**	**2**	**3**	**4**	**5**	**6**	**7**	**8**	**9**	**10**	**11**	**12**	**13**
$\mathbf{N_{time\text{-}points}}$	3	3	3	3	2	2	3	3	3	3	3	3	3
PBMC	3	3	3	3	2	2	3	3	3	3	3	3	3
Monocytes	3	3	3	3	2	2	3	3	3	3	3	3	3
Naive B cells	0	3	3	0	2	2	3	3	0	3	2	3	0
Memory B cells	0	3	2	0	2	2	3	3	0	3	3	3	0
Atypical B cells	3	3	1	0	2	2	3	3	0	3	0	3	0
T cells	3	3	3	3	2	2	3	3	3	3	3	3	3
NK cells	0	3	3	3	2	2	3	3	3	3	3	3	2
Total	12	21	18	12	14	14	21	21	12	21	17	21	11

Table S4. Change in TL between cell sub populations at each follow-up time-point separately (Chapter 4). *Results from LME model accounting for repeated measurements. Coefficients are interpreted as unit increase of TL in PBMC with one unit change of cell-type specific TL.*

Acute

	Monocytes		NK cells		Naive B cells		Memory B cells		Atypical B cells		T cells	
	Coef.	p	Coef.	p	Coef.	p	Coef.	p	Coef.	p	Coef.	p
Monocytes	1		0.84	**0.006**	0.71	**0.014**	0.59	**0.019**	0.57	0.196	0.82	**0.001**
NK cells	0.84	**0.006**	1		0.67	0.111	0.92	0.087	0.7	0.179	0.96	**<0.001**
Naive B cells	0.71	**0.014**	0.67	0.111	1		0.51	0.1	0.54	0.199	0.27	0.466
Memory B cells	0.59	**0.019**	0.92	0.087	0.51	0.1	1		0.71	0.196	0.65	0.168
Atypical B cells	0.57	0.196	0.7	0.179	0.54	0.199	0.71	0.196	1		0.09	0.811
T cells	0.82	**0.001**	0.96	**<0.001**	0.27	0.466	0.65	0.168	0.09	0.811	1	

10-30 days

	Monocytes		NK cells		Naive B cells		Memory B cells		Atypical B cells		T cells	
	Coef.	p	Coef.	p	Coef.	p	Coef.	p	Coef.	p	Coef.	p
Monocytes	1		1.12	**0.01**	0.94	**<0.001**	0.81	**0.004**	0.62	0.138	1.25	**0.008**
NK cells	1.12	**0.01**	1		1.1	**0.014**	1.01	**0.037**	0.23	0.678	0.33	**0.233**
Naive B cells	0.94	**<0.001**	1.1	**0.014**	1		0.82	**0.005**	0.49	0.266	1.13	**0.046**
Memory B cells	0.81	**0.004**	1.01	**0.037**	0.82	**0.005**	1		0.58	0.216	0.93	0.131
Atypical B cells	0.62	0.138	0.23	0.678	0.49	0.266	0.58	0.216	1		0.53	0.329
T cells	1.25	**0.008**	0.33	0.233	1.13	**0.046**	0.93	0.131	0.53	0.329	1	

6-12 months

	Monocytes		NK cells		Naive B cells		Memory B cells		Atypical B cells		T cells	
	Coef.	p	Coef.	p	Coef.	p	Coef.	p	Coef.	p	Coef.	p
Monocytes	1		0.69	0.291	0.74	**0.033**	1.6	**0.007**	1.66	0.113	0.85	0.056
NK cells	0.69	0.291	1		0.68	0.503	0.35	0.444	0.06	0.846	0.76	0.137
Naive B cells	0.74	**0.033**	0.68	0.503	1		1.2	0.22	3.18	0.168	-0.01	0.987
Memory B cells	1.6	**0.007**	0.35	0.444	1.2	0.22	1		0.55	0.532	0.45	0.093
Atypical B cells	1.66	0.113	0.06	0.846	3.18	0.168	0.55	0.532	1		0.57	0.346
T cells	0.85	0.056	0.76	0.137	-0.01	0.987	0.45	0.093	0.57	0.346	1	

Table S5. Study overview (Chapter 5): total number of telomere measurements and study time-points per child (n= 308). *In total, 308 children were enrolled in the study, 218 children from Junju and 90 children from Ngerenya. Majority of children account for three time points each (2007, 2010, 2013), while some children are lacking one of the study time-points due to unavailability during the yearly cross-sectional survey. Total number of telomere length measurements n= 886.*

Total N=308	**Junju** N=218	**Ngerenya** N=90
Survey 2007	190	83
Survey 2010	216	89
Survey 2013	218	90
$\mathbf{N_{measurements}}$	624	262

Table S6. Interaction between age and sex. Linear mixed effect model (Chapter 5).

	Est	SE	df	t	p
Intercept	3.99	0.30	327	13.2	**<0.001**
Age	-0.11	0.05	495	-2.02	**0.044**
Sex	0.29	0.16	290	1.82	0.071
Age*sex	-0.01	0.02	283	-0.07	0.94
Cohort	0.13	0.20	330	0.65	0.518
Survey year 2010	-1.38	0.14	580	-9.84	**<0.001**
Survey year 2013	-0.47	0.25	417	-1.50	0.134
Cumulative malaria episodes	0.02	0.014	432	1.22	0.22
Status at survey					
Non-malarial fever	-0.11	0.25	604	-0.44	0.663
Asymptomatic	0.22	0.10	703	2.14	**0.033**
Symptomatic	-0.18	0.37	470	-0.48	0.63
Sickle cell trait					
AS	-0.05	0.21	302	-0.22	0.829
SS	-1.64	1.46	248	-1.13	0.26
Thalassemia					
Heterozygous	0.25	0.17	303	1.45	0.149
Homozygous	0.45	0.23	299	1.95	0.052

Table S7. Demographic characteristics of the Nyamisati cohort including data from passive surveillance in Chapter 6*. Table includes data from 1002 participants and their respective time points when tested positive for Plasmodium sp. by microscopy, real-time PCR, and when asymptomatic. Data on HIV status was available for 459 individuals (n=972), out of which 14/1002 individuals were tested positive (n=20).*

	Total	**1986**	**1993**	**1994**	**1995**	**1996**	**1997**	**1998**	**1999**	**2010**	**2016**
	n=2604	n=140	n=187	n=343	n=351	n=208	n=176	n=291	n=354	n=271	n=283
Age median, (range), missing	18 (0 – 96) 0	13 (0 - 75)	20 (1-78)	16 (1-79)	12 (0-80)	34 (11-76)	17 (4-77)	24 (5-78)	14 (1-79)	30 (11-82)	12 (0-96)
Sex Ratio (M/F), missing	0.82 (1175/1429) 0	1.5 (84/56)	0.80 (83/104)	0.72 (144/199)	0.73 (148/203)	0.59 (77/131)	0.74 (75/101)	0.86 (135/156)	0.91 (169/185)	0.83 (123/148)	0.94 (137/146)
Microscopy and/or qPCR positive n (%), missing	1392/2427 (57.4) 37	ND	119/187 (63.6) 0	261/343 (76.1) 0	243/351 (69.2) 0	96/201 (47.8) 7	95/168 (56.5) 8	189/269 (70.3) 22	275/354 (77.7) 0	46/271 (17) 0	68/283 (24) 0
Microscopy positive n[a] (%), missing	495/1549 (31.96) 1055	ND	86/187 (45.99) 2	123/339 (36.28) 4	129/347 (37.18) 4	4/15 (26.67) 93	1 ND	13/26 (50) 265	100/354 (28.2) 0	ND	40/283 (14.1) 0
Parasite density median, (range), missing[b]	320 (8-660000) 17	ND	80 (8-30400) 0	240 (8.660000) 0	320 (8-72000) 0	ND 4	ND	ND 13	7261 (160-136000) 0	ND	560 (187-3440) 0
Real-time PCR positive n(%), missing	1442/2548 (56.6) 56	123/176 (69.89) 0	108/183 (59.02) 4	251/339 (74.04) 4	224/345 (64,93) 6	96/ 201(47,76) 7	95/168 (56.55) 8	189/269 (70.26) 2	2 269/349 (77.08) 5	46/271 (16.97) 0	68/215 (24.03) 0
Symptomatic n[c] (%), missing	151/200 (76) 5	ND	1/1 (100) 0	20/20 (100) 0	35/38 (92,11) 0	8/10 (90) 2	2/2 (100) 1	9/13 (69.23) 1	61/62 (98.4) 0	2/2 (100) 1	13/50 (26) 0
Asymptomatic infection n[d] (%), missing	1278/1746 (73.2) 513	ND	129/182 (70.8) 4	246/320 (76.9) 3	213/308 (69.2) 5	88/93 (94.6) 103	93/93 (100) 80	184/185 (99.5) 91	214/289 (74) 3	44/44 (100) 224	67/231 (29) 0
HIV positive (%)	20/972 (2.1) 1632	ND	2/99 (2) 88	4/204 (2) 139	2/258 (0.8) 93	4/207 (19) 1	0/84 (0) 92	ND	ND	8/120 (66.7) 151	ND

ND = No data; n[a] microscopy; n[b] missing data on parasite density for microscopy positive individuals; n[c] total number of microscopy and/or qPCR positive time points, when axillary temperature ≥37 ˚C; n[d] total number of microscopy and/or qPCR positive time points, when axillary temperature <37.5˚C.

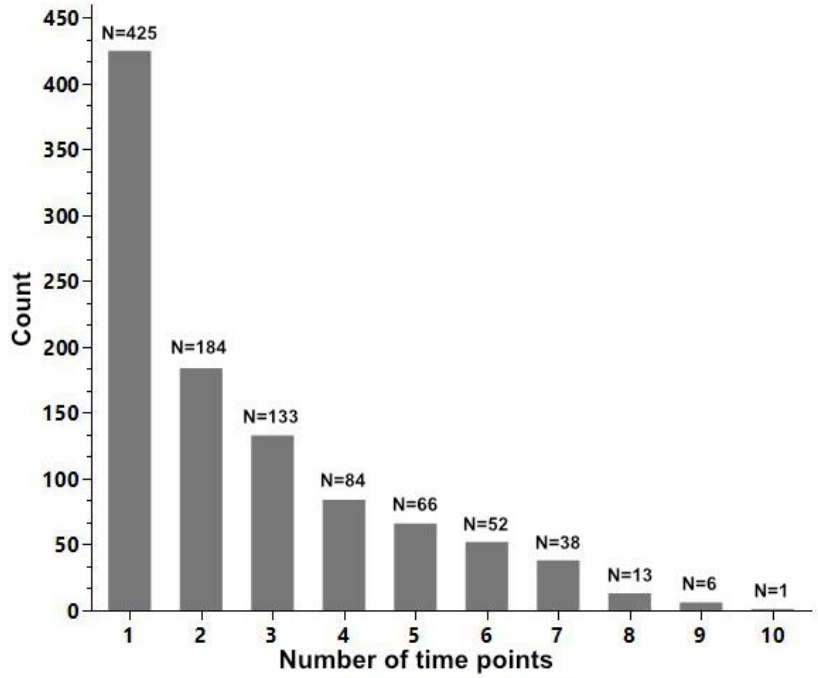

Figure S1. Overview of number of time points (Chapter 6). *Number of individuals N= 1002, mean number of time points per individual n=2.6 (median=3). The majority of individuals with a single time-point are school-children that were added to the data in a later step, to provide TL dynamics across all ages. The availability of the remaining follow-up data was strongly dependent on the villagers' availability at the cross-sectional survey, their oral consent at the day of cross-sectional survey and the death of study participants.*

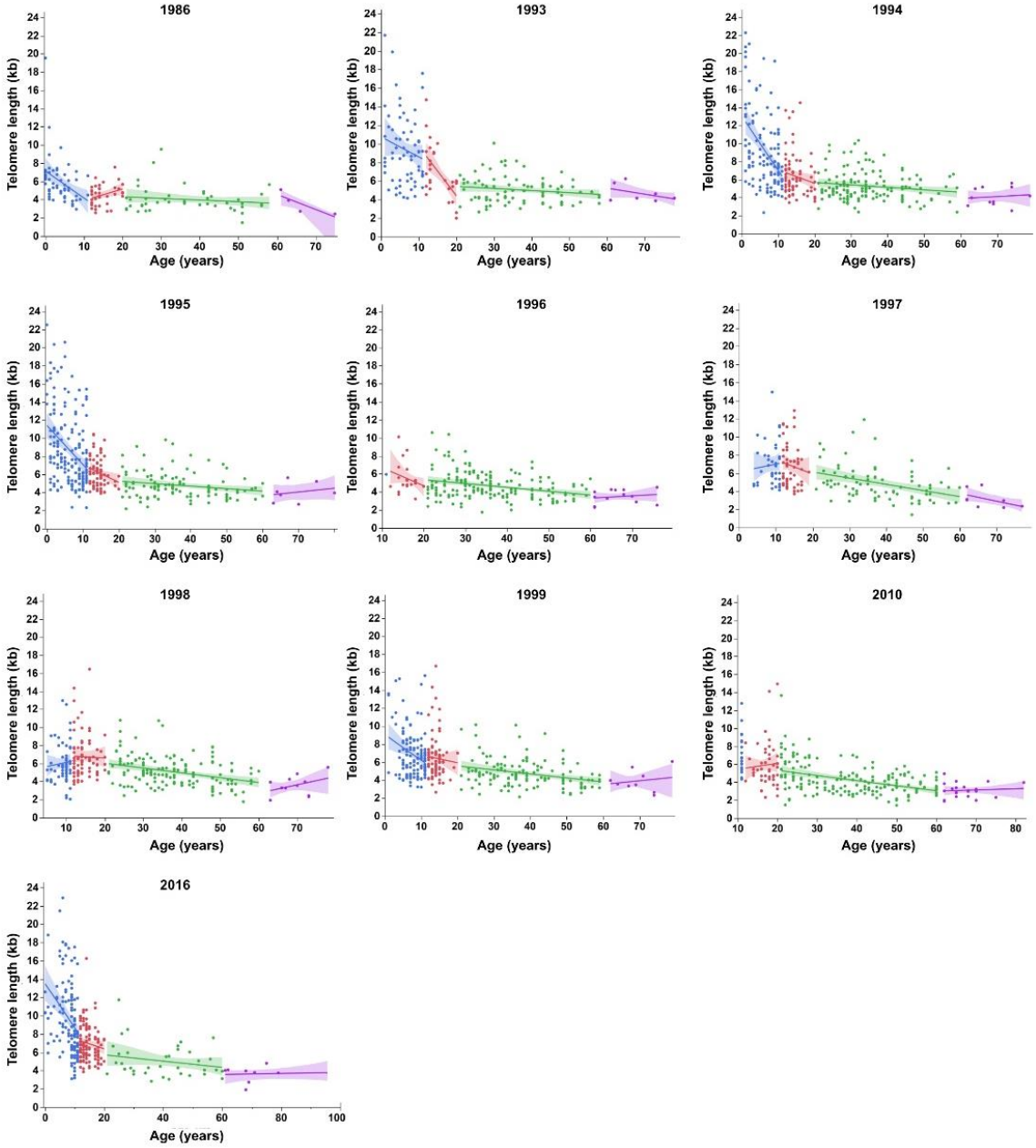

Figure S2. Age splines showing the decrease of TL with age in each survey years in Chapter 6*. Solid line represents the predicted mean, the shaded area denotes the 95% CI interval of the mean.*

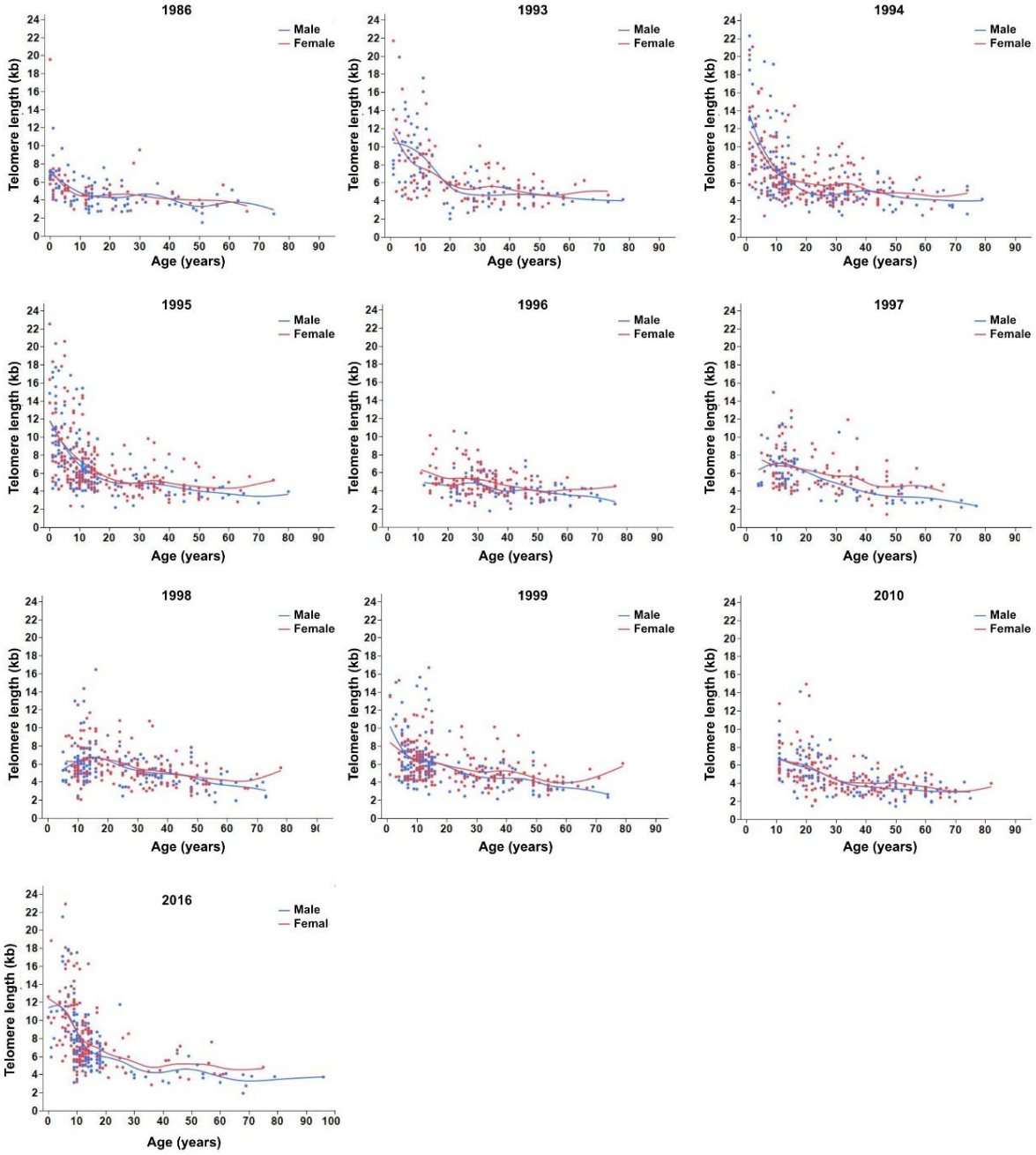

Figure S3. Sex-specific telomere dynamics with age in males (blue) and females across survey years in Chapter 6. *Dots represent the detected mean value ± standard error.*